

impact of light on the induction of programmed cell death in *B.amyloliquefaciens* biofilm cultures

Auteur : Kempgens, Justine

Promoteur(s) : Delvigne, Frank

Faculté : Gembloux Agro-Bio Tech (GxABT)

Diplôme : Master en bioingénieur : chimie et bioindustries, à finalité spécialisée

Année académique : 2017-2018

URI/URL : <http://hdl.handle.net/2268.2/5126>

Avertissement à l'attention des usagers :

Tous les documents placés en accès ouvert sur le site le site MatheO sont protégés par le droit d'auteur. Conformément aux principes énoncés par la "Budapest Open Access Initiative"(BOAI, 2002), l'utilisateur du site peut lire, télécharger, copier, transmettre, imprimer, chercher ou faire un lien vers le texte intégral de ces documents, les disséquer pour les indexer, s'en servir de données pour un logiciel, ou s'en servir à toute autre fin légale (ou prévue par la réglementation relative au droit d'auteur). Toute utilisation du document à des fins commerciales est strictement interdite.

Par ailleurs, l'utilisateur s'engage à respecter les droits moraux de l'auteur, principalement le droit à l'intégrité de l'oeuvre et le droit de paternité et ce dans toute utilisation que l'utilisateur entreprend. Ainsi, à titre d'exemple, lorsqu'il reproduira un document par extrait ou dans son intégralité, l'utilisateur citera de manière complète les sources telles que mentionnées ci-dessus. Toute utilisation non explicitement autorisée ci-avant (telle que par exemple, la modification du document ou son résumé) nécessite l'autorisation préalable et expresse des auteurs ou de leurs ayants droit.

IMPACT OF LIGHT ON THE INDUCTION OF PROGRAMMED CELL DEATH IN *B.amyloliquefaciens* BIOFILM CULTURES

KEMPGENS JUSTINE

**TRAVAIL DE FIN D'ÉTUDES PRÉSENTÉ EN VUE DE L'OBTENTION DU DIPLÔME DE
MASTER BIOINGÉNIEUR EN CHIMIE ET BIO-INDUSTRIES**

ANNÉE ACADÉMIQUE 2017-2018

PROMOTEUR : FRANK DELVIGNE

Toute reproduction du présent document, par quelque procédé que ce soit,
ne peut être réalisée qu'avec l'autorisation de l'auteur et de l'autorité académique
de Gembloux Agro-Bio Tech

Le présent document n'engage que son auteur

IMPACT OF LIGHT ON THE INDUCTION OF PROGRAMMED CELL DEATH IN *B.amyloliquefaciens* BIOFILM CULTURES

KEMPGENS JUSTINE

**TRAVAIL DE FIN D'ÉTUDES PRÉSENTÉ EN VUE DE L'OBTENTION DU DIPLÔME DE
MASTER BIOINGÉNIEUR EN CHIMIE ET BIO-INDUSTRIES**

ANNÉE ACADÉMIQUE 2017-2018

PROMOTEUR : FRANK DELVIGNE

Remerciements

Je tiens à remercier tous ceux qui m'ont aidée pendant la réalisation de mon TFE.

Je remercie les membres de mon jury, Christophe Blecker, François Coutte, Frank Delvigne, Philippe Jacques, Marc Ongena et Marianne Sindic d'avoir accepté de lire et d'évaluer ce travail.

Merci à Frank Delvigne pour votre aide, vos conseils et votre bonne humeur tout au long de la réalisation de ce travail.

Merci à Louise Carlier, ma chère voisine de bureau d'avoir supporté mon bordel et ma présence H24. Merci pour ces fous rire, ces soirées, ces délires ; la réalisation du TFE n'aurait pas été la même sans toi.

Un grand merci aux habitants de l'aquarium du laboratoire des pilotes, Andrew Zicler et Samuel Telek. Merci Sam pour ton aide, ton expertise, tes idées, ta méticuleuse organisation, ta bonne humeur... et juste merci d'avoir toujours été là. Merci le Français pour tes schémas et tes illustrations qui m'ont permis d'embellir ce travail et merci pour ces chouettes discussions.

Merci à Liu Wenzheng de m'avoir fait découvrir ...le MSgg ainsi que le cytomètre et toutes ces autres choses qui ont été précieuses pour mon TFE.

Merci à Sébastien Steels pour ta joie, ton sourire, ta bienveillance et pour ton obstination à tout comprendre.

Merci à Romain Bouchat de m'avoir fait découvrir le time laps même si mon Bacillus n'a pas voulu faire honneur à ton travail... et merci de nous avoir libérées de la chambre à 30°C, on commençait à perdre espoir.

Merci à Tamara pour ton écoute, tes bonnes idées et ton soutien.

Merci à Hosni pour tes explications et ta disponibilité à chacune de mes questions.

Merci à Sébastien Gofflot pour toutes les analyses HPLC et pour les isolants pour tuyaux sans quoi la colonne serait restée au froid.

Merci à Hannah pour ton analyse et ton aide avec 512. Bonne chance avec le réacteur!

Merci à Ariane, Olivia, Marie, Cathy, Barbara, Sokny, Sophia, Ben, Grégory, Henri, Antoine, Anthony,... pour votre accueil chaleureux! Vous faites régner une super ambiance au labo.

Merci à ma famille d'avoir supporté mes histoires de biofilm, à ma cousine d'avoir corrigé l'orthographe et à ma chère sœur (juste envie que tu apparaisses quelque part).

Résumé

Les molécules produites par les microorganismes tels que les *Bacillus* sp. font l'objet d'un nombre grandissant d'études. Leurs applications étant fort nombreuses, une large gamme d'industriels s'y intéressent. Certains de ces composés sont utilisés dans l'industrie agroalimentaire, chimique et/ou pharmaceutique comme c'est le cas des lipopeptides. Cette molécule possède des propriétés émulsifiantes intéressantes en production alimentaire mais également pour la protection des cultures via la production de biopesticides.

Afin de pouvoir utiliser cette molécule à grande échelle, sa production en réacteur doit être mise au point. La production de lipopeptides étant positivement influencée par la formation d'un biofilm, un réacteur à biofilm semble le plus adéquat. Dans ce genre de réacteur tel que celui développé par Q Zune et al., 2017, un biofilm se forme sur un support en inox (packing) suspendu au-dessus du milieu de culture qui est recirculé en permanence sur le packing. Toutefois, ce type de réacteur est difficilement extrapolable à une production industrielle de plus grande ampleur qui nécessiterait la sortie du support hors du réacteur. C'est pourquoi un réacteur à biofilm équipé d'une colonne séparée du système et contenant des packings a été développé avec la souche *B. amyloliquefaciens* GA1 en scale down.

Malheureusement, ce réacteur à biofilm engendre une lyse cellulaire et de ce fait, aucun biofilm ne s'y forme. La lumière émise par un spectromètre infrarouge présent dans le système a été initialement avancé comme déclencheur de cette lyse. Et un possible lien entre la lumière et le phénomène de mort programmé entraînant la lyse a été établi via l'étude du système de réponse aux stress et le réseau de régulation de *B. subtilis*.

Cependant, avant que ce lien n'ait pu être démontré, l'implication de la lumière dans ce phénomène a été démentie. Dès lors, une étude approfondie des possibles causes du problème a ensuite été menée. Les différents stress présents dans le réacteur à biofilm et pouvant mener à l'activation du système de réponses de *B. subtilis* ont été étudiés (les variations de température et de pH ainsi que la limitation en nutriments et en oxygène). Une analyse de la rétention des cellules dans la colonne à l'aide d'un modèle à compartiment a également été effectuée.

Ces multiples recherches ont abouti à la formation d'un biofilm grâce à un changement de milieu de culture (MSgg). De plus, le modèle à compartiments a permis de mettre en évidence l'influence du flux d'air dans la colonne sur la rétention des cellules sur les packings.

Néanmoins, la cause précise du phénomène de lyse observé avec l'ancien milieu (Optimized medium) reste inconnue. Aucun des stress étudiés n'a pu seul causer la mort des cellules.

Mots-clés : Réacteur à biofilm, lipopeptides, MSgg, Optimized medium, *Bacillus amyloliquefaciens* GA1, modèle à compartiments, réponse aux stress, mort cellulaire programmée

Abstract

Molecules produced by microorganisms such as *Bacillus* sp are the subject of many studies. Their manifold applications interest a large range of industries. Several components are used in the agro alimentary industry, chemistry and/or pharmaceutical, as the case of lipopeptides. These molecules present emulsifier properties interesting in food production and also in crops protection via the biopesticides production.

In order to use this molecule in a large scale, its production in reactor must be developed. Lipopeptides production is positively influenced by biofilm production and induces an important foam production. For these reasons, a biofilm reactor seems to be the more suitable. In this kind of reactor, such as the one developed by Q Zune et al., 2017, a biofilm is formed on a support in stainless steel (packing) suspended above the culture medium that recirculates permanently on the packing. However, this kind of reactor is not easily scalable. The output of the support out of the reactor is required for an industrial production in a larger scale. It is the reason why a biofilm reactor equipped with a column containing packings has been developed with the strains *B. amyloliquefaciens* GA1 in scale down.

Unfortunately, this biofilm reactor with a tower meets some difficulties. A cellular lysis is observed and thereby, no biofilm is formed on packings. The light emitted by a near infrared spectrometer placed in the system had been initially considered as the trigger of the cellular lysis. And a possible link between light and the phenomenon of programmed cell death had been established via the study of the general stress response and the regulation network of *B. subtilis*.

However, before this link had been demonstrated, the implication of the near infrared spectrometer in the phenomenon had been refuted. And the study of possible causes of this problem had been conducted. Different stresses present in the biofilm reactor and leading to the activation of the general stress response of *B. subtilis* had been studied (temperature and pH variation and nutrients and oxygen limitation). And an analysis of cells retention in column thanks to a compartments model had been carried out.

These multiple researches have ended up with a biofilm formation thanks to a change of culture medium (MSgg). And, the compartments model has allowed highlighting the influence of air flow in column on cells retention on packings. Nevertheless, the precise cause of the lysis phenomenon observed with the former medium (Optimize medium) remains unknown.

Key-words: Biofilm reactor, lipopeptides, MSgg, Optimized medium, *Bacillus amyloliquefaciens* GA1, compartments model, general stress response, programmed cell death

Table of contents

Introduction.....	1
1. General introduction	1
2. <i>Bacillus amyloliquefaciens</i> , strain characteristics	1
2.1. Generalities	1
2.2. Lipopeptides producer	2
2.2.1. Surfactin, iturin and fengycin	2
3. Stages of biofilm formation.....	3
3.1. Generalities	3
3.2. Physical stage in biofilm development.....	3
4. Regulation network of <i>Bacillus sp.</i>	5
4.1. Generalities	5
4.2. DegU	6
4.3. ComA	6
4.4. SpoOA.....	7
4.4.1. Impact of SpoOA-P evolution over time	7
4.4.2. SpoOA phophorelay fosters heterogeneity and response to external compounds	8
4.4.3. Matrix formation implications.....	9
4.5. Sporulation	10
4.6. Programmed cells death.....	11
5. General stress response in <i>Bacillus sp.</i>	12
6. Link between σ^B and network regulation.....	13
7. Biofilm reactor with stainless steels packings	16
7.1. Biofilm reactor.....	16
7.2. Scalable biofilm reactor design with a column	17
7.3. Potential stress in biofilm reactor with column	18
7.3.1. Temperature.....	18
7.3.2. PH	18
7.3.3. Light	19
7.3.4. Nutrient starvation	19
7.3.5. Oxygen limitation	19
Material and Method	21
1. Medium preparation	21

1.1.	Optimized medium	21
1.2.	PBS	21
1.3.	YPD	21
1.4.	MSgg	21
1.5.	TY	22
2.	Seed preparation	22
3.	Biofilm reactor	22
3.1.	Preculture preparation	22
3.2.	Reactor assembly and disassembly	22
3.3.	Near infrared spectrometer	22
3.4.	Reactor monitoring	22
3.4.1.	Optical density	23
3.4.2.	Analysis with cytometer	23
3.4.3.	Gas analysis	23
3.4.4.	Temperature, o ₂ dissolved and ph	23
3.4.5.	HPLC	23
3.5.	Reactors, different process parameters	24
3.6.	Quantification of cells on packings	25
4.	Determination of the cells path in column	26
4.1.	Experimental method with tracer	26
4.2.	Compartments model	26
5.	Toxins test	27
6.	Test of comparison between Msgg and Optimized medium	28
	Results and discussion	29
1.	Population instabilities in biofilm reactor with external packed bed	29
1.1.	Cells behaviors without biofilm formation	29
1.1.1.	Reactor exhibiting strong cells growth	29
1.1.2.	Reactor exhibiting low cells growth	33
1.1.3.	Possible origin of lysis phenomenon	34
1.2.	Cells behavior with matrix formation	34
1.3.	Causes of cells and biofilm instabilities	35
2.	Influence of culture medium	36
3.	Natural strains versus domesticated/engineered strains	39
4.	Instabilities generated by the biofilm reactor design	41

4.1.	Gas-liquid dispersion in column	41
4.2.	Packings colonization and biofilm instability with MSgg.....	43
4.3.	Attempt to improve cells adhesion with optimized medium.....	45
4.4.	Heterogeneities in environmental conditions and possible stresses expected at the single cell level	46
4.4.1.	Ph variation.....	46
4.4.2.	Column temperature	46
4.4.3.	Light	47
4.4.4.	Carbon source consumption	48
4.4.5.	Impact of the restriction of oxygen injection in column	50
4.4.6.	Conclusion	50
	Conclusion	51
	Outlooks	52
	References.....	54
	Annexes	65
	Annex 1 : Assembly and disassembly of the reactor and the column	65
	Annex 2: Code on Matlab for compartments model (part determinist).....	84
	Annex 3: Comparison test between fresh culture growing in fresh Optimized medium and in medium take out of the reactor.....	85
	Annex 4: Evolution of events number of <i>B. amyloliquefaciens</i> by μl and cells activity measured with a cytometer in FL1 and FL3 in biofilm reactor with MSgg.....	88
	Annex 5: Evolution of the numbers of events by μl of <i>B. amyloliquefaciens</i> growing in microplates in MSgg (red) and in Optimized medium (blue).....	89

List of figures

Figure 1: Summary diagram of DLVO (Hori & Matsumoto, 2010). The resultant force is represented in function of energy and distance between surfaces. In phase one, cell approaches surface but meets a repulsive resultant force. It needs its flagella to catch the surface to irreversibly hang on the support (phase two).....	4
Figure 2: Summary diagram of biofilm regulation with the 3 major regulators: ComA, Spo0A and DegU with their regulation networks (Mielich-Süss & Lopez, 2015)	5
Figure 3: Mechanism of ComA regulation by ComX and CSF (Lazazzera, Kurtser, Mcquade, & Grossman, 1999)	6
Figure 4: Evolution of Spo0A-P level during cell life and its influence on behaviors cells behaviors such as biofilm formation, Cannibalism and sporulation (José Eduardo González-Pastor, 2011).	7
Figure 5: Spo0A phosphorelay in presence of surfactin (José Eduardo González-Pastor, 2011).....	8
Figure 6: SinR and AbrB implication in matrix formation (José Eduardo González-Pastor, 2011).....	9
Figure 7: regulators interactions during sporulation (Piggot, P. J., & Hilbert, D. W. (2004)).....	10
Figure 8: Genes expression leading to the programmed cell death via the phosphorylation of Spo0A which allow the synthesis of Sdp ans Skf toxins (José Eduardo González-Pastor, 2011).....	11
Figure 9: Stress chains (Brody, M. S., Vijay, K., & Price, C. W. (2001)). Perception of energy stress involves the intervention of RsbP and RsbU in the case of environmental stress. Their excitation leads to the release of sigma which can synthesize genes implicated in stress response.....	12
Figure 10: Summary diagram of the hypothesis in <i>B. subtilis</i> , a gram+ bacterium (Adapted with Andrew Zicler works). Red arrows represent negative interaction (repression) and green arrows positive interaction (activation) between transcriptional regulators which regulates 3 cellular behaviors: sporulation, biofilm formation and cannibalism. Stresses activate sigmaB expression which encodes SpoOE. SpoOE has the ability to dephosphorylate Spo0A, a major regulator of the network. Thereby, stresses could induce programmed cell death and sporulation.	15
Figure 11: Configuration diagram of a biofilm reactor with only one packing suspended under the cells culture, with air injection done under the packing and with the recirculation of the liquid phase on it (Quentin Zune et al., 2014).	16
Figure 12 : Diagram of a biofilm reactor with column (A). Packings are placed in a vertical tower where oxygen is injected at its bottom and liquid phase enters by the top of the tower (B). (Illustration: Andrew Zicler).....	17
Figure 13 : diagram of compartments and flux.....	26
Figure 14 : Evolution of optical density (A) and O2 consumption measured in reactor (red) (B) in reactor with Optimized medium and high cell growth.	30
Figure 15 : Summary diagram of reactors with Optimized medium and rapid sucrose consumption. 3 phases of cells culture are noticed: cellular growth (red), lysis phase (blue) and end of sporulation (green). Not studied culture parts are predicted by calculation and appear in purple. This diagram is made thanks to 3 repetitions. Standard deviation for each sample is noted. Planktonic cells fingerprint gives information about cells activity. Spores are cells with an activity under 10^4 in FL1-A. The others ones are active cells.	31
Figure 16: Decrease of optical density (600nm) in reactor (left) and out of reactor (right) with Optimized medium and high growth rate (Adapted with Andrew Zicler works). A sample taken in the reactor was put in culture out of it, in the room at 30°C with agitation.	32

Figure 17 : Evolution of optical density (A) and CO ₂ emission in column (green) with O ₂ consumption measured in reactor (red) (B) in reactor with Optimized medium and low cell growth.	33
Figure 18 : Evolution of optical density (A) and CO ₂ emission in column (green) with O ₂ consumption measured in reactor (red) (B) in reactor with MSgg	35
Figure 19: Biofilm formation of GA1 culture in microplates after 24h, 48h, 72h at 30°C in Optimized medium (above) and in MSgg (below). A biofilm is observed with MSgg and nothing in Optimized medium.	36
Figure 20 : Acetoin concentration (blue) in Optimized medium with optical density in reactor (red). 38	
Figure 21: Evolution of optical density 600 (above) and CO ₂ production (below) for <i>B.subtilis</i> 512 (A) and GA1 (B).....	40
Figure 23: Mean distribution of tracers release measured at the bottom of the column over time for 3 repetitions (blue) in wet column, A: in absence of oxygen injection, B: in presence of oxygen (0.1L/min). The green line is obtained thanks to the determinist model and is adjusted to the tracers exit.....	41
Figure 23 : Distribution of tracers release measured at the bottom of the column over time without air injection for a humid column (blue) and for a dry column (green)	43
Figure 24: Distribution of cells (dry matter in gr) on packings numbered in order. The first packing is at the top of the column and the 6 th at the bottom for the reactor with MSgg and <i>B. subtilis</i> 512.....	44
Figure 25: Cytometer fingerprint of cells GA1 activity after 48h of culture in Msogg: planktonic phase growing in microplate (left), planktonic phase growing in reactor at the end of the cultue (in the midst) and cells from biofilm formed in microplate (right)	45
Figure 26 : The hollow support with packings. The 1l of medium introduced in column in red and the part in contact with packings (300ml) in green.....	45
Figure 27 : Emission spectrum of (A) tungsten lamp and (B) white led lamp for the wavelengths between 350 to 750 nm (visible light) with their relative intensity (adapted to http://www.sunkissedsolar.com.au/led-light-globes-detrimental-health-environment/).	48
Figure 28 : Evolution of optical density 600 (red), acetoin (green) and sucrose (blue) concentration (g/L) in reactor with Optimized medium and a high growth rate. A low residual concentration of sucrose stay in reactor and is consumed after 40h of culture. Acetoin production is high but it is never consumed.....	49
Figure 29 : Evolution of sucrose concentration (g/L) in reactor with Optimized medium and low growth phase (A) and glycerol concentration (g/L) in reactor with MSgg (B). Values at 0 in MSgg correspond at a concentration inferior at 1g/L.....	49

List of tables

Table 1: Concentration of glucose and other compounds of the calibration solution for MSgg analyze	24
Table 2 : References of compounds used in external standard for MSgg analyze	24
Table 3 : Summary table of reactors parameters.....	25

Abbreviation

EPS: exopolysaccharides

NIRS: Near Infrared spectrometer

DLVO: Derjaguin–Landau–Verwey–Overbeek

CSF: Competence and sporulation factor

Sdp: sporulation delaying protein

Skf: sporulation killing factor

PP2C: Protein phosphatase 2C

PAS domain: Per-ARNT-Sim domain

Introduction

1. General introduction

This master thesis is the continuity of precedent works about the optimization of a biofilm reactor with *Bacillus amyloliquefaciens* GA1. This reactor has as purpose the production of lipopeptides with the formation of a biofilm on a support in stainless steel. Unluckily, a cellular lysis followed by sporulation is observed and thereby, no biofilm formation is recorded. Therefore, this work aims to understand the phenomenon by the study of the general stress response and the network regulation of *Bacillus sp.* and by highlighting a link between them.

2. *Bacillus amyloliquefaciens*, strain characteristics

2.1. Generalities

Bacillus amyloliquefaciens is a Gram-positive bacterium known to live in plant-association in rhizosphere. They promote plant growth and protection against pathogens like nematodes, fungi and viruses (Klopper, Ryu, & Zhang, 2004; Koumoutsi et al., 2004). They stimulate the induced systematic resistance which protects plants against external attacks (Ongena et al., 2007). These abilities are possible thanks to the secretion of secondary metabolites such as lipopeptides (surfactin, iturin and fengycin) which represents a great interest for a large range of industries (Koumoutsi et al., 2004; Ongena et al., 2007).

The microorganism used in this work is *B. amyloliquefaciens* GA1. This stains was isolated in Italy on strawberries (Touré, Ongena, Jacques, Guiro, & Thonart, 2004) and shows interesting characteristics, such as its ability to produce lipopeptides in considerable amount (Arguelles-arias et al., 2009). This feature made this strain interesting for industrial production of lipopeptides.

There are more articles on *B. subtilis* in the literature for the mechanisms involved in matrix formation. Because of that, this introduction is based on *B. subtilis* but it is applicable for *B. amyloliquefaciens* GA1. *B. amyloliquefaciens* contains all genes involved in biofilm formation in *B. subtilis* (X. H. Chen et al., 2007).

2.2. Lipopeptides producer

Bacillus subtilis produces three different lipopeptides: surfactin, iturin, fengycin. They have three important functions as: swarming motility, biofilm formation and plant colonization.

These compounds have also interesting properties for industrial applications. Lipopeptides are biosurfactant. They reduce the surface and the interfacial tension and then, allow the mix between liquid, gas and solid by reducing their free energy. They have a growing interest because they are biodegradable, weakly toxic and renewable (Nitschke & Pastore, 2005). A large range of industries used them as in food processing, health care, textile manufacturing, lubricants... (Banat, Makkar, & Cameotra, 2000).

Lipopeptides are constituted by a peptide chain (hydrophilic part) and a fatty acid chain (hydrophobic part) and are formed by non-ribosomal peptide synthetase (Besson & Michel, 1992). Peptide chain can be linear or cyclic. In fact, lipopeptides have a large variety of structures thanks to the variation of the type and number amino acid residues, of peptide cyclization and of fatty acid chain composition (Ongena & Jacques, 2008).

2.2.1. *Surfactin, iturin and fengycin*

Surfactin is a good emulsifier (interfacial tension reduction) (Ahimou, Jacques, & Deleu, 2000). It has important foaming properties but it can also influence the cell membrane. Its effect depends on its concentration in the environment. At low concentration, surfactin can disturb the normal behavior of the cell membrane and change its permeabilization (Ongena & Jacques, 2008). And at higher ratio, surfactin inserts itself in lipid layer and forms pores. When the concentration of surfactin reaches the critical micellar concentration, it can lead to the destruction of biological membranes. For these properties surfactin has a considerable interest in a large range of domains as the fight against cancer, plants resistance and the fabrication of antibacterial products (Ongena et al., 2007).

Iturin does not have the same properties as surfactin. It is a great antifungal but a poor antibacterial and has no antiviral effect. Its activity is also different. Iturin leads to an osmotic perturbation thanks to the formation of ion-conducting pores (Ongena et al., 2007). The iturin family contains 7 variants which are iturin A and C and bacillomycin D.

Fengycin is a great antifungal. It disturbs the biological membrane by changing its fluidity. And at high ratio, fengycin can completely disorganize the phospholipid bilayer (Deleu, Paquot, & Nylander, 2005).

3. Stages of biofilm formation

3.1. Generalities

Bacillus subtilis forms a complex structure called a biofilm. Bacterial biofilm is an agglomeration of cells bound together to a surface by an extracellular matrix containing EPS (exopolysaccharides), proteins, nucleic acids and humic substances (Branda, Chu, Kearns, Losick, & Kolter, 2006; Costa, Silva, & Tavares, 2017; Liaqat, Ahmed, & Jahan, 2013). The conformation in biofilm protects cells against stress and some external attacks as antibiotics (Costa et al., 2017). Biofilm curbs the diffusion of antibiotics thanks to its secretion and disposition and therefore limits antibiotic effects. It promotes also access to substrates. Nutrients diffuse themselves in biofilm thanks to channels.

3.2. Physical stage in biofilm development

There are 3 phases in biofilm formation: adhesion, proliferation and detachment (Liaqat et al., 2013).

First of all, the liquid passage on surface charges it. This phenomenon allows retention of proteins, cations and organic molecules on support. Thanks to that, surface becomes a good environment for cells growth (Costa et al., 2017). Then, cells can catch the support and adhere to it.

This adhesion is described by the DLVO theory and depends on the surface properties of the material and cells and on the ionic strength of medium (Hori & Matsumoto, 2010; Van Loosdrecht, Lyklema, Norde, & Zehnder, 1989). In fact, global electrical charges of surface and cells are generally negative. But, in liquid, there are counter ions which tend to neutralize charges. They form next to surfaces the electric double layer.

Different forces interact between these surfaces, including electrostatic, hydrophobic and van der Waals interaction. Electrostatic force is usually a repulsive interaction and it refers to the force of the double layer. Its value increases with the decrease of ionic strength. Van der Waals force is generally attractive. It includes force between dipoles as Debye and Keersom. Together, they form the resultant force which is sometimes attractive and sometimes repulsive. That depends on ionic

strength and distance between surfaces. In fact, electrostatic force is dominant at high distance and Van der Waals at a low one. However, ion concentration has also a major role on resultant force and on energy barrier (Hermansson, 1999). Indeed, at high ionic concentration, bacterial cells can attach surface irreversibly directly. But, at lower ionic strengths and at 10nm of the surface, cells meet a resultant force that is repulsive. Bacterial cells cannot pass this energy barrier by swimming or Brownian motion. Therefore, it uses its flagella, pili or EPS to reach the surface (Figure 1) (Hori & Matsumoto, 2010).

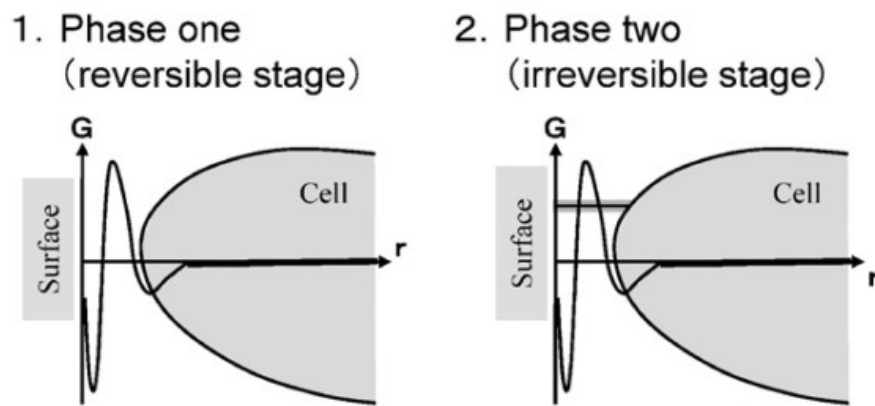


Figure 1: Summary diagram of DLVO (Hori & Matsumoto, 2010). The resultant force is represented in function of energy and distance between surfaces. In phase one, cell approaches surface but meets a repulsive resultant force. It needs its flagella to catch the surface to irreversibly hang on the support (phase two).

In the second phase, when cells hang on support, they proliferate and secrete molecules implicated in matrix formation such EPS (Liaqat et al., 2013). Biofilm begins its formation and can mature. Biofilm swells and forms channels to allow the nutrient transport to cells. They also secrete different molecules to communicate with each other. It is called the quorum sensing (Roilides, Simitopoulou, Katragkou, & Walsh, 2015).

After, bacterial cells trigger their dissemination. Nutrient limitation, liquid flow and enzyme that digest the matrix foster biofilm disintegration and cells dispersion. To destroy biofilm, *Bacillus* cells produce a cocktail of amino acid (D-tyrosine, D-leucine, D-tryptophan and D-methionine) which dissolve the structure (Lam et al., 2009; Manuscript, Blood, & Count, 2009).

4. Regulation network of *Bacillus* sp.

4.1. Generalities

During these different stages of biofilm life, various regulators are expressed in several concentrations and regulate them. In fact, they control three important behaviors known in cells, as biofilm formation, programmed cell death (cellular lysis by the production of toxins) and sporulation.

A complex network of transcriptional regulators is involved but 3 major one govern it: ComA, DegU, Spo0A (Figure 2) (Mielich-Süss & Lopez, 2015). According to their phosphorylation status, they regulate gene expression and so, cell behaviors.

Even if cells have the same genome, gene expression can differ. It is phenotypic heterogeneity. It depends on the position in biofilm and secretion in extracellular matrix. But the stimulation by phosphorylation also promotes heterogeneity thanks to different concentrations of phosphatase and dephosphatase in cells (J.-W. Veening et al., 2008; J. W. Veening, Hamoen, & Kuipers, 2005). That allows cells differentiation.

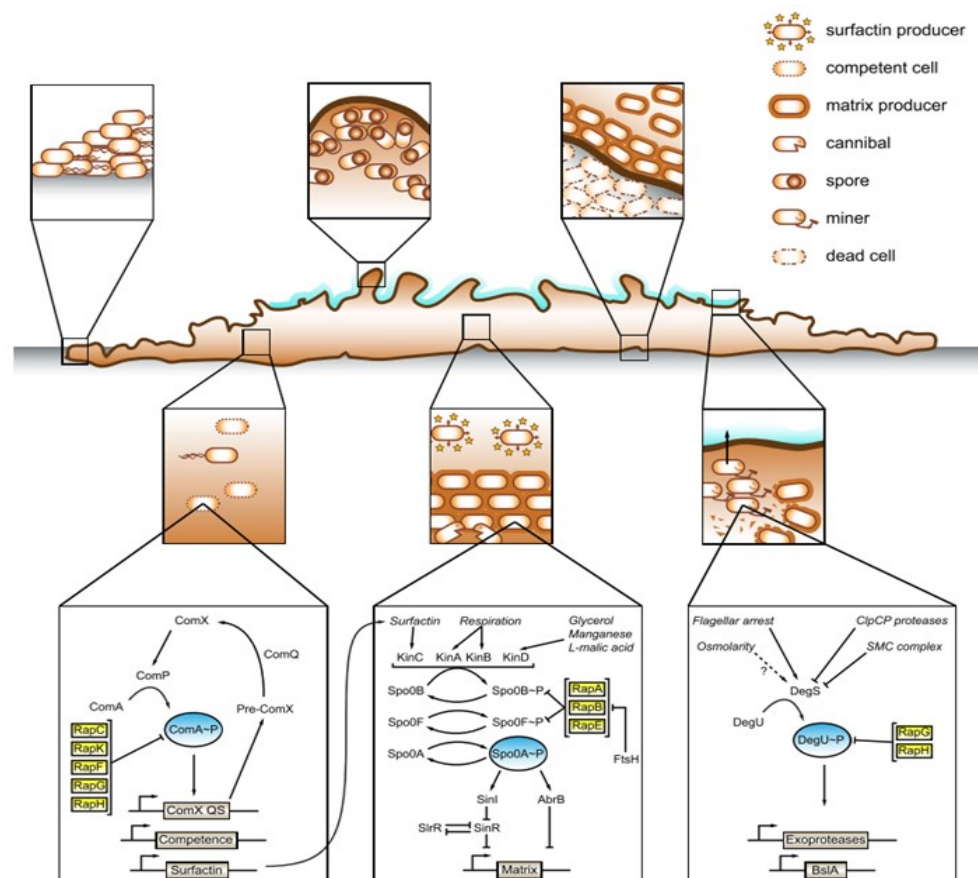


Figure 2: Summary diagram of biofilm regulation with the 3 major regulators: ComA, Spo0A and DegU with their regulation networks (Mielich-Süss & Lopez, 2015)

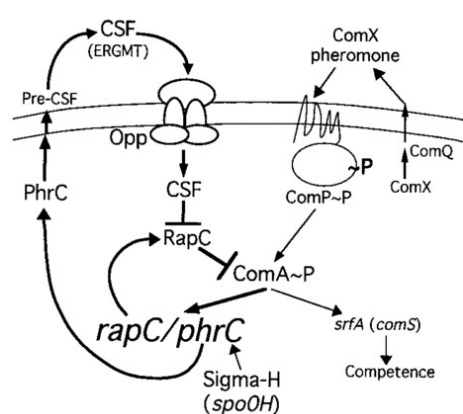
4.2. DegU

DegU regulates the matrix formation thanks to the control of BslA (Kobayashi & Iwano, 2012) and exoproteases (Kobayashi, 2007) and the repression of other genes involved in the biofilm formation (Marlow et al., 2014; Mielich-Süss & Lopez, 2015).

This control depends on the phosphorylation level of DegU (Murray, Kiley, & Stanley-Wall, 2009). DegU is phosphorylated by a sensor histidine kinase, DegS (Dahl, Msadek, Kunst, & Rapoport, 1991). This activation is not well known but the restriction of the flagellum rotation can promote the DegU phosphorylation (Kobayashi, 2007). And the dephosphorylation could be carried out by Clpc-mediated proteolysis (Ogura & Tsukahara, 2010).

DegU activation (DegU-P) leads to different phenomena as the differentiation of a subpopulation of cells which secretes exoproteases degrading polymers in smaller peptides more nutritive (Kobayashi, 2007; Mielich-Süss & Lopez, 2015). A high level of DegU-P leads also to BslA secretion and to *epsA* and *tapA* transcription inhibition (Branda et al., 2006). BslA is a hydrophobic protein that covers the biofilm and plays the role of water-repellent (Kobayashi & Iwano, 2012). *tapA* control the TasA production. TasA is a protein which, once assembled in amyloid filament, is anchored in the cell wall by TapA (Romero, Aguilar, Losick, & Kolter, 2010). Its filaments form a network which connect cells together and organize biofilm components (Romero, Vlamakis, Losick, & Kolter, 2014). *epsA* encodes exopolysaccharides (EPS).

4.3. ComA



ComA is a transcriptional regulator which control the expression of a large number of gene as *srfA* (M M Nakano & Zuber, 1993) and *rap A, C, E, F* when it is phosphorylated (M Jiang, Grau, & Perego, 2000; Solomon, Lazazzera, & Grossman, 1996). Rap phosphatases can dephosphorylate the three master regulators and then, have an important impact on genes expression.

Figure 3: Mechanism of ComA regulation by ComX and CSF (Lazazzera, Kurtser, Mcquade, & Grossman, 1999)

Com A phosphorylation is influenced by ComX and by CSF (Figure 3) (Comella & Grossman, 2005;

Solomon et al., 1996). CSF and ComX are the two most important quorum sensing signals of *Bacillus subtilis* (Comella & Grossman, 2005). CSF (competence and sporulation factor) gives a signal by repressing RapC that is a dephosphorylator of ComA-P (Comella & Grossman, 2005; Solomon et al., 1996). ComP, a membrane histidine kinase, autophosphorylates and gives its phosphate to ComA when ComX pheromone is presented in the extracellular environment (Comella & Grossman, 2005). By their implications on ComA phosphorylation, CSF and ComX allow the regulation of Rap phosphatases and surfactin synthesis.

srfA controls surfactin production (M M Nakano, Marahiel, & Zuber, 1988). Surfactin is the first inductor of Spo0A-P identified. It creates a pore in the cell membrane and thereby, leads to an evacuation of potassium which activates KinC (Lopez, Fischbach, Chu, Losick, & Kolter, 2009). Then, KinC, a kinase, phosphorylates Spo0A (Mielich-Süss & Lopez, 2015).

4.4. Spo0A

4.4.1. Impact of Spo0A-P evolution over time

Spo0A seems to be the most interesting regulator for this work. In fact, Spo0A is the most implicated in programmed cell death and in sporulation in addition to biofilm formation.

Spo0A is a transcriptional regulator which controls the expression of more than 500 genes (Molle et al., 2003; Piggot & Hilbert, 2004). By the concentration of its phosphorylated form, Spo0A regulates cells behavior (Fujita, González-Pastor, & Losick, 2005). An intermediate level of Spo0A-P induces the matrix formation (Molle et al., 2003) and a higher level the sporulation (Fujita et al., 2005; José Eduardo González-Pastor, 2011; Hamon & Lazazzera, 2001; Vlamakis, Chai, Beauregard, Losick, & Kolter, 2013). This phenomenon is explained by a different affinity of Spo0A-P for the regulatory region (Fujita et al., 2005).

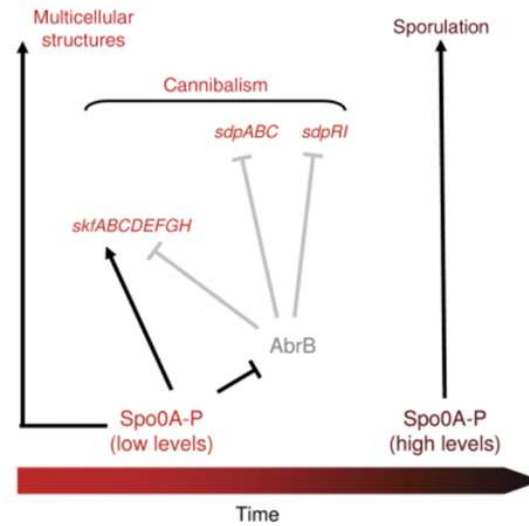


Figure 4: Evolution of Spo0A-P level during cell life and its influence on behaviors cells behaviors such as biofilm formation, Cannibalism and sporulation (José Eduardo González-Pastor, 2011).

Moreover, Spo0A-P concentration is correlated to cells age. In fact, its concentration evolves in cells over time (José Eduardo González-Pastor, 2011; Vlamakis et al., 2013). Young cells present less Spo0A-P at the beginning of their life and this concentration will increase until leading to the sporulation (Figure 4). (Méndez, Orsaria, Philippe, Pedrido, & Grau, 2004).

4.4.2. *Spo0A phosphorelay fosters heterogeneity and response to external compounds*

The Spo0A phosphorylation is triggered by kinases: KinA, KinB, KinC et KinD (Min Jiang, Shao, Perego, & Hoch, 2000; Manuscript et al., 2009; Rudner, LeDeaux, Ireton, & Grossman, 1991). These kinases phosphorylate SpoOF which transfers phosphate to Spo0B. Then, Spo0B phosphorylates Spo0A (Figure 5) (Min Jiang et al., 2000; Manuscript et al., 2009).

Certain external compounds can activate kinases which lead to Spo0A phosphorylation. It is the case of surfactin which acts on KinC (as seen above : 4.3-ComA-pg 6) (Lopez et al., 2009).

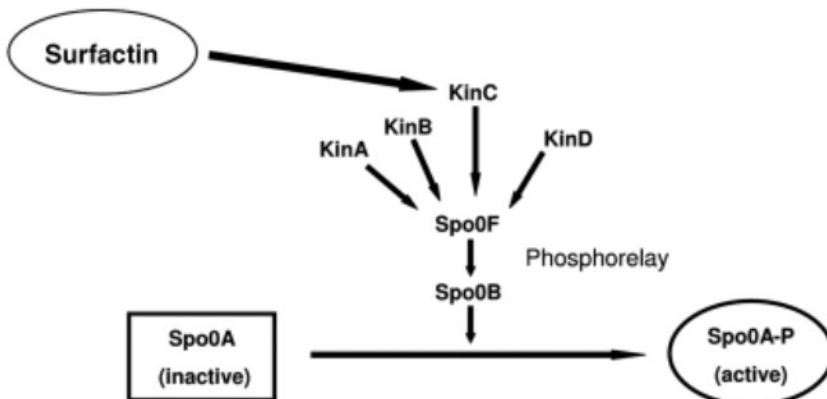


Figure 5: Spo0A phosphorelay in presence of surfactin (José Eduardo González-Pastor, 2011)

Spo0A synthesis and phosphorylation is also regulated by a positive boucle involving σ^H . σ^H is an activator of Spo0A synthesis and some phosphorelay compounds (SpoOF and KinA). Spo0A-P stimulates its synthesis by inactivating AbrB which is σ^H repressor. This way, Spo0A controls its own synthesis and phosphorylation at the same time (Fujita et al., 2005).

All the cells do not phosphorylate the same quantity of Spo0A. There is heterogeneity in stimulation (José Eduardo González-Pastor, 2011; J. W. Veening et al., 2005). This phenomenon is related to the positive boucle of σ^H , to RapA and SpoOE (M Jiang et al., 2000; Mielich-Süss & Lopez, 2015). By their implication and concentration, they induce variability in genes expression and then, in cells differentiation.

4.4.3. Matrix formation implications

Spo0A has an important role in cells differentiation but also in biofilm formation. By its repression on main regulators SinR and AbrB, Spo0A governs matrix transcription compounds (Branda et al., 2006; Manuscript et al., 2009; Strauch et al., 1989).

SinR and AbrB are repressors of operons *tasA-sipW-tapA*, *eps* (A-O) (Branda et al., 2006). These operons are involved in synthesis of molecules essential for the biofilm formation. *tasA-sipW-tapA* operons encode TapA and TasA (function seen above, 4.2 DegU-pg6) (Branda et al., 2006) and *eps* (A-O) express exopolysaccharides (EPS) (Kearns, Chu, Branda, Kolter, & Losick, 2004).

Spo0A governs SinR repression thanks to SinI synthesis. SinI is a repressor of SinR. Its expression depends on Spo0A-P level. In fact, the SinI promoter contains a high affinity activator and some low affinity operators for Spo0A-P. A cell with a low Spo0A-P level express SinI. SinI binds SinR and prevents the operons repression. When cells present a high Spo0A-P level, the SinI synthesis decreases (Figure 6). It is the reason why cells with a low level of Spo0A-P express matrix genes and not cells with a higher level (Chai, Chu, Kolter, & Losick, n.d.; Manuscript et al., 2009; Spring, York, York, York, & York, 1993; Vlamakis et al., 2013).

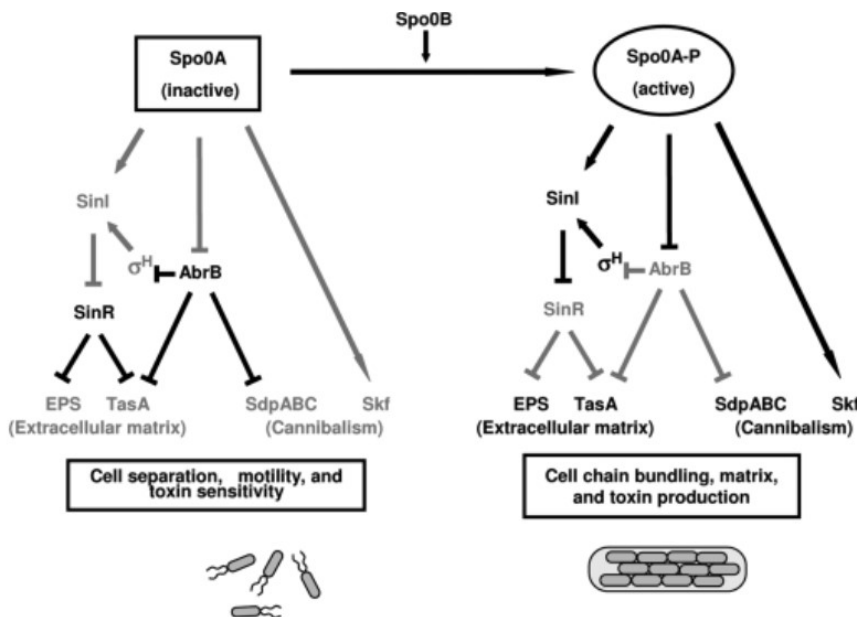


Figure 6: SinR and AbrB implication in matrix formation (José Eduardo González-Pastor, 2011)

SinR governs also its own synthesis thanks to the control of SlrR, a SinR repressor. As a result, SinR can control its own synthesis and then, introduce heterogeneity. If the level of SlrR is high in the cell, SinR is repressed and the SlrR level remains high. Conversely, a low level of SlrR is insufficient to

prevent inactive SinR and increases its own expression (Kearns et al., 2004; Kobayashi, 2008; Manuscript et al., 2009; Mielich-Süss & Lopez, 2015; Vlamakis et al., 2013).

4.5. Sporulation

During cells life, Spo0A-P and σ^H concentration increase (seen above: 4.4.1 Impact of Spo0A-P evolution over time-pg7) (José Eduardo González-Pastor, 2011; Hamon & Lazazzera, 2001; Vlamakis et al., 2013). At high Spo0A-P concentration, an asymmetric division appears. Septum cuts mother cell in two parts (Figure 7) (Burbulys, Trach, & Hoch, 1991). This separation become irreversible when σ^F is activated in spores and σ^E in mother cell (Xenopoulos & Piggot, 2011). After that, the mother cell produces proteins which degrade septum (Piggot & Hilbert, 2004). After spore detachment, σ^G is produced in spore and σ^K in mother cell (Piggot & Losick, 2002). σ^G is a transcriptional regulator which activates proteins synthesis involved in spores resistance (Fujita & Losick, 2003).

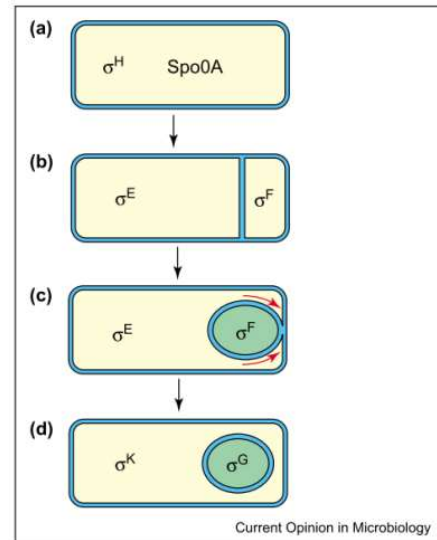


Figure 7: regulators interactions during sporulation (Piggot, P. J., & Hilbert, D. W. (2004))

Spo0A-P regulates sporulation by 2 ways : initiating it and allowing factor transcription in mother cell after septum formation (Fujita & Losick, 2003). In fact, Spo0A-P triggers sporulation by SpolIIE stimulation (Piggot & Losick, 2002). SpolIIE is a phosphatase that dephosphorylates SpolIAA. Then, SpolIAA can bind SpolIAB and release σ^F (Piggot & Losick, 2002). σ^F stimulate synthesis of the SpolIIR protein which permits σ^G expression in spores and σ^E in mother cell. σ^F also allows the synthesis of SpolVB which stimulate σ^K synthesis in mother cell (Losick & Stragier, 1992; Wang et al., n.d.).

Spores of *Bacillus* are brown (Driks, 1999). The spore coat produces CotA that provides this color. CotA is a laccase which catalyses the O₂ oxidation thanks to its copper cofactor (Dick, Torpey, Beveridge, & Tebo, 2008; Oise Hullo, Moszer, Danchin, & Martin-verstraete, 2001). This brown pigment protects spores against UV radiation (Riesenman & Nicholson, 2000).

4.6. Programmed cells death

Spo0A is also involved in cannibalism phenomena (José E González-Pastor, Hobbs, & Losick, 2003). When nutrients disappear, cells with high Spo0A-P level induce expression of 2 toxins : SdpC (sporulation delaying protein) and Skf (sporulation killing factor) (José E González-Pastor et al., 2003). This synthesis leads to a release of nutrients by the death of neighboring cells.

These toxins affect only cells that do not produce them. This resistance mechanism to Skf is not well-known. But, it seems possible that an ABC transporter releases toxins out of cells (José E González-Pastor et al., 2003). For SdpC, cells producer also secretes the resistant protein Sdpl (José E González-Pastor et al., 2003; José Eduardo González-Pastor, 2011). This Sdpl cannot be produced in cells with a low Spo0A-P level because they secrete AbrB, which is the repressor of Sdpl and Sdp (Figure 8) (Molle et al., 2003).

High Spo0A-P level cells are presented in sporulating or old cells (Fujita et al., 2005; José Eduardo González-Pastor, 2011; Hamon & Lazazzera, 2001; Vlamakis et al., 2013). So, cannibalism promotes old cells by killing the others and releasing nutrients (José Eduardo González-Pastor, 2011; Manuscript et al., 2009; Mielich-Süss & Lopez, 2015; Vlamakis et al., 2013).

Before sporulation, cells try to adapt to their environment and cannibalism is a proof of this phenomenon. When spores appear, they produce toxins to kill their neighbors and so provide nutrients. This phenomenon delays the complete cells sporulation (José Eduardo González-Pastor, 2011; Manuscript et al., 2009; Mielich-Süss & Lopez, 2015; Vlamakis et al., 2013).

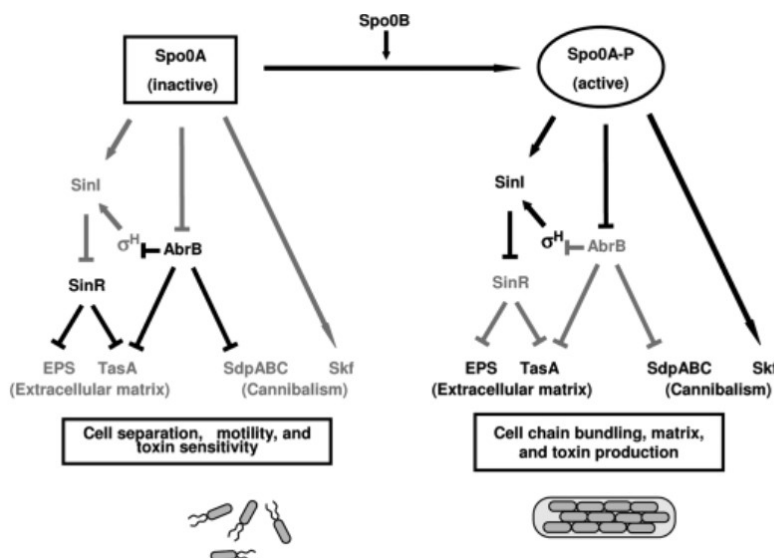


Figure 8: Genes expression leading to the programmed cell death via the phosphorylation of Spo0A which allow the synthesis of Sdp ans Skf toxins (José Eduardo González-Pastor, 2011).

5. General stress response in *Bacillus* sp.

When conditions become unfavorable, *Bacillus subtilis* synthesizes molecules that allow its adaption and its survival. This stress answer needs σ^B activation. This alternative transcription factor, when associated with RNA polymerase allows the synthesis of more than 200 molecules implicated in stress response (Hecker & Völker, 1998).

σ^B can be activated by 2 separate phosphorylation chains. These different branches involve 2 PP2C serine phosphatases (Figure 9). One, RsbU, is activated in environmental stress condition (heat shock, acid shock, salt,...) and the other one, RsbP, is triggered by energetic stress (glucose starvation, light, oxygen limitation) (S. Zhang & Haldenwang, 2005). RsbP and RsbU induction are additive (Voelker, Voelker, et al., 1995).

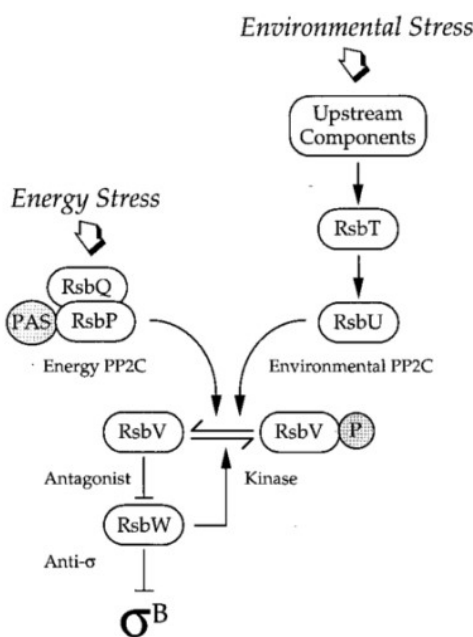


Figure 9: Stress chains (Brody, M. S., Vijay, K., & Price, C. W. (2001)). Perception of energy stress involves the intervention of RsbP and RsbU in the case of environmental stress. Their excitation leads to the release of sigma which can synthesize genes implicated in stress response.

When a stress signal occurs, RsbP and RsbU dephosphorylate the RsbV protein which can bind RsbW and thereby, leads to σ^B release (Vijay, Brody, Fredlund, & Price, 2000). In fact, in favorable condition, RsbV is phosphorylated, it cannot repress RsbW activity which is free to bind σ^B and by this fact inactivate it.

It is important to note that σ^B , RsbV and RsbW synthesis depends on sigma B (Voelker, Dufour, & Haldenwang, 1995). If σ^B is released, RsbV, σ^B and RsbW concentrations increases in cells and then, ensure an adapted response to stress.

RsbP protein presents a PAS domain (a sensor module) on its amino terminal region and a PP2C phosphatase on its carboxyl terminal chain (Taylor & Zhulin, 1999; Vijay et al., 2000; S. Zhang &

Haldenwang, 2005). Its PAS domain is sensible to the variation of potential redox, electron transport and proton motive force (Vijay et al., 2000) or ATP (S. Zhang & Haldenwang, 2005). Once activated, the PAS domain leads to the phosphatase domain activation that can dephosphorylate RsbV.

RsbP activation needs the RsbQ presence. RsbP is synthesized in an inactive form and RsbQ intervention gives the ability to RsbP to perceive stress signals (Brody, Vijay, & Price, 2001).

On its side, RsbU need the intervention of RsbT. This RsbT regulators perceives stresses and then, bind the N-terminal RsbU_N domain of RsbU (Brody, Stewart, & Price, 2009; Rothstein, Lazinski, Osburne, & Sonenshein, 2017; Voelker, Dufour, et al., 1995). This stage actives the phosphatase RsbU.

6. Link between σ^B and network regulation

It seems evident that a link exists between σ^B and the network regulation. It seems very likely that the presence of stresses in environmental surroundings leads to changes in network regulation and therefore, generates several behaviors as programmed cell death and sporulation.

A possible connection has been highlighted by Reder, Albrecht, Gerth, & Hecker, 2012 to explain sporulation inhibition after an exposition to ethanol (Reder, Gerth, & Hecker, 2012). In fact, σ^B encodes a large number of genes such as Spo0E (Reder, Gerth, et al., 2012). This protein has the capacity to dephosphorylate Spo0A-P and then, disturbs network regulation (Ohlsen, Grimsley, & Hoch, 1994). The study demonstrates that, after an exposition to ethanol, Spo0E concentration increases leading to Spo0A-P dephosphorylation. As seen above (4.5-Sporulation-pg10), sporulation initiation depends on the level of Spo0A-P in cells. A high concentration is required for the septation. This way, Spo0E synthesis can inhibit or delay sporulation.

Indeed, several sporulation delays have also been observed in cases of UV and blue light (Ondrusch & Rgen Kreft, 2011; Propst-Ricciui & Lubin, 1976) and red light expositions (Ávila-Pérez, Van Der Steen, Kort, & Hellingwerf, 2010). Moreover, after a cold stress, a larger concentration of Spo0A-P, σ^F , σ^G , σ^E is observed in σ^B -mutants than in wild-type strains (Méndez et al., 2004) (see 4.5-Sporulation-pg10).

This link could be extrapolated to other functions of Spo0A-P. As seen above, Spo0A-P has a major role in biofilm formation and in cannibalism by directly repressing AbrB (Perego, Spiegelman, & Hoch, 1988)(see 4.4.3-Matrix formation implications-pg9 and 4.6-Programmed cells death-pg11). In fact, the action of Spo0E on Spo0A-P leads to an increase of AbrB concentration in cells exposed to stress.

Indeed, an AbrB augmentation in bacterial cells leads to SinR expression. SinR is a master repressor of genes implicated in biofilm formation (operons tasA-sipW-tapA, eps (A-O), see above 4.4.3 -Matrix formation implications-pg 9). Consequently, this increase of AbrB concentration can clearly impact normal biofilm development.

Introduction

Moreover, high AbrB repressor concentration brings to the cessation of cannibalism toxins production but also to its resistance (4.6-Programmed cells death-pg11) (José E González-Pastor et al., 2003; José Eduardo González-Pastor, 2011). This makes cells sensitive to toxins.

However, all cells do not produce SpoOE. Indeed, cells with high SpoOA-P level synthesize a repressor called Rok (Figure 10) (Hoa, Tortosa, Albano, & Dubnau, 2002). This SpoOE repressor acts on the same promoter than σ^B and is able, in large concentration, to inhibit SpoOE expression (Reder, Albrecht, et al., 2012). This way, Rok can impede effects of SpoOE on SpoOA-P and then, the response to stresses.

Therefore, cells with enough SpoOA-P normally continue to produce toxins and its resistance. Thereby, stress would lead to a brutal augmentation of the number of cells sensible to toxins and only spores or sporulating cells would stay alive.

SpoOA-P concentration at stress moments seems to be decisive for cells survival. This phenomenon reminds the importance of heterogeneity in SpoOA production and phosphorylation (as seen above: 4.4.2 SpoOA phophorelay fosters heterogeneity and response to external compounds-pg8).

However, this hypothesis depends on the intensity of interaction. And network regulation is complex. Everything must be considered. For their implication on biofilm compound synthesis, DegU and ComA are not negligible (see 4.2-DegU-pg6 and 4.3-ComA-pg6). Moreover, they also influence SpoOA phosphorylation. For example, ComA is responsible of surfactin, RapA and Rap E synthesis which all impact SpoOA phosphorylation.

Introduction

Summary diagram

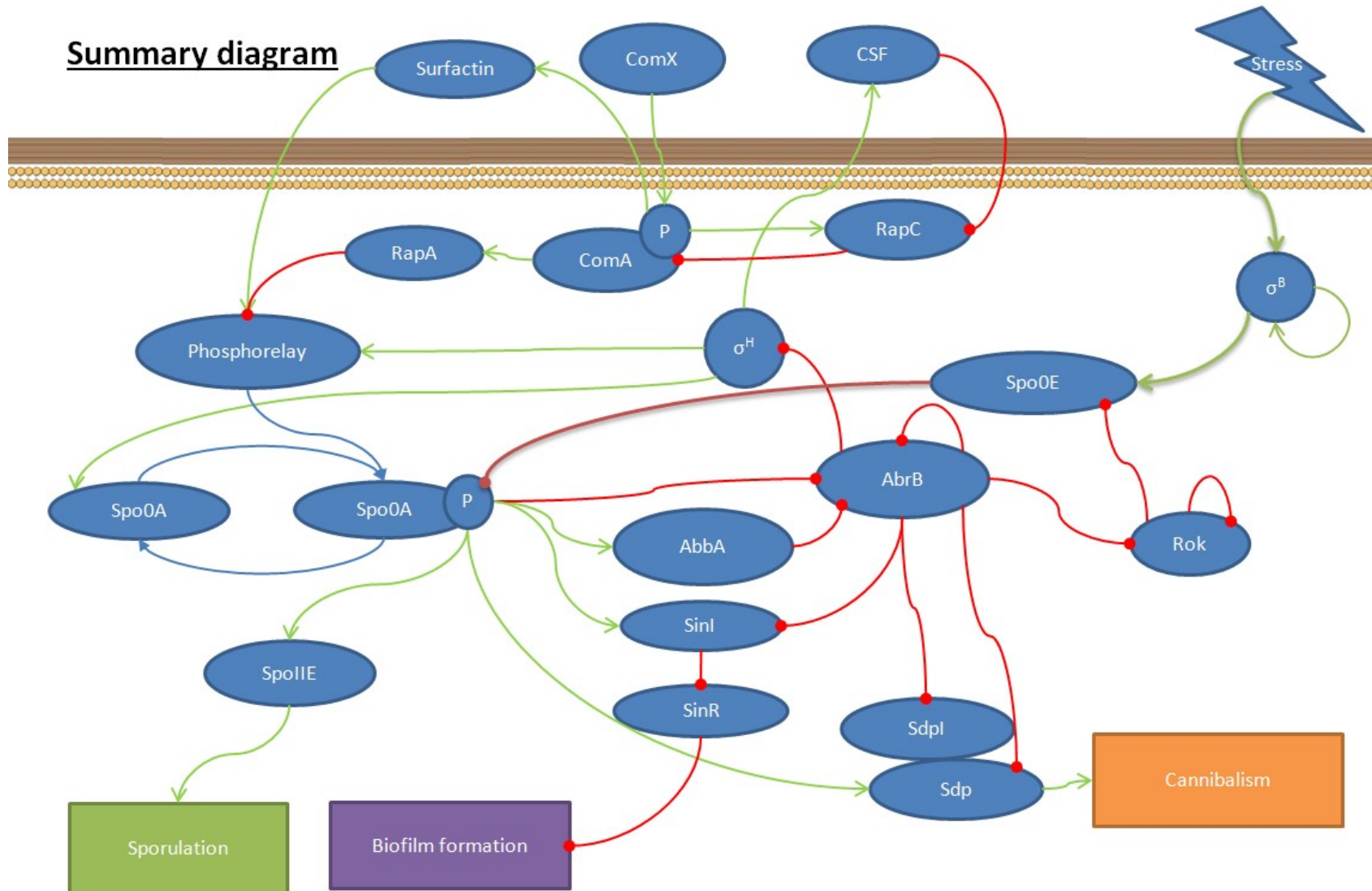


Figure 10: Summary diagram of the hypothesis in *B. subtilis*, a gram+ bacterium (Adapted with Andrew Zicler works). Red arrows represent negative interaction (repression) and green arrows positive interaction (activation) between transcriptional regulators which regulates 3 cellular behaviors: sporulation, biofilm formation and cannibalism. Stresses activate sigmaB expression which encodes SpoOE. SpoOE has the ability to dephosphorylate SpoOA, a major regulator of the network. Thereby, stresses could induce programmed cell death and sporulation.

7. Biofilm reactor with stainless steels packings

7.1. Biofilm reactor

Usually, lipopeptides production by *B. subtilis* is performed in a submerged stirred tank (Q Zune et al., 2017; Quentin Zune et al., 2014). This technique requires an intense agitation and aeration and this way, fosters foam production. This foam production is problematic and is not so easy to suppress. Antifoam and foam breaker disturb cells culture and otherwise, a decrease of aeration and agitation limits surfactin production and cells growth.

The biofilm reactor with packing seems to be a good compromise to solve this problematic. In this kind of reactor, air injection is carried out to the bottom of a stainless steel packing which is suspended over the liquid phase (Figure 11) (Quentin Zune et al., 2014). Liquid is pumped under packing and is spilled at its upper surface. This way, air-liquid mixing is avoided. Moreover, in biofilm reactor, around 92% of dry biomass adhere to packing thanks to its large contact surface ($1735\text{m}^2/\text{m}^3$) (Quentin Zune et al., 2014). And lipopeptide production is easier when cells are immobilized in biofilm.

This reactor has also the advantage of being possibly extrapolated for industrial application. Numerous packings can be increased and volume of cells culture can be upgraded. To manage that, the exit of packing out of the reactor seems to be a good way. It is the reason why a biofilm reactor with a column out of the reactor has been created.

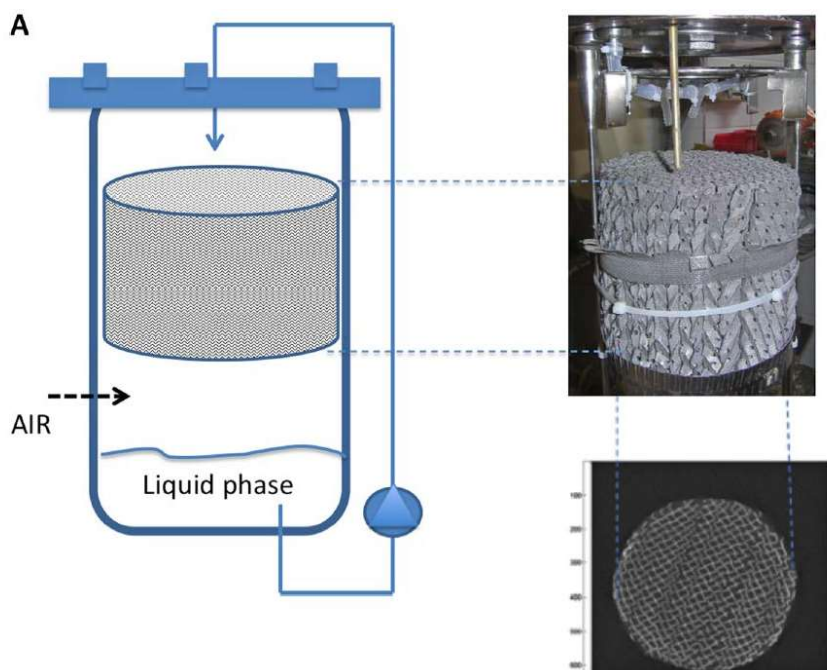


Figure 11: Configuration diagram of a biofilm reactor with only one packing suspended under the cells culture, with air injection done under the packing and with the recirculation of the liquid phase on it (Quentin Zune et al., 2014).

7.2. Scalable biofilm reactor design with a column

In a biofilm reactor with a tower, packings are brought together in a column out of the reactor (Figure 12). Medium with cells culture is injected at its top and circulates in packings at atmosphere pressure. Oxygen injection is done at the bottom of the column and ascends it. Thanks to that, no oxygen is injected in the reactor and therefore, foam production is limited.

Then, medium returns in a 2L reactor tank which is only mixed to allow pH equilibration.

This configuration can be used easily in little and large scale for industrial applications. In this work, this reactor design is used with a 2L reactor and six packings in a tower with a NIRS presents in the loop.

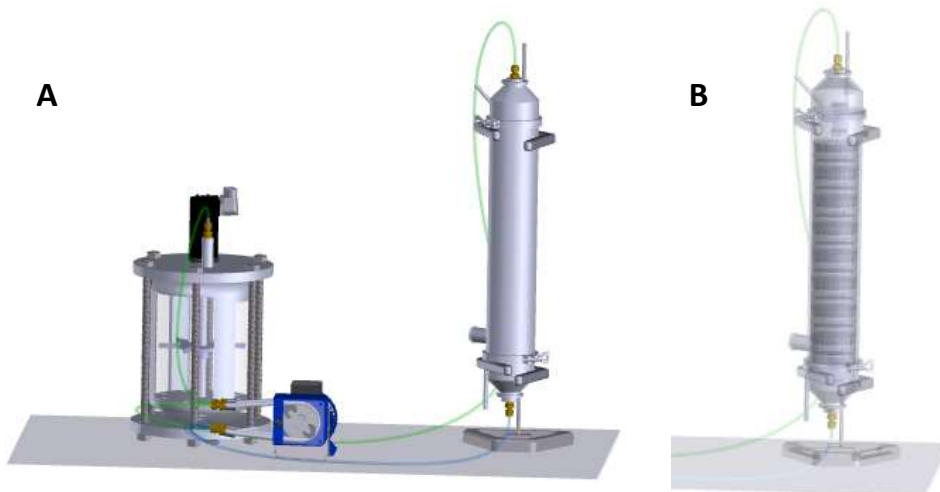


Figure 12 : Diagram of a biofilm reactor with column (A). Packings are placed in a vertical tower where oxygen is injected at its bottom and liquid phase enters by the top of the tower (B). (Illustration: Andrew Zicler)

Unfortunately, this system introduces some stresses which lead to biofilm formation unstable. In fact, 5 major parameters are identified to potentially affect biofilm development in this kind of reactor: temperature, pH variation, nutrient starvation, oxygen limitation and light.

Indeed, reactor content is heated but not the column and all parts of the reactor are connected by silicon pipes which loses a lot of heat. Because of all these aspects, the temperature in the column is lower than in normal growth conditions in the reactor.

Secondly, pH is only adjusted in the reactor and not in the column. Therefore, pH neutrality cannot be ensured in packings.

Then, if no biofilm is formed on packings cells can suffer from nutrient deprivation. In fact, planktonic cells are more affected by nutrient starvation than in biofilm conformation. If they are in large quantity, they can disturb biofilm behavior.

Oxygen is only injected in column and not in the reactor tank. Therefore, planktonic cells meet different concentration of dissolved oxygen in the different parts of the biofilm reactor.

And the last one is light. It is shown that intense light exposition of cells can delay spore production via an excitation of general stress response (Ávila-Pérez, Hellingwerf, & Kort, 2006; Ávila-Pérez et al., 2010; Ondrusch & Rgen Kreft, 2011; J. B. Van Der Steen & Hellingwerf, 2015). And in the reactor, all parts except the column are transparent. Moreover, a NIRS that emits light thanks to a tungsten lamp is present in the system.

All these stresses can lead to sigma B activation and then, influence cells behaviors such as generate programmed cell death and sporulation.

7.3. Potential stress in biofilm reactor with column

7.3.1. Temperature

B. subtilis is a soil bacterium. Thereby, even though its optimal growth temperature is 37°C, it can grow in a large range of temperature from 11°C to 53°C (Weber & Marahiel, 2002). However, temperature variation requests some adaptations from cells. In fact, a drop in temperature affects the fluidity of the cytoplasmic membrane, primary metabolism, protein folding and reduce protein activity (Budde, Steil, Scharf, Vö Lker, & Bremer, 2018; Weber & Marahiel, 2002).

In some cases of temperature variation, general stress response seen in the previous section is induced but not only. When cells grow at low temperature from the beginning, the sigma B induction is considerable (Brigulla et al., 2003). The same is noticed in the case of a sharp temperature increase of the cells culture (Voelker, Voelker, et al., 1995). But when cells were cultivated at high temperature and then, put at a lower, cells use some other system to respond as incorporating fatty acid in the double membrane layer. But in this case of stress, no activation of sigma B is observed (Brigulla et al., 2003; Méndez et al., 2004; Weber & Marahiel, 2002).

7.3.2. PH

B. subtilis has the ability to maintain an internal ph between 7.3 and 7.6 even if environmental ph varies from 6 to 9 (Martinez et al., 2012; Wilks et al., 2009). However, ph variation can impact their growth rate and their survival (Wilks et al., 2009). Indeed, a mild ph modification leads to a lag in growth rate. But, this lag is more important in case of augmentation of ph than a decrease. In fact, they do not implicate the same mechanism. High external ph values involves Na^+/H^+ antiporters and other Na^+ transporter to maintain a neutral ph in cytoplasm . And the adaptation to a

low pH activate sigma B (Kovács, Hargitai, Kovács, & Mécs, 1998; Padan, Bibi, Ito, & Krulwich, 2005; Wilks et al., 2009; S. Zhang & Haldenwang, 2005).

7.3.3. Light

It has been shown that visible light can also influence the normal behavior of cells. In fact, when cells grow exposed to red (625-655 nm) or blue light (430-470nm), a delay in sporulation can be noticed (Ávila-Pérez et al., 2010; Ondrusch & Rgen Kreft, 2011; Propst-Ricciui & Lubin, 1976). This mechanism looks like a “circadian clock” to foster sporulation during night (Ávila-Pérez et al., 2010).

This phenomenon also depends on σ^B (Ávila-Pérez et al., 2006, 2010). Blue light is perceived by a LOV domain containing a photoprotein Ytva which transmits excitation to σ^B by RsbU chain (Ávila-Pérez et al., 2006; J. B. ; Van Der Steen, Nakasone, Hendriks, Hellingwerf, & Biosystems, n.d.; J. B. Van Der Steen & Hellingwerf, 2015). And red light gives signal to an unidentified chromophore bound to RsbP (Ávila-Pérez et al., 2010; Vijay et al., 2000). With the same intensity, the blue light induces a higher σ^B excitation than the red one (Ávila-Pérez et al., 2010). By their σ^B activation, red and blue lights can influence phosphorylation of important transcriptional regulators and therefore, influence single cells and biofilm behavior.

7.3.4. Nutrient starvation

A nutrient limitation is obviously also a major stress origin. Cells spend more time in nutrient deprivation than in exponential growth. Following that, they have developed some behaviors to ensure their survival such as cannibalism, biofilm formation and in ultimate cases, spores development (Chubukov & Sauer, 2014). Biofilm conformation protects cells to stresses and allows growth under less favorable condition. In fact, a low nutrient depletion triggers matrix formation (Stanley & Lazazzera, 2004) by, for instance, an increase of EPS production (W. Zhang et al., 2014). However, conversely, a severe starvation leads to programmed cell death follow by sporulation (Stanley & Lazazzera, 2004). These behaviors require SpoOA phosphorylation.

Cells are able to detect starvation conditions thanks to RsbP that perceived a drop of ATP in cytoplasm (Antelmann et al., 1997; Boylan, Redfield, Brody, & Price, 1993; Voelker, Voelker, et al., 1995). Then, RsbP activate sigma B (see 5-General stress response in *Bacillus* sp.-pg12).

7.3.5. Oxygen limitation

Bacillus subtilis is an aerobe bacterium. Nevertheless, it can grow under anaerobic condition by using nitrate or nitrite as electron acceptor or by fermentation (Clements, Streips, & Miller, 2002;

Introduction

M M Nakano, Dailly, Zuber, & Clark, 1997; Michiko M. Nakano & Hulett, 1997; Sun et al., 1996; Ye et al., 2000). In absence of oxygen, cells can continue its growth by using nitrate or nitrite as electron acceptor and form by this way ammonia thanks to its 2 nitrate reductases (Hoffmann, Troup, Szabo, Hungerer, & Jahn, 1995). Only after, when no more electron acceptors are present, fermentation can occurs and leads to the production of acetate, lactate and 2,3-butanediol (Cruz Ramos et al., 2000). But fermentation is not efficient (M M Nakano et al., 1997; Ye et al., 2000). Some cases of lysis has been observed when sucrose or nitrate are depleted (J. Espinosa-de-los-Monteros · A. Martinez · F. Valle, n.d.).

Oxygen limitation actives sigma B by the same mechanism as nutrient starvation (Boylan et al., 1993; Hecker & Völker, 1998; Voelker, Voelker, et al., 1995; Voelker, Voelker, & Haldenwang, 1996). A drop of ATP occurred and is perceived by RsbP which activate sigma B (see 7.3.4-Nutrient starvation-pg19).

Material and Method

1. Medium preparation

1.1. Optimized medium

Optimized medium contains 30g/L of casein peptone (Becton, Dickinson and Company), 7g/L of yeast extract (Becton, Dickinson and Company), 1,9g/L of KH₂PO₄ (Merck KGaA), 0,9g/L of MgSO₄ (Merck KGaA), 10mg/l of citric acid (Merck KGaA), 100µl of solution 1, 100µl of solution 2, 100µl of antifoam Ks911 and 20g/L of sucrose (sigma). Sucrose solution is prepared separately to avoid Maillard reaction. Solution 1 contains 100mg/l of H₃BO₃ (sigma), 40mg/l of NaMoO₄ (Alfa Aesar), 50mg/l of FeCl₃*6H₂O (Merck KGaA), 20mg/l of KI (VWR) and 10mg/l of CuSO₄ (Merck Eurolab). Its pH is adjusted at 7. Solution 2 is prepared with 36g/L of MnSO₄*H₂O (VWR) and 140mg/l of ZnSO₄*7H₂O (VWR). All is autoclaved at 121°C during 20 minutes (5807 MBG).

1.2. PBS

PBS solution contains 8g/L of NaCl (Merck KGaA), 0,2 g/L of KCl (Merck KGaA), 1,44 g/L of Na₂HPO₄ (1,81g/L de Na₂HPO₄*2H₂O) (Merck KGaA) and 0.24g/L of KH₂PO₄ (Merck KGaA).

1.3. YPD

YPD solution contains 20g/L of casein peptone (Becton, Dickinson and Company), 10g/L of yeast extract (Becton, Dickinson and Company) and 20g/L of glucose (Merck KGaA). Glucose solution is prepared separately to avoid Maillard reaction. All is autoclaved at 121°C during 20 minutes and then, mixed together when there are cold. YPD solution is stocked at 4°C.

1.4. MSgg

MSgg solution for 1 litre is made with 1ml of solution A, 10ml of solution B, 10ml of solution C, 1ml of a 0.54g/L filtered thiamine solution (Sigma), 100ml of a 50g/L filtered glutamic acid solution (Sigma), 100ml of a 50g/L autoclaved glycerol solution (Merck), 100ml of a 209,26g/L filtered Mops solution (Sigma) and 680ml of autoclaved distilled water. Solution A contains 6.3g/L of MnCl₂ (Merck), 0.136g/L of ZnCl₂ (VWR), 8,12g/L of FeCl₃ (Merck), 77,7g/L of CaCl₂ (Merck). Solution is filtered. Solution B contains 68g/L of KH₂PO₄ (Merck), 19g/L of MgCl₂ (VWR) and is autoclaved. Solution C contains 5g/l of tryptophan (Sigma) and of phenylalanine (Sigma) and is filtered.

The pH of MSgg solution is adjusted to 7 with sterilized 3M KOH.

1.5. TY

TY contains 10g/L of bactotryptone (Becton, Dickinson and Company), 5g/L of Bactoyeast (Becton, Dickinson and Company), 2.5g/L of NaCl (Merck) and 0.1mM of MnCl₂ (VWR).

2. Seed preparation

100ml of YPD and a seed are added in a 1L Erlenmeyer with baffles. The Erlenmeyer is incubated at 37°C at 160rpm during 16h00 (Gallenkamp Orbital incubator). Then, 30ml of the Erlenmeyer are added to 20ml (26gr) of sterilized glycerol (Merck). After, freezing tube (Greiner Bio-One GmbH) can be filled with 1.8ml of the mix.

3. Biofilm reactor

3.1. Preculture preparation

100ml of Optimized medium and a seed of GA1 are added in a 1L Erlenmeyer with baffles. The Erlenmeyer is incubated at 37°C at 160rpm during one night (Gallenkamp Orbital incubator). The OD 600 is measured (Genesys 10S UV vis spectrometer Thermo Scientific at 600nm).

3.2. Reactor assembly and disassembly

The protocol of assembly and disassembly of the 2L reactor (Sartorius Biostat B plus) and of the column (Carter gaz in stainless steel 316 PALL) with 6 packings (83/53 Sulzer) are joined in annex (Annex 1 : Assembly and disassembly of the reactor and the column- pg65).

3.3. Near infrared spectrometer

The near-infrared spectrometer with HPLC analyzes allow having a continuous monitoring of compounds in the reactor. Transmission cell is included in reactor system (IN243 miniplant, 1mm, Brucker). Cap is connected to the Matrix-F (Brucker, FT-NIR) thanks to optical fibers. Near Infrared spectrometer (NIRS) emits in continuous a light at a power of 35mW thanks to it tungsten lamp.

3.4. Reactor monitoring

Each hour or 2 hours, 7-8ml is taken in the reactor. The optical density and sometimes, cytometer fingerprints was studied.

3.4.1. Optical density

The optical density is measured thanks to Genesys 10S UV vis spectrometer Thermo Scientific at 600nm.

3.4.2. Analysis with cytometer

Sample is diluted with PBS to have approximately 0.025 of OD600 in an eppendorf tube. 1 μ l of green redox sensor and 2 μ l of PI is added (*BacLight™ RedoxSensor™ Green Vitality Kit Thermo Scientific*). Eppendorf are mixed and kept 10min protected from light. Then, fluorescence in FL1 and FL3 can be measured with the cytometer (BD biosciences, NJ USA).

3.4.3. Gas analysis

Gas in the column is analyzed by INNOVA -1316 A-3 Multi Gas Monitor (LumaSense Technologies). Each 4 seconds, the concentration in ppm and in percent of CO₂ and O₂ is measured.

3.4.4. Temperature, o₂ dissolved and ph

Temperature (pt100 Sartorius), o₂ dissolved (Hamilton Visiferm DO) and ph (Hamilton PH EasyFerm Plus PHI K8 200) are followed thanks to sondes placed in the reactor during all the culture.

3.4.5. HPLC

2ml of sample are centrifuged (Beckman Avanti J-25i)(8000rpm, 4°C and 5 minutes). Then, supernatant is conserved at -20°C. Before analyze, sample is thawed and filtered directly in a vial with a filter HPLC Chromafil® RC-45/15 MS.

The HPLC used is UPLC WatersAcquity Class H with the detector Détecteur RI (Acquity Class H).

Glycerol, acetoin, acid lactic and glucose is analyzed for samples of reactors with MSgg and sucrose concentration for Optimized medium.

For sucrose analyze, the external calibration is carried out with 7 concentrations: 0.002%, 0.01%, 0.02%, 0.1%, 0.2%, 1%, 2% prepared with a standard solution with 2% of sucrose (sigma, 057K00652, purity of 99,9).

For glycerol analyze, the standard solution is prepared with 2% of sucrose and 0.5% of each other compound (Table 2). After, this solution is diluted in 7 concentrations (Table 1).

Material and Method

Table 1: Concentration of glucose and other compounds of the calibration solution for MSgg analyze

Standard	Glucose (%)	Other compounds
STD1	0,002	0,0005
STD2	0,010	0,001
STD3	0,020	0,005
STD4	0,100	0,01
STD5	0,200	0,05
STD6	1,000	0,1
STD7	2,000	0,5

Table 2 : References of compounds used in external standard for MSgg analyze

Compounds	Label	Lot	Purity
Glucose	Sigma	108K0031	99,9
Acid acetic	Fluka	1387360	99,0
acid lactic lithium salt	Acros	A0277279	99,0
Acetoin	Merck	S7001864 611	99,0
Glycerol	Sigma	125K01532	99,0

Glycerol, glucose, acid acetic, acid lactic and acetoin are analyzed thanks to a UPLC WatersAcquity Class H with a column Aminex HPX87-H 300X 7.8 mm heated at 65°C. The technique used is the isocratic method with a mobile phase of 0.005M H₂SO₄ flowing at 0.6ml/min.

For sucrose, the column used for some samples is the CARBOSep CHO682 Pb and for the others Aminex HPX 87P. The method is the same but the mobile phase is only milliQ water heated at 80°C with a flow of 0.4ml/min for CARBOSep and 0.6ml/min for Aminex.

3.5. Reactors, different process parameters

10 reactors were carrying out during this master thesis. For all, some parameters were the same: recirculation flow of 44,5ml/min, preculture in Optimized medium, airflow of 0,1l/min and a ph of 6,95.

The two first reactors were exactly identical. The NIRS was switched on and a growing phase in reactor was done at 30°C during 3 hours but without column heating. One of the two was stopped after 25h of culture to see if a biofilm was present in column.

For the next reactor, parameters were exactly the same but the NIRS was turn off to verify the absence of light impact.

The fourth and the fifth reactors did not have a growth phase and the column was heated only for fifth.

For the sixth, a growth phase was carried out in column during 4h40 with air injection in column with 1liter of medium. The column was vertical and isolated but not heated. So, temperature decreased in reactor. To avoid these problems in another reactor, preculture was injected in column directly. And in sterilized conditions, the column was separated of the system and put in the room at 30°C horizontally without air injection during 6 hours. Sucrose injection was also made differently. Only 50ml of the 200ml at 150grsucrose/l was injected at the beginning in 1.3l of medium. The rest was injected in the reactor at a rate of 139 μ l/min to ensure metabolisms maintenance.

For following reactor medium was changed. The MSgg was used without a growth phase for the eighth, ninth and eleventh reactor. Preculture was in Optimized medium. Before the injection in reactor, cells were washed and the Optimized medium removed thanks to the centrifuge at 800rpm during 5minutes (Beckman Avanti J-25i). 100ml of MSgg were required to put cells in solution.

Table 3 : Summary table of reactors parameters

Batch number	Strains	Culture medium	Column heating	Growth phase before recirculation	Temperature
1	GA1	Optimized medium	no	yes, in reactor	30°C
2	GA1	Optimized medium	no	yes, in reactor	30°C
3	GA1	Optimized medium	no	yes, in reactor	30°C
4	GA1	Optimized medium	no	no	30°C
5	GA1	Optimized medium	yes	no	30°C
6	GA1	Optimized medium	yes	yes, in column vertically	30°C
7	GA1	Optimized medium	yes	yes, in column horizontally	30°C
8	GA1	MSgg	yes	no	30°C
9	GA1	MSgg	yes	no	30°C
10	<i>B. subtilis</i> 512	MSgg	yes	no	37°C

For all: recirculation flow of 44,5ml/min; preculture in Optimized medium; airflow of 0,1l/min; ph 6,95

3.6. Quantification of cells on packings

Each packing is covered by distilled water in a 1L berlin. Berlins are placed in a sonicator (Branson 3200) during 15minutes. Water is recovered and then, packings are washed 2 times with distilled water to remove all of the cellular materials. After, this water is centrifuged (with the sorval RC12bp) at 8000rpm during 45 minutes. Cells are recovered and diluted in 100ml of distilled water. 50 μ l are taken to carry out cells quantification thanks to the cytometer (BD biosciences, NJ USA). The

remainder stays one night in a stove (memmert UN 55) during one night at 105°C. Then, berlins are weighed to have the dry matter for each packing.

4. Determination of the cells path in column

4.1. Experimental method with tracer

The column is assembled with the same configuration than in the reactor (see: Reactor assembly and disassembly- pg 22) with same pumps and silicon pipes. 20 μ l of red tracer (1010beats/ml, 1 μ m, life technologies, fluorosphere, polystyrene) are injected at the top entrance of the column. Each 3 seconds, 1.5ml is taken at the bottom of the column. Then, the quantity of beats is measured thanks to the cytometer (BD biosciences, NJ USA). All data is processed with Matlab 7.5.0 R2007b.

This studied was carried out 3 times in reactor with and without air injection (0.1ml/min) in a column previously moistened and only one time in a column not humidify.

4.2. Compartments model

The cells way in column was estimate thanks to a determinist model on Matlab 7.5.0 R2007b. A previous version (Nguyen et al., 2014) was modified for the column design.

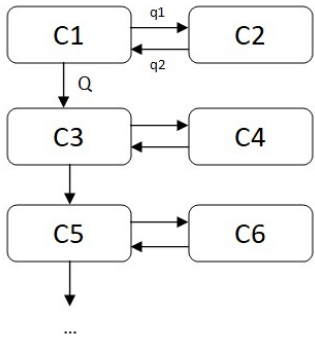


Figure 13 : diagram of compartments and flux in column for the elaboration of determinist model

This model is based on an exchange of flux between lateral and vertical compartments such as Q, q1 and q2. Different value of debit is given to these fluxes and are proportional to the debit (m^3/s) of the pump used for the recirculation (44,7ml/min, so $7,45 \times 10^{-6} m^3/s$) (see 3.5-Reactors, different process parameters-pg24). Thanks to these values, a matrice of flux is created on Matlab where each line equals 0 and represents what goes in and out the compartment.

Material and Method

Thanks to this matrice, the way used by cells can be estimated during time. For the comparison with data collected with the tracer, the observation point is placed at the last compartment and all results are divided by the maximum value in order to make data proportional to 1.

Some tests were done with equal and different values of q1 and q2. Results were quite similar for numbers of compartments but compare to data collected with tracer, the distribution time of cells release was more similar to tracer with q1 and q2 different.

The entire code in matlab for this model is in annex (Annex 2: Code on Matlab for compartments model (part determinist)-pg84). This code is equilibrate (each line equals 0) for q1 and q2 with different and equal value. Moreover, during its realization, another flow called q was studied between compartments with a pair number (between C2 and C4, C4 and C6,...) but its value was fixed at 0 for the final result.

5. Toxins test

One Petri dish is inoculated with GA1. Then, it is incubated at 30°C (Binder). After one night, 100ml of Optimized medium in a 1-liter flask are inoculated with a colony taken in the Petri dish. The flask is incubated at 37°C at 160rpm one night (Gallenkamp Orbital incubator). Then, OD 600 is measured (Genesys 10S UV vis spectrometer Thermo Scientific at 600nm). A specific volume is taken (to have 3, 1.5 or 0.1 of OD600 by ml in 10ml) and put in 6 falcons of 15ml. Cells are washed once with a centrifuge (Beckman Avanti J-25i) at a speed of 7,884rpm during 5minutes at 4°C).

In erlenmeyers of 100ml, 5ml of the fresh Optimized medium are added to 5ml of sterile distilled water or to 5ml of the medium sampled in the reactor after 28h of cell culture.

Cells prepared with the same OD 600 are injected in erlenmeyers. After, Erlenmeyers are put at 30°C and 120rpm.

Each hour, each sample is analyzed with the UV spectrometer and the cytometer to see the number of cells and their activities in FL1 and FL3. A part of samples is diluted with PBS to have approximately 0.025 of OD600 in an eppendorf tube. 1 μ l of redox sensor and 2 μ l of PI is added to samples (*BacLight™ RedoxSensor™ Green Vitality Kit Thermo Scientific*). Eppendorf are mixed and kept 10min protected from light. Then, fluorescence in FL1 and FL3 can be measured with the cytometer (BD biosciences, NJ USA).

6. Test of comparison between Msgg and Optimized medium

One Petri dish is inoculated with GA1. Then, it is incubated at 30°C (Binder). After one night, 100ml of Optimized medium in a 1-liter flask are inoculated with a colony taken in the Petri dish. The flask is incubated at 30°C at 160rpm one night (Gallenkamp Orbital incubator).

OD600 of the preculture is measured (Genesys 10S UV vis spectrometer Thermo Scientific at 600nm). A volume of the preculture is taken to prepare a solution with 0.15 of D600 by ml. Cells of preculture are washed once with a centrifuge (Beckman Avanti J-25i) (speed of 7,884rpm during 5minutes at 4°C). The Msgg or the Optimized medium is added to cells. Then, 2ml of the two cultures is put in sterile tissue culture plate (24wells, VWR). The sterile plate is incubated at 30°C during 24h, 48h, and 72h (Binder).

If there is a biofilm in plate, biofilm is removed and put in 2ml of PBS. Afterwards, cells are separated thanks to the sonicator (Bandelin sonopuls electronic) with two cycles of 12sec with 9 cycles separated by 2 sec. To avoid heating them, they are kept in ice during this stage. If cells do not form a biofilm, this stage is not useful but sonication can be to avoid cells aggregate.

After, a part of samples is diluted with PBS to have approximately 0.025 of OD600 in an eppendorf tube. 1 μ l of redox sensor and 2 μ l of PI is added to samples (*BacLight™ RedoxSensor™ Green Vitality Kit Thermo Scientific*). Eppendorf are mixed and kept 10min protected from light. Then, fluorescence in FL1 and FL3 can be measured with the cytometer (BD biosciences, NJ USA).

Results and discussion

1. Population instabilities in biofilm reactor with external packed bed

In the biofilm reactor with a tower (see 7.2- Scalable biofilm reactor design-pg 17), difficulties were encountered to ensure cells growth and survival. In fact, cells multiplication in reactor is followed by a cellular lysis and the sporulation of the population. That leads to the absence of biofilm formation in column.

Several parameters of the reactor were modified to enhance cells and biofilm growth as column heating, a first contact phase in column without recirculation, progressive sucrose feeding, a change of medium... (See 3.4.5-Reactors, different process parameters-pg 23). For all of these different reactors, only 3 distinct behaviors were observed, two without biofilm formation and one with a biofilm development in column.

For all reactors, gaseous CO₂ emission was measured in column and dissolved O₂ consumption (see 3.4.3-Gas analysis- pg 23) and optical density of planktonic cells (see 3.4.1-Optical density- pg 23) in reactor. And for some of them, cells activity was observed by flow cytometry fingerprinting with RSG and PI (see 3.4.2 - Analysis with cytometer – pg 23). RSG represented by the axis FL1 on cytometer fingerprint gives information on the electron chain of the cells membrane and PI represented by the axis FL3 on its permeability.

1.1. Cells behaviors without biofilm formation

First reactors were carried out with Optimized medium. With it, no biofilm grows and a lack of repeatability was noticed. For some of them, a high growth phase was observed and for the others, only a low one.

1.1.1. Reactor exhibiting strong cells growth

In some reactors, after exponential growth, cells concentration drops without biofilm formation and is quickly followed by sporulation (Figure 14).

Thanks to the Figure 15, we can see that, at the beginning of the culture, optical density increases sharply and reaches a value around 9. Thanks to fingerprints obtain with the cytometer, the presence of a large number of active cells is confirmed. In fact, on fingerprint, active cells appear

Results and discussion

above 10^4 in FL1. And in exponential growth, the majority of the cells has their activity above 10^4 and therefore, are active.

But then, after 20h of culture, the number of cells drop in medium. This stage could have been an immobilization on packings but, the column was opened during this phase and no biofilm was noticed (see 3.5-Reactors, different process parameters- pg24).

Moreover, this cells disappearance continues and after 30h of culture, oxygen consumption stops (Figure 14). Moreover, cells activity has changed on cytometer fingerprints. The majority of cells has their activity under 10^4 in FL3 (PI) and in FL1 (RSG) (Figure 15). Unluckily, this spot corresponds to the activity of spores. Therefore, cells population in reactor is sporulating.

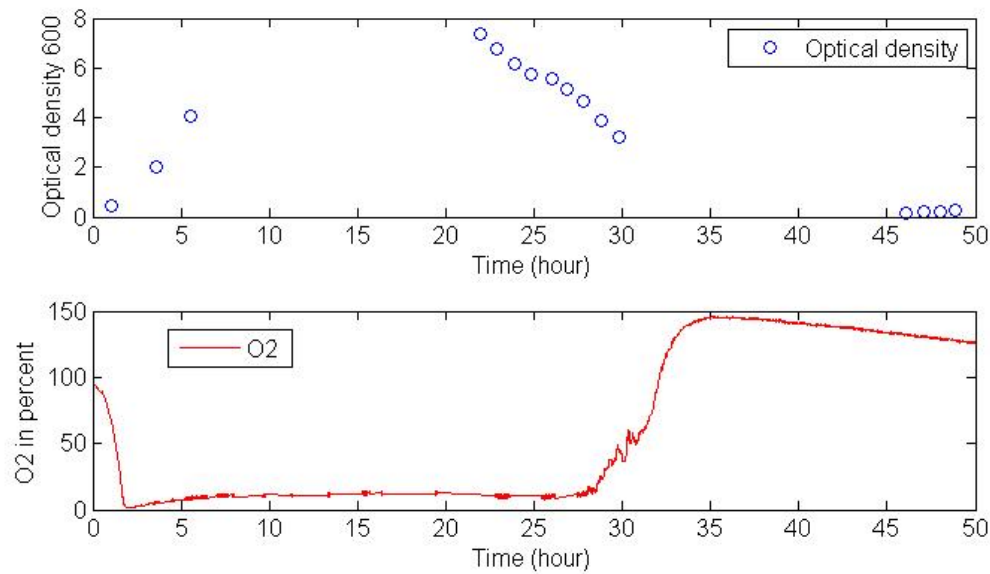


Figure 14 : Evolution of optical density (A) and O2 consumption measured in reactor (red) (B) in reactor with Optimized medium and high cell growth.

Results and discussion

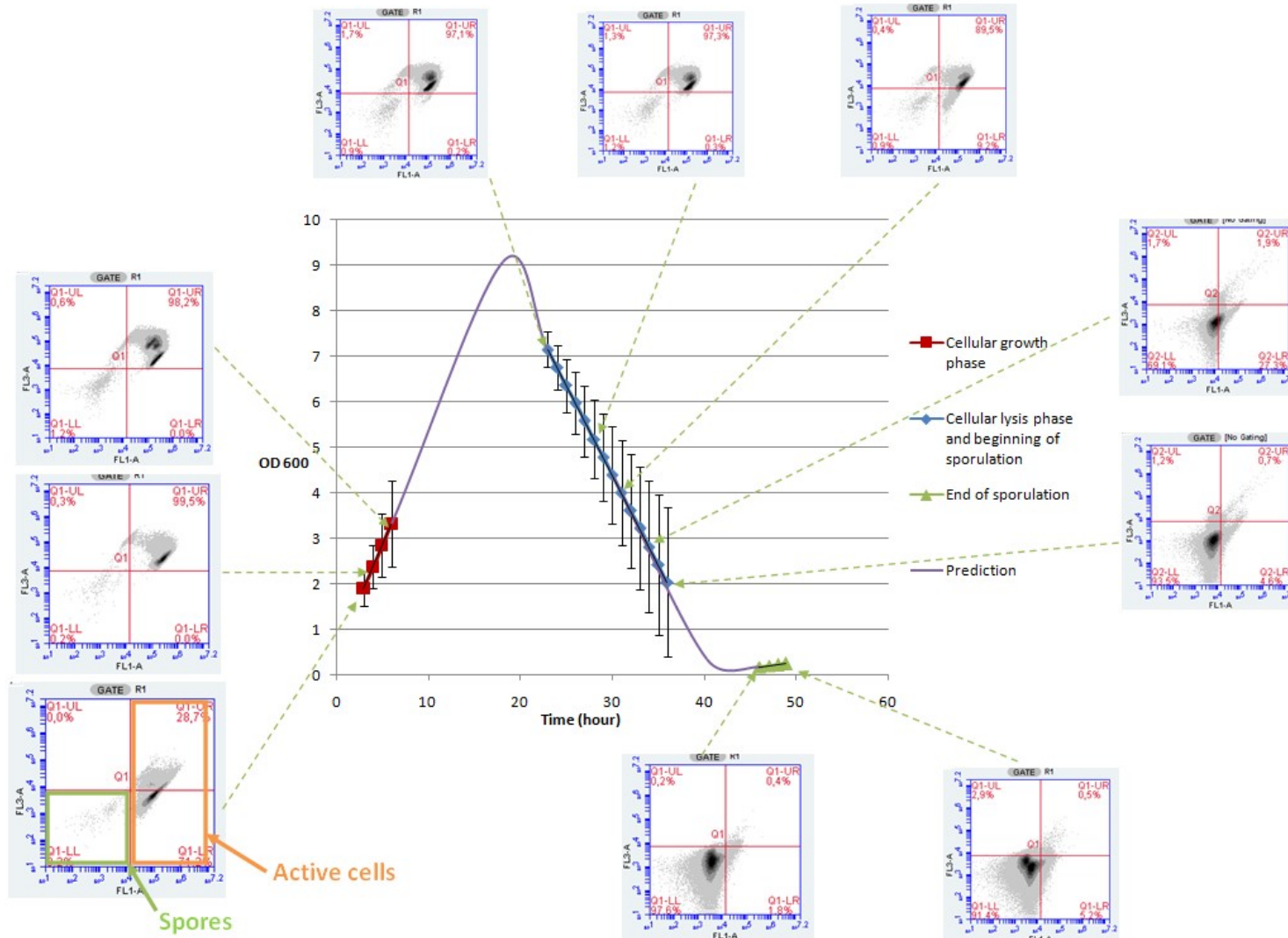


Figure 15 : Summary diagram of reactors with Optimized medium and rapid sucrose consumption. 3 phases of cells culture are noticed: cellular growth (red), lysis phase (blue) and end of sporulation (green). Not studied culture parts are predicted by calculation and appear in purple. This diagram is made thanks to 3 repetitions. Standard deviation for each sample is noted. Planktonic cells fingerprint gives information about cells activity. Spores are cells with an activity under 10^4 in FL1-A. The others ones are active cells.

Results and discussion

This phenomenon observed in the biofilm reactor seems to be a cellular lysis followed by sporulation.

A possible origin of that is the programmed cell death (see 4.6-Programmed cells death- pg 11). During this cells behavior, Sdp and Skf proteins are produced by cells under stress conditions to ensure their survival. These toxins lead to cells lysis and it is the stage before sporulation.

This mechanism is really similar to the phenomenon observed in the biofilm reactor. Moreover, a part of reactor content was taken out and put in culture protected from reactor stresses (30°C, without light, O₂). And the same optical density drop was observed (Figure 16).

Upon induction, cell death is independent of the biofilm reactor. Something in medium or related to cells generates this lysis.

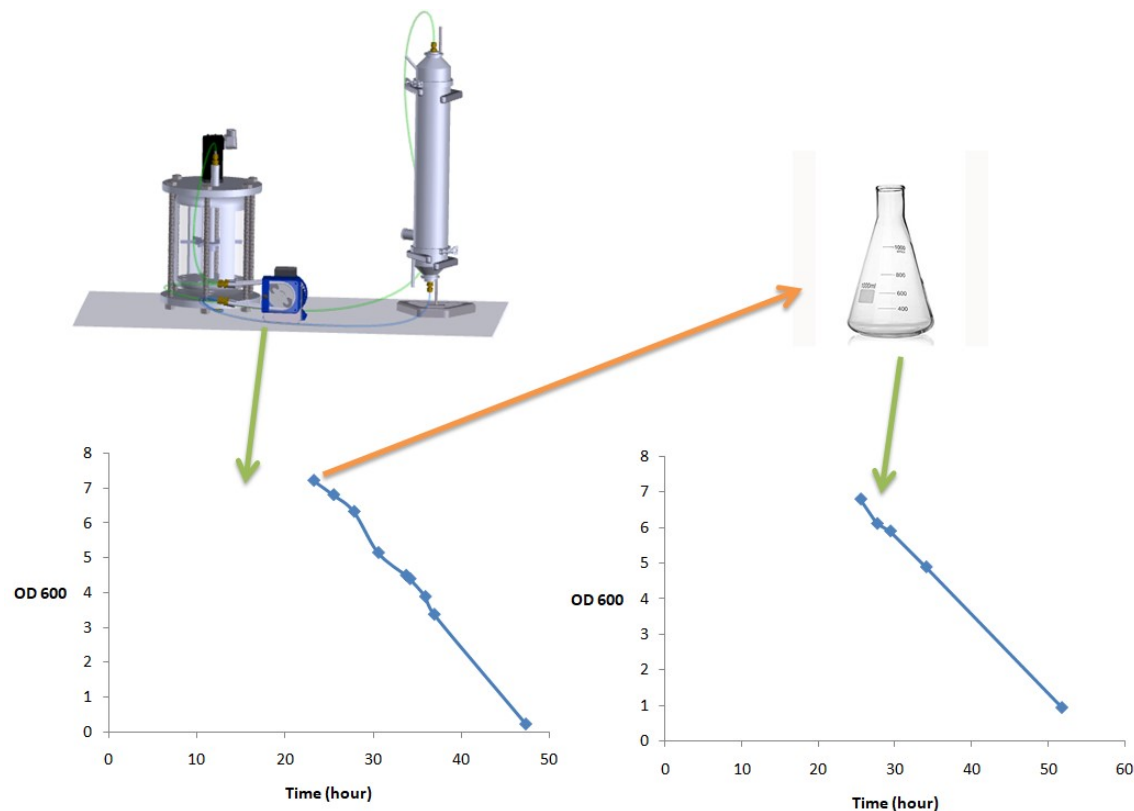


Figure 16: Decrease of optical density (600nm) in reactor (left) and out of reactor (right) with Optimized medium and high growth rate (Adapted with Andrew Zicler works). A sample taken in the reactor was put in culture out of it, in the room at 30°C with agitation (source picture of Erlenmeyer: Amazon.ca).

But, to highlight toxins production in reactor, some tests were done to compare growth of fresh culture growing in medium from reactor and in fresh medium (see 5-Toxins test-pg 27). And a lag phase was noticed but no cells death (see results in Annex 3: Comparison test between fresh culture growing in fresh Optimized medium and in medium take out of the reactor-pg85). It is then difficult

to conclude their presence or not. Toxins could be denatured during its conservation, fresh culture could be insensible to them depending on its SpoOA-P level (see 4.6-Programmed cells death-pg11) or cells from reactor could produce it and assimilate it rapidly.

However, by this method, only the medium was studied but cells present during the lysis phase could also be considered. In order to see their influence and to understand the phenomenon, cells can be taken out of the reactor and put in culture in fresh medium to see if the lysis continues and if then, once triggered, lysis is independent of medium and so only related to cells.

1.1.2. Reactor exhibiting low cells growth

This rapid and high cell growth in first reactors did not seem to be favorable for biofilm formation. It seemed to promote planktonic cell multiplication to the detriment of biofilm development. Following that, for some other reactors, parameters were modified in order to limit cells growth and enhance cells adhesion on packings (with no growth phase in reactors but in column, progressive sucrose addition, control of column temperature and recirculation directly) (see 3.5-Reactors, different process parameters- pg24). Unluckily, it was not enough; another behavior of cellular lysis without matrix formation was noticed.

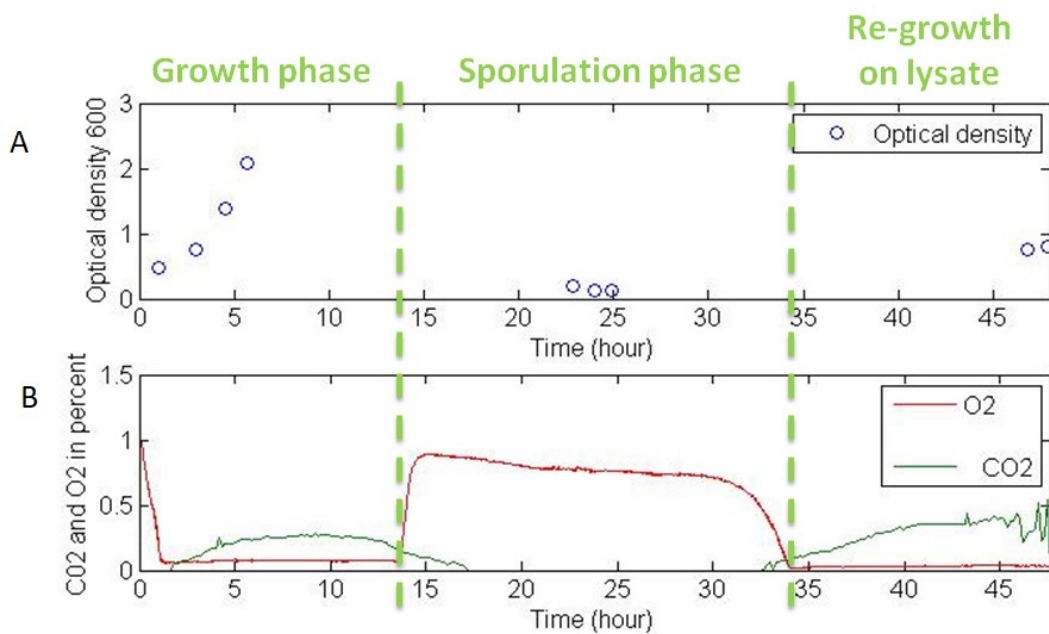


Figure 17 : Evolution of optical density (A) and CO₂ emission in column (green) with O₂ consumption measured in reactor (red) (B) in reactor with Optimized medium and low cell growth.

But, in this case, optical density rises at the beginning of the culture but does not exceed 3. And after 15h, CO₂ emission and O₂ consumption drop (Figure 17). The cells number goes down and

population activity changes. The proportion of spores increases but a little part of the cells continues to be active and to consume sucrose but in less quantity. And then, after 35 hours of culture, cells activity and multiplication restart.

The major difference with the previous case is the comeback of active cells at the end of the culture and the low cell growth. Despite this, no biofilm grew and a phenomenon of lysis was also observed.

1.1.3. Possible origin of lysis phenomenon

A cell lysis was observed each time in reactor with Optimized medium. And once triggered, the phenomenon seems to be independent of the reactor design.

Medium can impact this lysis behavior. In fact, programmed cell death is generally caused by a weak accessibility to nutriments as nutrient deprivation, oxygen limitation... (See 4.6- Programmed cells death- pg 11). Optimized medium may not be optimal for cells and air injection only in column may not be enough (see 7.2- Scalable biofilm reactor design-pg 17).

Otherwise, *B. amyloliquefaciens* GA1 used in the culture is a natural isolates and then, less adapted to reactor conditions (Touré et al., 2004). This cells death phenomenon can be related to difficulties of GA1 to adapt to reactor. Or reactor conditions may not be adapted to GA1 growth.

1.2. Cells behavior with matrix formation

Ultimately, culture medium was changed. Optimized medium was replaced by MSgg which is known to enhance biofilm formation. And with it, a biofilm was obtained and a radically different behavior was observed: no lysis was recorded and at the end, a biofilms were present on packings.

However, planktonic cells concentration stays high. Only a little part of the cells holds packings. And when CO₂ increases in column, optical density goes up also. It seems that the rise of CO₂ is also related to planktonic cells growth (Figure 18).

Moreover, biofilms is unstable. A beginning of disintegration is noted after 40 hours of culture. Indeed, optical density and numbers of cells increase while oxygen consumption and CO₂ emission drops (Annex 4: Evolution of events number of *B. amyloliquefaciens* by µl and cells activity measured with a cytometer in FL1 and FL3 in biofilm reactor with MSgg -pg88).

Results and discussion

Otherwise, also thanks to O₂ and CO₂ measures, we can see that cells needed 7h to adapt to the reactor. In fact, preculture was done in Optimized medium to keep a maximum of similar conditions between reactors. This change of medium causes an important lag phase.

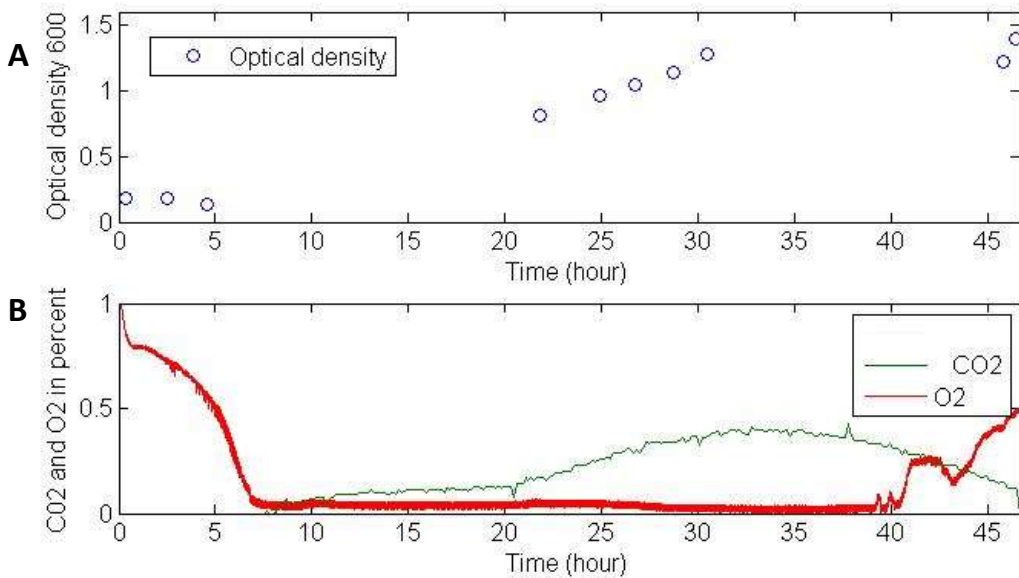


Figure 18 : Evolution of optical density (A) and CO₂ emission in column (green) with O₂ consumption measured in reactor (red) (B) in reactor with MSgg

1.3. Causes of cells and biofilm instabilities

On the one hand, a lysis is observed with Optimized medium. And on the other hand, a biofilm is obtained with MSgg but is not stable and is accompanied by an important planktonic phase. Cells and biofilm growth does not seem to be optimal in scalable biofilm reactor.

Reasons of these population instabilities can be multiple. Firstly, in view of results, medium seems to have an important influence on this phenomenon and can promote the programmed cell death.

Furthermore, characteristics of the strain can also foster the phenomenon of sporulation. *Bacillus amyloliquefaciens* GA1 used in reactors (see 3.5-Reactors, different process parameters- pg 24) is an undomesticated isolate and as a result, more difficult to grow in reactor by comparison with other strains.

And thirdly, the design of the scalable reactor does not seem to be innocent in this phenomenon. It can clearly influence cells and biofilm development by the creation of a large range of stresses.

These three distinct potential sources of instabilities were studied in order to understand what destabilizes cells and biofilm development.

2. Influence of culture medium

After different biofilm reactor tests with Optimized medium, the effectiveness of this medium to produce a biofilm was questioned. In fact, this medium was selected for its efficiency to produce lipopeptides and not promote biofilm formation (Akpa et al., 2001; Jacques et al., 1999). Therefore, the medium was replaced by another known to foster biofilm formation: MSgg (Shemesh & Chai, 2013). And finally, a biofilm grew on packings.

To compare abilities of both medium to promote biofilm formation, a culture in microplates for 3 days was performed. And the results are unequivocal: cells growing in MSgg showed a pellicle after only 24h and a structured and robust biofilm after 48h and no matrix formation was noted in Optimized medium (Figure 19).

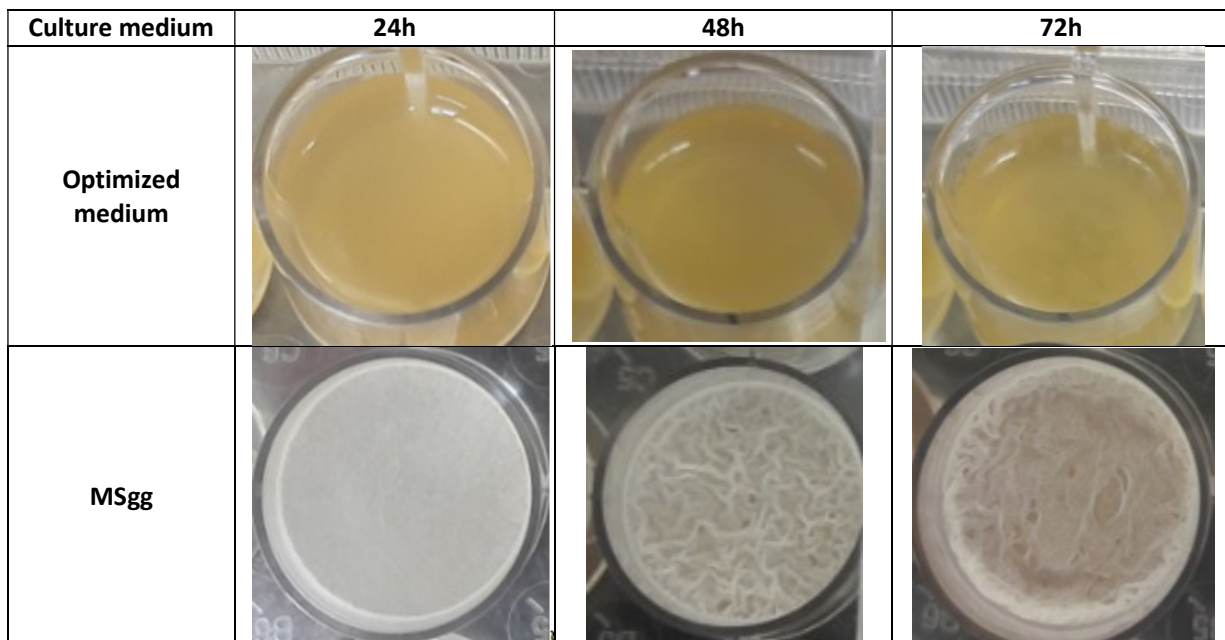


Figure 19: Biofilm formation of GA1 culture in microplates after 24h, 48h, 72h at 30°C in Optimized medium (above) and in MSgg (below). A biofilm is observed with MSgg and nothing in Optimized medium.

MSgg and Optimized medium compositions are completely different (see 1-Medium preparation- pg21). The major carbon source of Optimized medium is sucrose present in large amount (20g/L), and accompanied by yeast extract (7g/L) and casein peptone (30g/L). It is a rich medium in contrast to MSgg containing only 5g/L of glycerol and 5g/L of glutamic acid.

A first, rich medium does not seem to promote biofilm formation (Morikawa, 2006; Stanley, Britton, Grossman, & Lazazzera, 2003; Stanley & Lazazzera, 2004; W. Zhang et al., 2014). Cells require

Results and discussion

a decrease in carbon source to trigger biofilm formation. In exponential growth, nutrients concentration is high, cells multiply and it is only at the beginning of carbon source deprivation in stationary phase that Spo0A is phosphorylated and the expression of genes involved in matrix formation begins (Kearns et al., 2004; Morikawa, 2006; J D Quisel, Burkholder, & Grossman, 2001; W. Zhang et al., 2014).

Glucose and fructose have been studied for their repression effect on biofilm development (Morikawa, 2006; Stanley et al., 2003). And it was demonstrated that they activate a repressor of a large number of genes: CcpA (Henkin, 1996). During this growth phase, sugar curbs matrix formation via the activation of transcriptional factor CcpA (catabolite control protein) (Morikawa, 2006; Stanley et al., 2003). This way, high carbon source concentration inhibits biofilm formation which can only begin when sugar concentration has decreased.

But once sugar concentration has dropped, by-products of glucose metabolism enhance biofilm formation. It is the case of the acetoin. Acetoin is produced in case of an excess of sugar concentration in culture medium (ex: sucrose fructose, glucose, glycerol, xylose and ribose) (T. Chen, Liu, Fu, Zhang, & Tang, 2013; Stanley et al., 2003; Tian, Xu, et al., 2016; Tian, Fan, Liu, Zhao, & Chen, 2016; Y. Zhang, Li, Liu, & Wu, 2013). During sugar metabolism, cells synthesize acetoin via the condensation of 2 molecules of pyruvates and excrete its extracellular medium (Renna, Najimudin, Winik, & Zahler, 1993; Speck* A N, 1973). And when sugar disappears, in stationary phase, acetoin is reabsorbed and metabolized. This carbon source is used more slowly than sugar and only for metabolism maintenance, not for cellular multiplication (Silbersack et al., 2006). By an unknown mechanism, this metabolism triggers phosphorylation of Spo0A and thereby, enhances biofilm formation and sporulation (4.4.3-Matrix formation implications-pg9) (John D Quisel, Burkholder, & Grossman, 2001; Stanley et al., 2003). A higher stimulation of biofilm formation and sporulation have been noticed in presence of acetoin (John D Quisel et al., 2001; Stanley et al., 2003).

Acetoin production is directly related to carbon source concentration and is an indicator of the rapid consumption of sugar (Sharma & Noronha, 2014; Stanley et al., 2003; Tian, Fan, et al., 2016). In a reactor carried out with Optimized medium, its concentration amounts to 9,6 g/L (Figure 20). This high production seems logical when we see the sucrose concentration in Optimized medium (see 1-Medium preparation- pg21). However, in reactor, acetoin is poorly reabsorbed. The low residual concentration of sucrose and oxygen limitation impede its assimilation (Speck* A N, 1973). And its metabolism is required to trigger Spo0A phosphorylation. Therefore, acetoin effects were weak: cells died before its assimilation. So, enough carbon source was present in medium to ensure cells survival and positive effect of acetoin on biofilm development did not take place.

Results and discussion

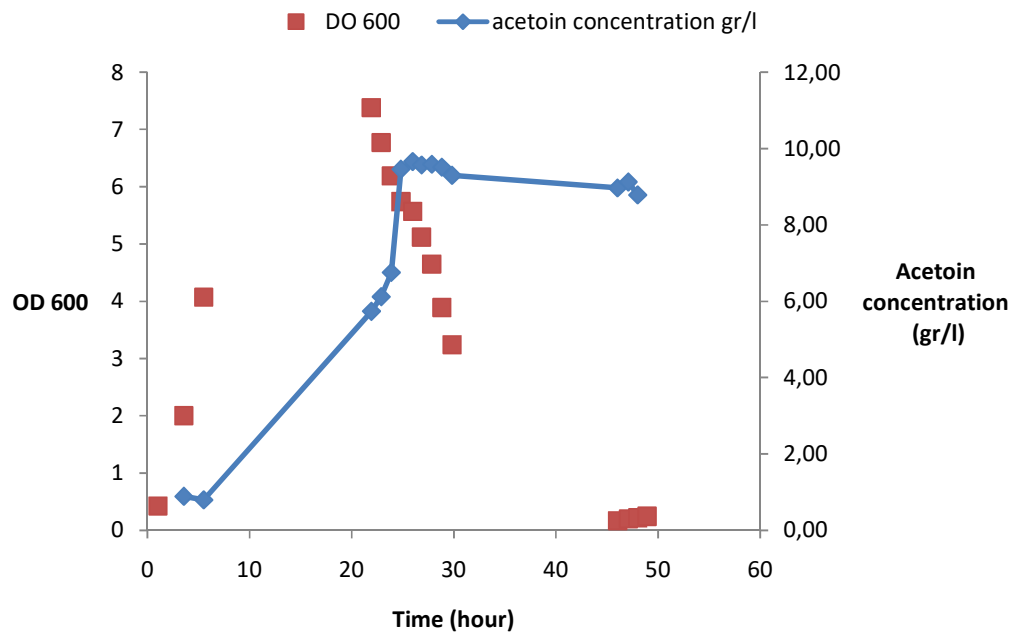


Figure 20 : Acetoin concentration (blue) in Optimized medium with optical density in reactor (red)

Otherwise, the mix of Mn^{2+} and glycerol present in MSgg has shown interesting effectiveness of matrix development stimulation (Shemesh & Chai, 2013). This mix promotes the activation of KinD, a kinase that phosphorylates SpoOA that encode genes involved in matrix formation (see 4.4-SpoOA-pg7).

Nevertheless, biofilms were not stable over time in MSgg. Their deterioration began after 72h of culture in microplates.

Unluckily, the goal of this reactor is the lipopeptides production. And, Optimized medium was elaborate to enhance this production (Akpa et al., 2001; Jacques et al., 1999). Moreover, cells multiply less in MSgg than in Optimized medium. Number of cells in microplates is 6 times higher in Optimized medium than with MSgg (see Annex 5: Evolution of the numbers of events by μl of *B. amyloliquefaciens* growing in microplates in MSgg (red) and in Optimized medium (blue)-pg89). And the number of cells in the biofilm can impact lipopeptides concentration found in medium. No analysis was carried out on lipopeptides concentration but it seems really probable that their production is higher in Optimized medium. But an analysis is required.

3. Natural strains versus domesticated/engineered strains

The strain commonly used in our reactor was *Bacillus amyloliquefaciens* GA1. It is interesting for its abilities to produce exopolysaccharides and lipopeptides. It was discovered on strawberries and therefore, is a natural isolate (see 2-Bacillus amyloliquefaciens, strain characteristics-pg1. However, undomesticated strains are less easy to manipulate in laboratory than the conventional laboratory strains *B. subtilis* 168. Unfortunately, because of mutations appeared during its domestication, this strain has lost several abilities such as synthesizing surfactin and exopolysaccharides and then, shaping a robust biofilm (Branda, Gonzá Lez-Pastor, Ben-Yehuda, Losick, & Kolter, n.d.; McLoon, Guttenplan, Kearns, Kolter, & Losick, 2011; Nye, Schroeder, Kearns, & Simmons, 2017).

However, some engineered strains of *B. subtilis* 168 have retrieved these competences. It is the case of *B. subtilis* 512. This strain was obtained after 3 mutations. One is an activation of a gene involved in exopolysaccharides synthesis called, *epsC*. Another one was the activation of *sfp*, which is required for surfactin production; and the last one is the deletion of *sepF*. SepF is a protein that recruits FtsZ, a protein involved in the divisome of *B. subtilis* (Hamoen, Meile, de Jong, Noirot, & Errington, 2006). FtsZ forms a ring on the future position of the septum and its deletion generates a cells division defect. This phenotype allows the cells filamentation which is the stage before biofilm formation. Thanks to these 3 mutations, *B. subtilis* 512 is able to form a robust biofilm and is adapted to laboratory conditions. That makes this strain attractive for this work in order to compare its ability to develop a biofilm in the reactor to *B. amyloliquefaciens* GA1. Two reactors with MSgg were carried out, one with *B. amyloliquefaciens* GA1 and the other with *B. subtilis* 512. Their CO₂ emission and optical density were analyzed in order to collect information on their biofilm development.

CO₂ emission analysis in column gives us information about cells adhesion on packings, biofilm and cells growth and cells detachment (Figure 21). CO₂ emission begins later for *B. subtilis* 512. A conceivable reason is the adaptation period. Indeed, preculture of *B. subtilis* 512 and *B. amyloliquefaciens* GA1 is carried out in Optimized medium. Once in the reactor with Msgg, they need a variable adaptation period. This phase can be longer for *B. subtilis* 512 than for *B. amyloliquefaciens* GA1. But it is also possible that cells catch packing later and then, before that, CO₂ emission is too low to be measured.

Two point of view of the colonization by *Bacillus amyloliquefaciens* GA1 can be done. In one hand, the apparition of CO₂ in column after 7 hours of culture can be related to the recovery of cells activity after the lag phase followed by the packing colonization after 20hours. In fact, O₂ consumption reaches is lower value after 7 hours (Figure 18). But it is also possible that colonization

Results and discussion

begins after 7 hours and then, the slow increase of CO₂ after 20h of culture is related to biofilm growth. And CO₂ emission before 7h can be too weak to be measured. It is difficult to know which possibility is the right. Moreover, we can notice that CO₂ emission is also related to the growth of planktonic cells. Only a little part of cells proportional to culture density hangs on packing. Indeed, when CO₂ rises in column, optical density increases also.

Otherwise, *B. subtilis* 512 is a filamentous strain. The fast CO₂ soaring observed after 15h of culture could be related to this characteristic. In fact, cells can catch packings when cells have filament. Filaments have a bigger size and then, can be more retained on packings. Or cells immobilized on packing can filament. It can explain this fast augmentation of CO₂ emission in column with this low optical density of planktonic cells.

In reactor with *B. subtilis* 512, CO₂ emission goes up higher in column than *Bacillus amyloliquefaciens* GA1. With the low planktonic cells concentration at this emission peak, we can think that more *B. subtilis* 512 are retained in column and then, conditions are more favorable for the biofilm formation. Nevertheless, a part of the cells is not held permanently, that can explain this fast rapid decline following the CO₂ peak.

Moreover, cells adhesion durability is not promoted with the utilization of *B. subtilis* 512. In both cases, a release of cells is noted. CO₂ emission in column decreases continuously while the optical density of planktonic cells goes up. In different test carried out with MSgg, biofilm deterioration was also observed relatively quickly.

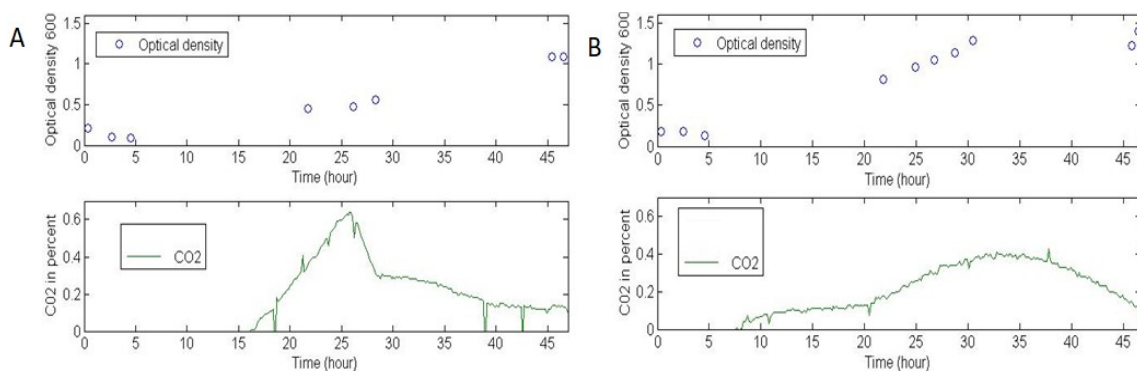


Figure 21: Evolution of optical density 600 (above) and CO₂ production (below) for *B. subtilis* 512 (A) and GA1 (B)

B. subtilis 512 seems not really enhance biofilm development. However, it was not used with Optimized medium. Therefore, we do not know if this strain is more stable than *B. amyloliquefaciens* GA1 in conditions that lead to cells death. A reactor can be carried out with *B. subtilis* 512 and optimized medium to see if the same behavior of lysis is observed or if is specific of this strain.

However, it is important to note that *B. subtilis* 512 require 37°C for its growth. So, temperature differs between reactors with *B. subtilis* 512 and *B. amyloliquefaciens* GA1. It can affect their growth.

4. Instabilities generated by the biofilm reactor design

The biofilm reactor can have an important impact on this phenomenon of lysis, on cells adhesion and biofilm formation and on biofilm disintegration. Its design may not enhance cells immobilization on packings as for example with the airflow injection in column; and therefore, leads to a continuous cells circulation in the different parts of the reactor (the column, the 2L tank and silicon pipes) (7.2-Scalable biofilm reactor design-pg 17). But, all of these components of the reactor generate a lot of different environmental surroundings with their specific stresses and then, can destabilize cells. Therefore, its influence is studied in this part.

4.1. Gas-liquid dispersion in column

In order to understand why no biofilm was formed in the biofilm reactor, an analysis of cells retention in column was conducted. The time required for cells release was measured thanks to a tracer (see 4-Determination of the cells path in column-pg 26). And with the repartition of cells output and a compartment model, the number of interactions between cells and packings was estimated.

In fact, the compartment model gives us information about the number of compartments where cells can go and the portion of the flow going to this compartment. Thanks to this precious information, we can estimate the way used by the cells and their different time of retention in column. These analyses were done for 3 cases: in a column previously moistened with and without air injection and in a column without humidification.

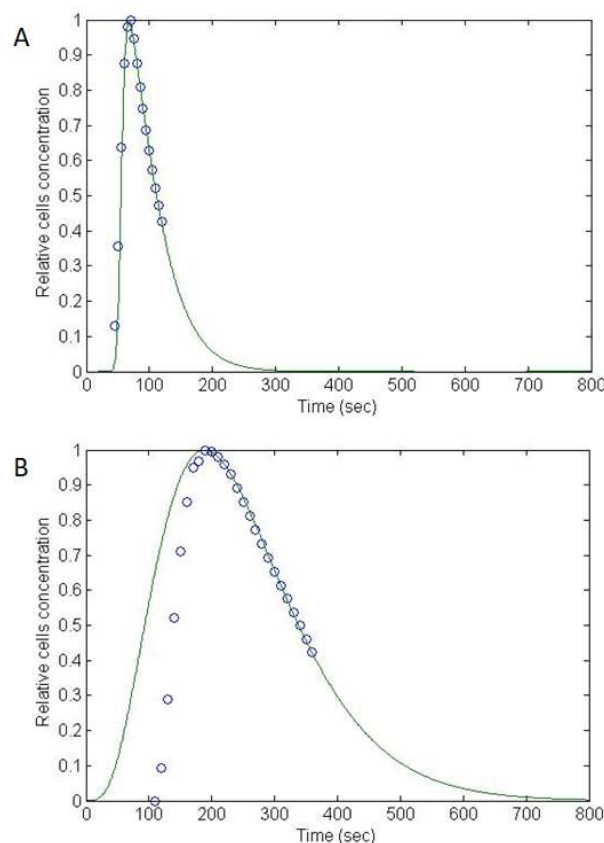


Figure 22: Mean distribution of tracers release measured at the bottom of the column over time for 3 repetitions (blue) in wet column, A: in absence of oxygen injection, B: in presence of oxygen (0.1L/min). The green line is obtained thanks to the determinist model and is adjusted to the tracers exit.

Results and discussion

Flow exchange and number of compartments were determined by the adjustment of their values in order to fit with the distribution of tracer release. However, we have no experimental data on flow exchanges as basis for their studies. Therefore, there were estimates. But, different method can be used to determine it. As explain above (4.2-Compartments model-pg 26), different ways were investigated by example with different values of flows between lateral compartment or the introduction of another downstream... And one method was chosen. But, all gives different results of flow values and number of compartments. By example, for the case of air injection in column, number of compartments varies from 7 to 12. Then, no precise value can be given with certitude to flow exchange and numbers of compartments but all results are enough similar to allow the comparison between the different cases studied here.

All these analyses were done in a column previously moistened with and without air injection. In fact, airflow can influence cells retention and liquid dispersion and then, impacts cells adhesion and distribution on packing. Indeed, the presence of airflow in column increases the time required for cells release and then, their retention. In fact, in absence of air injection, cells need 45 to 300 seconds to go out of column and 75% of cells are out after 95 seconds (Figure 23). Otherwise, in case of air injection, 110 to 750 seconds are required for the output of cells and 280 seconds are needed for 75% of cells. Airflow curbs cells output and so helps for their retention.

The number of interaction also changes with airflow. In case of air injection, the majority of cells goes in lateral compartments (high liquid flow part) but in a lower number of times (less compartments). Conversely, without air, there are a lot of compartments but less participation at the same number of them (weak liquid flow part). In a technical view, without air, it seemed that a lot of cells are not retained in lateral compartments and when it is the case, they are not stopped at same localities. And with air injection, large quantity of cells is curbed at the same spots in the column, which are not numerous. In absence of air injection, lateral compartment could be related to interaction or retention on packings because it is the only source which slows down liquid flow. But, in case of air injection, lateral compartment can correspond to a curbing by airflow and by packings.

It is also important to note that the column humidity influences a lot cells release (Figure 23). Indeed, when column is not moistened and without air injection before the analysis with tracer, the number of compartments is high and very few cells go to each compartment compare to wet column. Then, in dry conditions in column, some cells have a high retention, but the majority of the others is not held and is rapidly released. That looks like the preferential way. When packings are dry, the majority of the liquid goes in the same direction and only some particles are strongly retained.

Results and discussion

This observation is interesting in order to understand what happens in column when airflow is present. In fact, next to the air inlet, it seems probable that humidity is lower than next to liquid entrance. Therefore, air injection could generate a gradient of humidity in column. Distribution of cells release in wet columns and in dry ones can be handsets in order to give an idea of the way used by cells in a wet column with air injection. Thanks to a comparison between them, we can think that preferential way appears next to the air inlet. Cells may pass quicker the bottom of the column than the top. Therefore, cells retention could be lower on packings placed near air inlet (bottom of the column). Moreover, if some “dry” and “wet” area appeared in column, liquid could pass in humid zone than dry. These elements could give information about possible position of cells retention in the column.

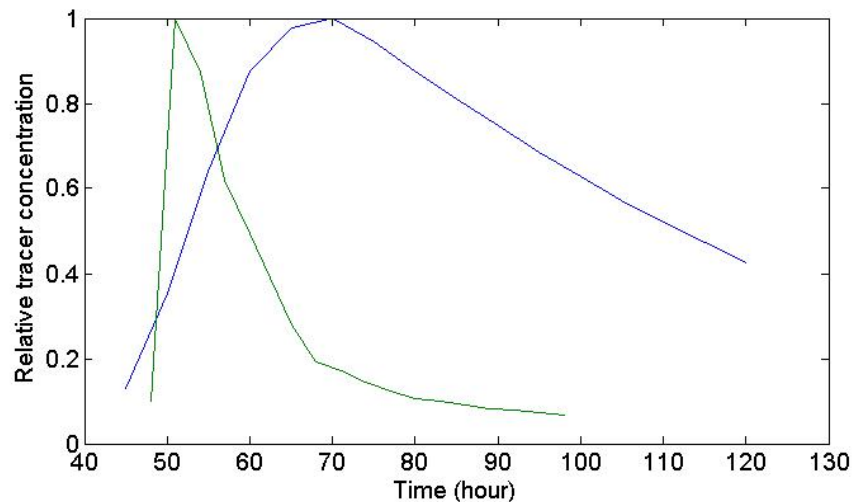


Figure 23 : Distribution of tracers release measured at the bottom of the column over time without air injection for a humid column (blue) and for a dry column (green)

Airflow modifies and curbs liquid flow paths. It seems probable that air injection impedes normal liquid flow by forcing it to use some define way in packings but also to help to cells retention by curbing liquid flow.

4.2. Packings colonization and biofilm instability with MSgg

Packings colonization also gives information about this influence of air injection. In reactor with MSgg and *B. subtilis* 512, more biofilm was formed at the top of the column. And this amount decreases as it approaches the source of airflow (Figure 24). This observation corroborates the previous analysis with the model. Liquid seemed to pass quicker in the bottom of the column. That can explain this low cells retention on packings. Moreover, air injection curbs liquid flow and

Results and discussion

therefore can increase cells retention in some area such as packings in the top of column. A thorough analysis is however needed to confirm that because we have no information about the colonization position on packings. And this biofilm quantification was carried out with *B. subtilis* 512, which is a filamentous strain. This characteristic can modify its ability to hold packings.

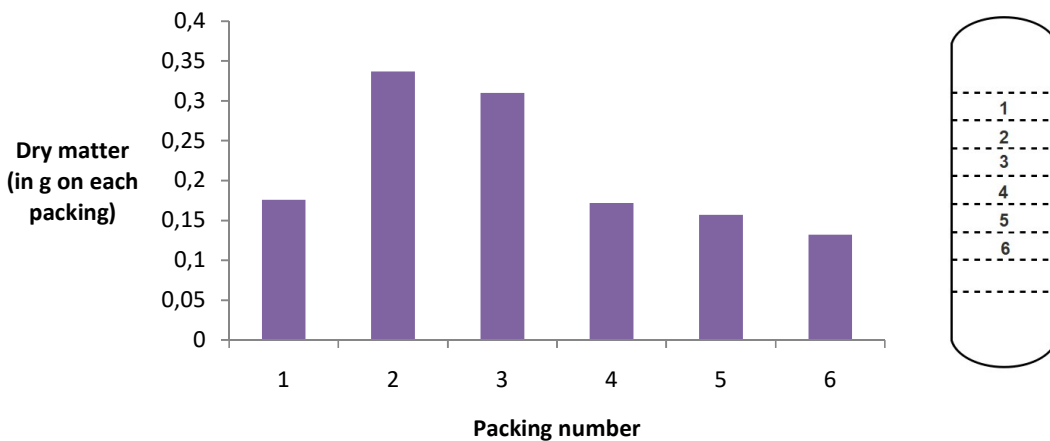


Figure 24: Distribution of cells (dry matter in gr) on packings numbered in order. The first packing is at the top of the column and the 6th at the bottom for the reactor with MSgg and *B. subtilis* 512.

Even if a biofilm was formed, cells immobilization was not optimal. As an illustrative examples, at the end of the culture with *Bacillus subtilis* 512, biofilm concentration on packings was only 45 times higher than planktonic cells (7.8×10^{13} cells hang packings for 1.7×10^{12} in medium). A lot of cells go out of the column without enough interaction to allow their adhesion.

In addition, the biofilm formed with MSgg is not stable. There is a cells release. At the end of the batch (45h of culture), cells concentration in medium suddenly goes up whereas CO₂ emission drops in column. Thanks to fingerprints, we can see the apparition of a population in planktonic cells, more active and with a similar activity of cells biofilm (Figure 25) (Annex 4: Evolution of events number of *B. amyloliquefaciens* by μ l and cells activity measured with a cytometer in FL1 and FL3 in biofilm reactor with MSgg -pg88). These cells seem to come from biofilm.

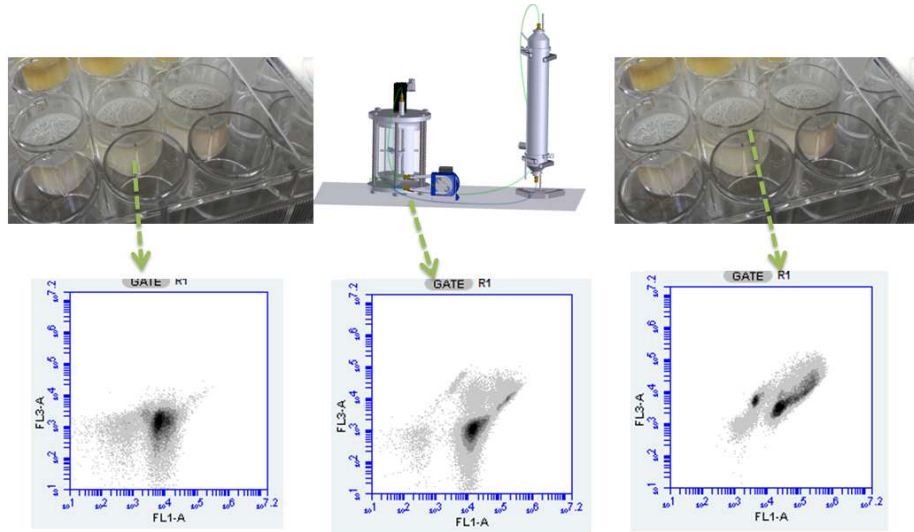


Figure 25: Cytometer fingerprint of cells GA1 activity after 48h of culture in Mgg: planktonic phase growing in microplate (left), planktonic phase growing in reactor at the end of the culture (in the midst) and cells from biofilm formed in microplate (right)

Possible reasons can explain this disintegration as nutrient deprivation, too strong liquid and air flow, instability of strains or biofilm... Nevertheless, glycerol is exhausted after 45h of culture (<1g/L) exactly when a cell release is noticed (Figure 29). That can clearly impact biofilm disintegration if no other carbon source is consumed.

4.3. Attempt to improve cells adhesion with optimized medium



Figure 26 : The hollow support with packings. The 1L of medium introduced in column in red and the part in contact with packings (300ml) in green

In reactor with optimized medium, a method was used to promote cells immobilization in column in order to avoid cell death. A first contact phase between cells and packings before recirculation was carried out. This stage allows to condition cells to form a biofilm. 2 reactors with Optimized medium were tested with this phase but, it was not enough to trigger biofilm development.

In fact, for technical reasons, only 1l on 1.6l of medium used in reactor can filled the column. Unfortunately, packings are placed on a hollow support (Figure 26). Because of that, on the 1l of culture, only 300ml are in contact with packings. Namely, only 1/5 of all the cells are directly in contact with packings in a column at 22°C degrees (see after 4.4.2-Column temperature-pg46). Moreover, the support with these few holes does not facilitate the migration of the others cells to packings. Therefore, in order to optimize this contact phase, in another reactor, all the preculture was directly injected in column with 1l of

medium. And then, column was placed horizontally in the room at 30°C. Thanks to that, all the cells were in contact with packings at 30°C. However, no biofilm grew either. It was also not enough.

4.4. Heterogeneities in environmental conditions and possible stresses expected at the single cell level

As seen above, planktonic cells represent a large part of culture cells with MSgg (7.8×10^{13} cells hang packings for 1.7×10^{12} in medium) and all the cells for Optimized medium. Contrary to the biofilm in column, planktonic cells continue to pass in the different parts of the reactor. With its design, single cells go through different kinds of environment with their specific particularities. In fact, culture cells stay 35 minutes in the tank where optimal conditions are maintained (but without oxygen) and then, cells leave it and are exposed to different surroundings and stresses during 7 minutes with 4,7 in column¹ and 2.3 minutes in silicon pipes. All these stress can destabilize biofilm formation and in the case of Optimized medium, trigger cells lysis. Ph, temperature variation, light and nutrients accessibility were studied here to see their impact on sigma B activation and then, on programmed cell death and on biofilm development in column.

4.4.1. Ph variation

For example, ph is controlled and measured only in 2L tank and can vary in column. However, little variation has been observed in tank reactor. Therefore, it seems unluckily that ph fluctuate highly in column.

4.4.2. Column temperature

During these 7 minutes out of reactor, culture cells are exposed to a decrease of heat. Actually, the length of pipes is enough to bring culture medium to room temperature and as a result, limits temperature at 22°C in the column where a biofilm must grow. These low degrees in column can affect cells and biofilm growth in column (see 7.3.1-Temperature-pg18).

The temperature impact was studied with 2 reactors. Only one parameter was changed between them: the column heating. And cells behaviors observed were clearly different. Without heating, sugar consumption was slow and optical density remained small (behavior seen above 1.1.2-Reactor exhibiting low -pg 33). It was not the case with column maintained at 30°C: sucrose concentration

¹This duration is the time required for the release of 75% of the cells so 280 seconds (wet column with airinjection). That was calculated on the basis of the release distribution in column. (as seen above: 3.4.3-Gas analysis-pg23)

Results and discussion

dropped quickly and OD600 rises also sharply (behavior seen above 1.1.1-Reactor exhibiting -pg29). The low temperature in tower seemed to slow down cells metabolism and then, limited cells growth rate and curbed nutrients consumption. Therefore, this low temperature in column can impact biofilm formation. When cells must create a biofilm, they have a slow metabolism. Thereby, temperature control of the column is an important parameter to ensure biofilm growth in it.

Nevertheless, cell lysis is observed also with column heating. Moreover, cells just pass in column. In this case, they adapt too this cold conditions but without sigma B excitation (see 7.3.1-Temperature-pg18). Therefore, column temperature could not be a trigger of cells lysis.

For following reactors, to avoid temperature variation, silicon pipes were heated and column isolated to maintain 30°C in the whole system. However, this heating can generate a gradient of temperature and then, favors biofilm development at some places instead of others. A maximum loss of 2 degrees was measured at the bottom of column.

4.4.3. Light

Cells bacteria are exposed for 2.2 minutes to direct light from led lamps of the laboratory and for 0.11 minutes to the light emitted by the tungsten lamp of the near infrared spectrometer (see 3.3-Near infrared spectrometer-pg22). Wavelength of the led lamp light above the reactor goes from 375 nm to 775 nm with a more intense peak at 450nm (so, in blue) (Figure 27). Otherwise, tungsten lamp emits more in the infrared light than the visible one. Light emission reaches a peak at 910nm and goes from 400 to 2200 nm.

So, both lamps emit in red and blue wavelengths. As seen above (7.3.3-Light-pg19), red (625-655 nm) and blue lights (430-470nm) can active σ^B and then, influence phosphorylation of transcriptional regulator.

However, that depends on the power of the light (Ávila-Pérez et al., 2010). Led lamp above the reactor has a power of 44W (TRILUX C-Line B LED6000-840 ET C). Even if silicon transmits only 95%² of the intensity, power of led lamp stays higher than the 35mW emitted by tungsten lamp. Therefore, the light emitted by the NIRS is negligible and so, the near infrared spectrometer cannot be the origin of programmed cell death. Moreover, the led lamp has a peak in blue. And the blue light leads to higher σ^B activation than the red one (Ávila-Pérez et al., 2006, 2010; Ondrusch & Rgen Kreft, 2011; J. B. Van Der Steen & Hellingwerf, 2015). The duration of exposure is also important:

² Industrial information : https://www.thorlabs.com/newgroupage9.cfm?objectgroup_id=3983

Results and discussion

0.11 minutes seems too short. To prove that, two reactors with and without NIRS were studied and the same phenomenon of lysis was observed. Moreover, for following reactors with MSgg, NIRS was switched on and cells did not die.

However, the impact of the light emitted by led lamp on sigma B excitation was not studied and can be present but 2.2 minutes seems to be really short to be the cause of the death behavior.

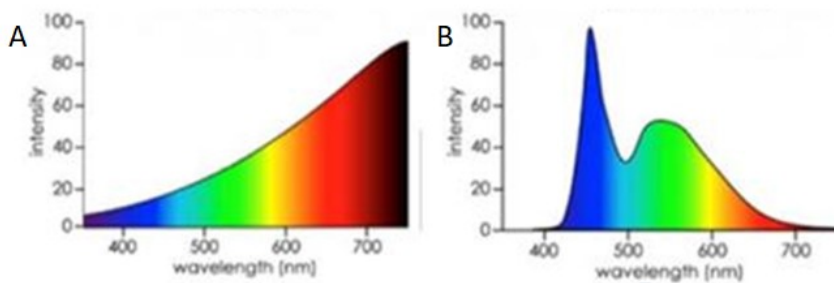


Figure 27 : Emission spectrum of (A) tungsten lamp and (B) white led lamp for the wavelengths between 350 to 750 nm (visible light) with their relative intensity (adapted to <http://www.sunkissedsolar.com.au/led-light-globes-detrimental-health-environment/>).

4.4.4. Carbon source consumption

Nutrient starvation is a usual trigger of programmed cell death (see 4.6- Programmed cells death-pg 11). However, biofilm conformation protects cells from this kind of stress and helps to their survival. In nutrient depletion, cells can form a biofilm to ensure their growth (W. Zhang et al., 2014). But in this biofilm reactor, cells meet difficulties to catch the packings surface and to form a biofilm and consequently, single cells concentration remains high. Unluckily, they are more sensible to a decrease of nutrients than biofilm and their toxins production can destabilize its development.

In the first reactors (behavior seen above 1.1.1 - Reactor exhibiting -pg 29), sucrose consumption was quick. Nutrient deprivation was a hypothesis of death. However, sucrose concentration does not reach zero rapidly. A low residual concentration of sucrose is not consumed and stays in reactor. For an unknown reason, cells do not consume it. They might begin their lysis before its complete assimilation or consume another source of carbon.

Moreover, when sugar concentration is high in medium, sucrose is transformed in acetoin which is a major carbon source consumed after the nutrient depletion in medium (see 2-Influence of culture medium-pg36). In this reactor, its production is high (9.6g/L) (Figure 28). Unluckily, its concentration remains stable. Cells never absorb it. They could assimilate another source as acetate

Results and discussion

or 2,3-butanediol (Renna et al., 1993; Speck* A N, 1973; Y. Zhang et al., 2013). Nevertheless, carbons sources were available. A starvation does not seem to be the origin of death.

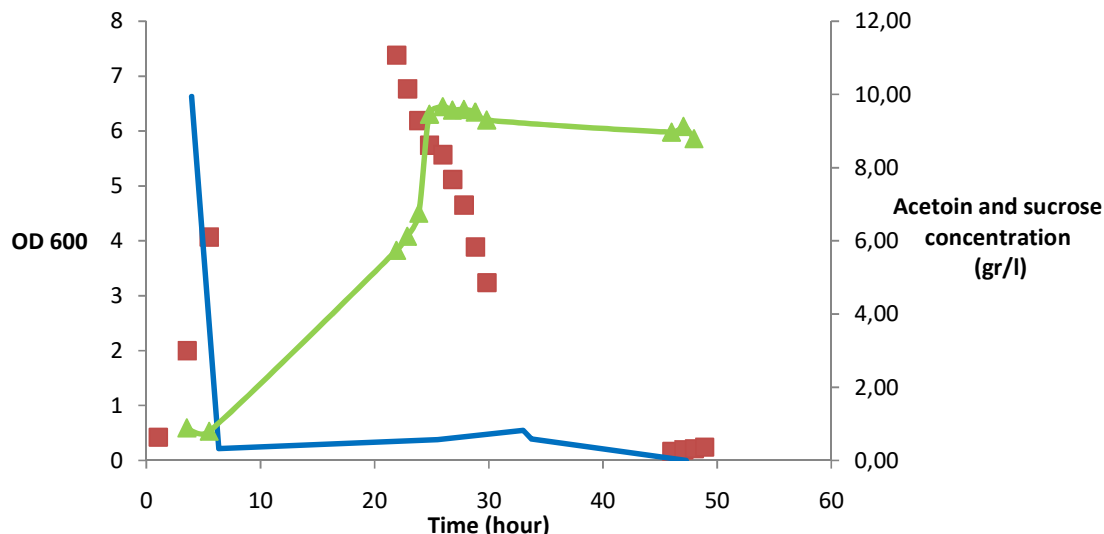


Figure 28 : Evolution of optical density 600 (red), acetoin (green) and sucrose (blue) concentration (g/L) in reactor with Optimized medium and a high growth rate. A low residual concentration of sucrose stay in reactor and is consumed after 40h of culture. Acetoin production is high but it is never consumed.

We can think that this fast sucrose consumption can destabilize biofilm formation by promoting cells growth at the expense of biofilm development. In reactor with MSgg, the rate of carbon consumption was lower and a biofilm grew (Figure 29). This consumption rate could be more beneficial for cells survival. But, when the culture medium used is the Optimized medium and the cell growth is low (1.1.2-Reactor exhibiting low cells growth-pg33), cells go through a phase where most of the cells are less active whereas nutrients are available during all the culture. Something else destabilizes cells in Optimized medium or in reactor design.

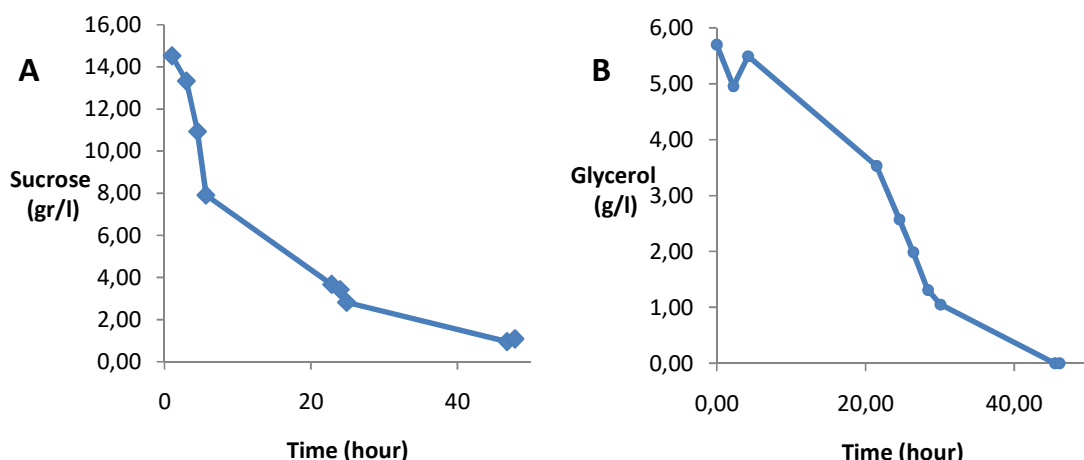


Figure 29 : Evolution of sucrose concentration (g/L) in reactor with Optimized medium and low growth phase (A) and glycerol concentration (g/L) in reactor with MSgg (B). Values at 0 in MSgg correspond at a concentration inferior at 1g/L.

4.4.5. Impact of the restriction of oxygen injection in column

It is also important to note that oxygen is only injected in column and not in reactor. That allows limitation of foam production and promotes cells growth in column. However, this method can limit accessibility to oxygen for cells at some moments. In fact, the majority of cells does not stay a long time in column (4,7 minutes) and then, spend more time under oxygen limitation (37,3 minutes) (see 4.4-Heterogeneities in environmental conditions and possible stresses expected at the single cell level-pg46). In fact, cells stay 35minutes in the reactor tank and 2,3 minutes in the silicon pipes without air injection. This limitation can influence nutrient consumption and is also a source of stress (7.3.5-Oxygen limitation-pg 19). Moreover, oxygen rate impacts surfactin production which is higher when dissolved oxygen is important (Yeh, Wei, & Chang, 2006).

Dissolved O₂ in reactor was followed and its rate was under 10% with sometimes under 2% in all reactors. But, that is not enough to know if cells were in oxygen limitation. Unluckily, the impact of oxygen limitation was not studied in this work. The following of the production of lactate, ethanol and acetate could give information on the importance of this stress (see 7.3.5-Oxygen limitation-pg 19).

4.4.6. Conclusion

The origin of the lysis was not identified. All stresses studied here (temperature, carbon starvation, ph, light) can destabilize cells but none of them was identified as the major source of sigma B activation and then, the source of programmed cell death. Temperature variation does not trigger sigma B activation. Cells were not in nutrient starvation. Light was present but the exposition is not really important. And ph variation seems improbable. The only one stress not studied is oxygen limitation. Its analysis could be interesting.

Conclusion

Medium seems to have a major impact on cells behaviors in biofilm reactor. Only the Optimized medium which is a rich medium, leads to cellular lysis. On the contrary, MSgg allows a biofilm formation and ensures their survival. However, biofilm was already obtained in reactor with Optimized medium. It is then, normally possible to form a biofilm with it.

The design of the column does not also enhance cells attachment. And the biofilm reactor generates a lot of different environmental surroundings with their specific stresses by variation of light, oxygen rate, agitation, ph, temperature. All these different environments lead to a bacteria destabilization. They must adapt quickly to a large range of stresses. If cells form a biofilm, the cellular environment stops changing. A quick attachment to packings decreases these stresses exposition.

MSgg allows this rapid cell adhesion. Its positive influence on biofilm formation helps this adhesion. That is not the case of Optimized medium.

The reason of cells death in Optimized medium is unknown but, enhancing a rapid adhesion on packings seems to be an effective solution.

No real improvements were noticed with using *B. subtilis* 512 in reacor with MSgg by comparison to *B. amyloliquefaciens* GA1. More cells are immobilized on packings during a several hours but not permanently. And the same disintegration is noticed at the end of the culture. However, no reactor was done in Optimized medium with this strain. This reactor could produce better result with *B. subtilis* 512.

Outlooks

A qRT-PCR analysis can be conducted in order to visualize the level of σ^B and SpoOA synthesis in cells culture in order to know the importance of excitation by stresses.

And, it can be interesting to verify the hypothesis of link between σ^B and programmed cell death (see 6-Link between σ^B and network regulation-pg13). The analysis of SpoOE and SdpABC can also be carried out with σ^B and SpoOA.

Nevertheless, a qRT-PCR cannot be used to identify the major source of the excitation of σ^B in the biofilm reactor. Indeed, all stresses of the reactor are perceived by RsbP or RsbU in terms of their types. However, RsbP and RsbU expressions are independent of their chain in general stress response (see 5-General stress response in *Bacillus* sp.-pg12). In fact, RsbP which perceives energy stresses (nutrient starvation, red light and oxygen limitation) have an expression completely independent of stress chains and of general stress response (Vijay et al., 2000). And the expression of RsbU implicating in the perception of environmental stresses (heat, ph and blue light) is directly influence by sigma B. And therefore, all excitations of sigma B lead to an overproduction of RsbU (Voelker, Dufour, et al., 1995). Thereby, the analysis of RsbP and RsbU synthesis does not allow the identification of the major type of stresses involved in the biofilm reactor. Another way must be found.

A lysis is observed in reactor with optimized medium but we have no certitude about the mechanism involved. Sdp and Skf could be analyzed in culture medium of the reactor in order to know if they are produced during cells culture. Their identification has already made in previous study thanks to mass spectrometry (Liu et al., 2010).

And a reactor with *B. subtilis* 512 and Optimized medium can be performed in order to know if the lysis can be avoid with this strain more adapted to the culture in reactor.

In another domain, in order to enhance cells adhesion on packings, a study of the influence of the air and liquid flow velocity can be conducted. Indeed, air injection curbs liquid flow and then, permits a longer contact time between cells and packings. The modification of their values can be performed in order to optimize the time spent by cells in column.

Moreover, for the same purpose, the volume of medium could be decreased. That allows the reduction of the time spent in reactor without changing the time passed in column. It can be helpful for the transition of cells from planktonic phase to the development of a biofilm. However, this

Outlooks

reduction increases also the number of passages in each different environments of the biofilm reactor. A compromise must be found.

MSgg better promotes biofilm formation than Optimized medium but does not allow the same production of lipopeptides than with Optimized medium. Therefore, a possible improvement can be the utilization of MSgg at the beginning of the reactor to form a biofilm and then, change the medium for Optimized medium to allow the biofilm growth.

Furthermore, another option is the utilization of a medium which enhances biofilm formation and allows a higher lipopeptides production such as the Landy medium (1g/L of Yeast extract, 0,5g/L of MgSO₄, K₂HPO₄ of 1g/L, 0,5g/L of KCl, 1,6mg/L of CuSO₄, 1,2 mg/L of MnSO₄, 0,4 mg/L of FeSO₄, 20g/L of glucose, 5g/L of glutamic acid, 21g/L of MOPS and 16mg/L of L-tryptophane). Landy medium composition is quite similar to MSgg but differs for the carbon source concentration. It contains yeast extract and glucose that is not present in MSgg. Landy medium can possibly allow biofilm formation and increase cell density in reactors.

And finally, the ultimate goal of this biofilm reactor is the production of lipopeptides (see 7-Biofilm reactor with stainless steels packings-pg16). Their concentrations were not followed in this work but are important for further optimizations. Moreover, a comparison of the lipopeptides concentration between Optimized medium and MSgg can be conducted in order to know if its production in MSgg is efficient or if medium must be replaced by another one.

References

- Ahimou, F., Jacques, P., & Deleu, M. (2000). Surfactin and iturin A effects on *Bacillus subtilis* surface hydrophobicity. *Enzyme and Microbial Technology*, 27(10), 749–754.
[https://doi.org/10.1016/S0141-0229\(00\)00295-7](https://doi.org/10.1016/S0141-0229(00)00295-7)
- Akpa, E., Jacques, P., Wathelet, B., Paquot, M., Fuchs, R., Budzikiewicz, H., & Thonart, P. (2001). *Culture Conditions Influence on Lipopeptide Production 551 Influence of Culture Conditions on Lipopeptide Production by Bacillus subtilis. Applied Biochemistry and Biotechnology* (Vol. 91). Retrieved from <https://link.springer.com/content/pdf/10.1385%2FABAB%3A91-93%3A1-9%3A551.pdf>
- Antelmann, H., Engelmann, S., Schmid, R., Sorokin, A., Lapidus, A., & Hecker, M. (1997). Expression of a stress- and starvation-induced dps/pexB-homologous gene is controlled by the alternative sigma factor sigmaB in *Bacillus subtilis*. *Journal of Bacteriology*, 179(23), 7251–7256.
<https://doi.org/10.1128/JB.179.23.7251-7256.1997>
- Arguelles-arias, A., Ongena, M., Halimi, B., Lara, Y., Brans, A., Joris, B., & Fickers, P. (2009). *Bacillus amyloliquefaciens* GA1 as a source of potent antibiotics and other secondary metabolites for biocontrol of plant pathogens, 12, 1–12. <https://doi.org/10.1186/1475-2859-8-63>
- Ávila-Pérez, M., Hellingwerf, K. J., & Kort, R. (2006). Blue light activates the σB-dependent stress response of *Bacillus subtilis* via YtvA. *Journal of Bacteriology*, 188(17), 6411–6414.
<https://doi.org/10.1128/JB.00716-06>
- Ávila-Pérez, M., Van Der Steen, J. B., Kort, R., & Hellingwerf, K. J. (2010). Red light activates the σB-mediated general stress response of *Bacillus subtilis* via the energy branch of the upstream signaling cascade. *Journal of Bacteriology*, 192(3), 755–762. <https://doi.org/10.1128/JB.00826-09>
- Banat, I. M., Makkar, R. S., & Cameotra, S. S. (2000). Potential commercial applications of microbial surfactants. *Applied Microbiology and Biotechnology*, 53(5), 495–508.
<https://doi.org/10.1007/s002530051648>
- Besson, F., & Michel, G. (1992). Biosynthesis of iturin and surfactin by *Bacillus subtilis*: Evidence for amino acid activating enzymes. *Biotechnology Letters*, 14(11), 1013–1018.
<https://doi.org/10.1007/BF01021050>
- Boylan, S. A., Redfield, A. R., Brody, M. S., & Price, C. W. (1993). Stress-induced activation of the sigma B transcription factor of *Bacillus subtilis*. *Journal of Bacteriology*, 175(24), 7931–7.
<https://doi.org/10.1128/JB.175.24.7931-7937.1993>
- Branda, S. S., Chu, F., Kearns, D. B., Losick, R., & Kolter, R. (2006). A major protein component of the *Bacillus subtilis* biofilm matrix, 59, 1229–1238. <https://doi.org/10.1111/j.1365-2958.2005.05020.x>
- Branda, S. S., González-Pastor, J. E., Ben-Yehuda, S., Losick, R., & Kolter, R. (n.d.). Fruiting body formation by *Bacillus subtilis*. Retrieved from www.pnas.org/cgi/doi/10.1073/pnas.191384198
- Brigulla, M., Hoffmann, T., Krissp, A., Völker, A., Bremer, E., & Völker, U. (2003). Chill induction of the SigB-dependent general stress response in *Bacillus subtilis* and its contribution to low-

- temperature adaptation. *Journal of Bacteriology*, 185(15), 4305–14.
<https://doi.org/10.1128/JB.185.15.4305-4314.2003>
- Brody, M. S., Stewart, V., & Price, C. W. (2009). Bypass suppression analysis maps the signalling pathway within a multidomain protein: The RsbP energy stress phosphatase 2C from *Bacillus subtilis*. *Molecular Microbiology*, 72(5), 1221–1234. <https://doi.org/10.1111/j.1365-2958.2009.06722.x>
- Brody, M. S., Vijay, K., & Price, C. W. (2001). Catalytic Function of an α / β Hydrolase Is Required for Energy Stress Activation of the ζ B Transcription Factor in *Bacillus subtilis* Catalytic Function of an α / β Hydrolase Is Required for Energy Stress Activation of the ζ B Transcription Factor in *Bacillus subtilis*. *Society for General Microbiology Supplements*, 183(21), 6422–6428. <https://doi.org/10.1128/JB.183.21.6422>
- Budde, I., Steil, L., Scharf, C., Völkner, U., & Bremer, E. (2018). Adaptation of *Bacillus subtilis* to growth at low temperature: a combined transcriptomic and proteomic appraisal.
<https://doi.org/10.1099/mic.0.28530-0>
- Burbulys, D., Trach, K. A., & Hoch, J. A. (1991). Initiation of sporulation in *Bacillus subtilis* is controlled by a multicomponent phosphorelay. *Cell*, 64(3), 545–52. Retrieved from <http://www.ncbi.nlm.nih.gov/pubmed/1846779>
- Chai, Y., Chu, F., Kolter, R., & Losick, R. (n.d.). Bistability and biofilm formation in *Bacillus subtilis*.
<https://doi.org/10.1111/j.1365-2958.2007.06040.x>
- Chen, T., Liu, W., Fu, J., Zhang, B., & Tang, Y. (2013). Engineering *Bacillus subtilis* for acetoin production from glucose and xylose mixtures. *Journal of Biotechnology*, 168(4), 499–505. <https://doi.org/10.1016/J.JBIOTEC.2013.09.020>
- Chen, X. H., Koumoutsi, A., Scholz, R., Eisenreich, A., Schneider, K., Heinemeyer, I., ... Borris, R. (2007). Comparative analysis of the complete genome sequence of the plant growth-promoting bacterium *Bacillus amyloliquefaciens* FZB42. *Nature Biotechnology*, 25(9), 1007–1014. <https://doi.org/10.1038/nbt1325>
- Chubukov, V., & Sauer, U. (2014). Environmental dependence of stationary-phase metabolism in *Bacillus subtilis* and *Escherichia coli*. *Applied and Environmental Microbiology*, 80(9), 2901–9. <https://doi.org/10.1128/AEM.00061-14>
- Clements, L. D., Streips, U. N., & Miller, B. S. (2002). Differential proteomic analysis of *Bacillus subtilis* nitrate respiration and fermentation in defined medium. *Proteomics*, 2(12), 1724–1734. [https://doi.org/10.1002/1615-9861\(200212\)2:12<1724::AID-PROT1724>3.0.CO;2-S](https://doi.org/10.1002/1615-9861(200212)2:12<1724::AID-PROT1724>3.0.CO;2-S)
- Comella, N., & Grossman, A. D. (2005). Conservation of genes and processes controlled by the quorum response in bacteria: Characterization of genes controlled by the quorum-sensing transcription factor ComA in *Bacillus subtilis*. *Molecular Microbiology*, 57(4), 1159–1174. <https://doi.org/10.1111/j.1365-2958.2005.04749.x>
- Costa, F., Silva, B., & Tavares, T. (2017). Biofilm Bioprocesses. In *Current Developments in Biotechnology and Bioengineering* (pp. 143–175). Elsevier. <https://doi.org/10.1016/B978-0-444-63663-8.00006-9>
- Cruz Ramos, H., Hoffmann, T., Marino, M., Nedjari, H., Presecan-Siedel, E., Dreesen, O., ... Jahn, D.

- (2000). Fermentative metabolism of *Bacillus subtilis*: physiology and regulation of gene expression. *Journal of Bacteriology*, 182(11), 3072–80. Retrieved from <http://www.ncbi.nlm.nih.gov/pubmed/10809684>
- Dahl, M. K., Msadek, T., Kunst, F., & Rapoport, G. (1991). Mutational analysis of the *Bacillus subtilis* DegU regulator and its phosphorylation by the DegS protein kinase. *Journal of Bacteriology*, 173(8), 2539–47. Retrieved from <http://www.ncbi.nlm.nih.gov/pubmed/1901568>
- Deleu, M., Paquot, M., & Nylander, T. (2005). Fengycin interaction with lipid monolayers at the air–aqueous interface—implications for the effect of fengycin on biological membranes. *Journal of Colloid and Interface Science*, 283(2), 358–365. <https://doi.org/10.1016/J.JCIS.2004.09.036>
- Dick, G. J., Torpey, J. W., Beveridge, T. J., & Tebo, B. M. (2008). Direct identification of a bacterial manganese(II) oxidase, the multicopper oxidase MnXG, from spores of several different marine *Bacillus* species. *Applied and Environmental Microbiology*, 74(5), 1527–34. <https://doi.org/10.1128/AEM.01240-07>
- Driks, A. (1999). *Bacillus subtilis* Spore Coat INTRODUCTION OF MOLECULAR GENETICS TO THE PROBLEM OF SPORE. *Society*, 63(1), 1–20.
- Fujita, M., González-Pastor, J. E., & Losick, R. (2005). High- and low-threshold genes in the SpoOA regulon of *Bacillus subtilis*. *Journal of Bacteriology*, 187(4), 1357–1368. <https://doi.org/10.1128/JB.187.4.1357-1368.2005>
- Fujita, M., & Losick, R. (2003). The master regulator for entry into sporulation in *Bacillus subtilis* becomes a cell-specific transcription factor after asymmetric division. *Genes and Development*, 17(9), 1166–1174. <https://doi.org/10.1101/gad.1078303>
- González-Pastor, J. E. (2011). Cannibalism: a social behavior in sporulating *Bacillus subtilis*. *FEMS Microbiology Reviews*, 35(3), 415–424. <https://doi.org/10.1111/j.1574-6976.2010.00253.x>
- González-Pastor, J. E., Hobbs, E. C., & Losick, R. (2003). Cannibalism by sporulating bacteria. *Science (New York, N.Y.)*, 301(5632), 510–3. <https://doi.org/10.1126/science.1086462>
- Hamoen, L. W., Meile, J.-C., de Jong, W., Noirot, P., & Errington, J. (2006). SepF, a novel FtsZ-interacting protein required for a late step in cell division. *Molecular Microbiology*, 59(3), 989–999. <https://doi.org/10.1111/j.1365-2958.2005.04987.x>
- Hamon, M. A., & Lazazzera, B. A. (2001). The sporulation transcription factor SpoOA is required for biofilm development in *Bacillus subtilis*. *Molecular Microbiology*, 42(5), 1199–1209. <https://doi.org/10.1046/j.1365-2958.2001.02709.x>
- Hecker, M., & Völker, U. (1998). Non-specific, general and multiple stress resistance of growth-restricted *Bacillus subtilis* cells by the expression of the σ(B) regulon. *Molecular Microbiology*, 29(5), 1129–1136. <https://doi.org/10.1046/j.1365-2958.1998.00977.x>
- Henkin, T. M. (1996). The role of the CcpA transcriptional regulator in carbon metabolism in *Bacillus subtilis*. *FEMS Microbiology Letters*, 135(1), 9–15. [https://doi.org/10.1016/0378-1097\(95\)00370-3](https://doi.org/10.1016/0378-1097(95)00370-3)
- Hermansson, M. (1999). The DLVO theory in microbial adhesion. *Colloids and Surfaces B: Polymers and Biomolecules*, 23(1–3), 1–12. [https://doi.org/10.1016/S0927-3696\(98\)00123-7](https://doi.org/10.1016/S0927-3696(98)00123-7)

Biointerfaces, 14, 105–119. Retrieved from www.elsevier.nl/locate/colsurfb

- Hoa, T. T., Tortosa, P., Albano, M., & Dubnau, D. (2002). Rok (YkuW) regulates genetic competence in *Bacillus subtilis* by directly repressing comK. *Molecular Microbiology*, 43(1), 15–26. <https://doi.org/10.1046/j.1365-2958.2002.02727.x>
- Hoffmann, T., Troup, B., Szabo, A., Hungerer, C., & Jahn, D. (1995). The anaerobic life of *Bacillus subtilis*: Cloning of the genes encoding the respiratory nitrate reductase system. *FEMS Microbiology Letters*, 131(2), 219–225. <https://doi.org/10.1111/j.1574-6968.1995.tb07780.x>
- Hori, K., & Matsumoto, S. (2010). Bacterial adhesion: From mechanism to control. *Biochemical Engineering Journal*, 48, 424–434. <https://doi.org/10.1016/j.bej.2009.11.014>
- J. Espinosa-de-los-Monteros · A. Martinez · F. Valle. (n.d.). Metabolic profiles and aprE expression in anaerobic cultures of *Bacillus subtilis* using nitrate as terminal electron acceptor. <https://doi.org/10.1007/s002530100749>
- Jacques, P., Hbid, C., Destain, J., Razafindralambo, H., Paquot, M., De Pauw, E., & Thonart, P. (1999). *Optimization of Biosurfactant Lipopeptide Production from Bacillus subtilis S499 by Plackett-Burman Design* (Vol. 77). Retrieved from <https://link.springer.com/content/pdf/10.1385%2FABAB%3A77%3A1-3%3A223.pdf>
- Jiang, M., Grau, R., & Perego, M. (2000). Differential processing of propeptide inhibitors of Rap phosphatases in *Bacillus subtilis*. *Journal of Bacteriology*, 182(2), 303–10. <https://doi.org/10.1128/JB.182.2.303-310.2000>
- Jiang, M., Shao, W., Perego, M., & Hoch, J. A. (2000). Multiple histidine kinases regulate entry into stationary phase and sporulation in *Bacillus subtilis*. *Molecular Microbiology*, 38(3), 535–542. <https://doi.org/10.1046/j.1365-2958.2000.02148.x>
- Kearns, D. B., Chu, F., Branda, S. S., Kolter, R., & Losick, R. (2004). A master regulator for biofilm formation by *Bacillus subtilis*. *Molecular Microbiology*, 55(3), 739–749. <https://doi.org/10.1111/j.1365-2958.2004.04440.x>
- Kloepper, J. W., Ryu, C.-M., & Zhang, S. (2004). Induced Systemic Resistance and Promotion of Plant Growth by *Bacillus* spp. *Phytopathology*, 94(11), 1259–1266. <https://doi.org/10.1094/PHYTO.2004.94.11.1259>
- Kobayashi, K. (2007). Gradual activation of the response regulator DegU controls serial expression of genes for flagellum formation and biofilm formation in *Bacillus subtilis*. *Molecular Microbiology*, 66(2), 395–409. <https://doi.org/10.1111/j.1365-2958.2007.05923.x>
- Kobayashi, K. (2008). SlrR/SlrA controls the initiation of biofilm formation in *Bacillus subtilis*. *Molecular Microbiology*, 69(6), 1399–1410. <https://doi.org/10.1111/j.1365-2958.2008.06369.x>
- Kobayashi, K., & Iwano, M. (2012). BslA(YuaB) forms a hydrophobic layer on the surface of *Bacillus subtilis* biofilms. *Molecular Microbiology*, 85(1), 51–66. <https://doi.org/10.1111/j.1365-2958.2012.08094.x>
- Koumoutsi, A., Chen, X.-H., Henne, A., Liesegang, H., Hitzeroth, G., Franke, P., ... Borriis, R. (2004). Structural and functional characterization of gene clusters directing nonribosomal synthesis of

- bioactive cyclic lipopeptides in *Bacillus amyloliquefaciens* strain FZB42. *Journal of Bacteriology*, 186(4), 1084–96. <https://doi.org/10.1128/JB.186.4.1084-1096.2004>
- Kovács, T., Hargitai, A., Kovács, K. L., & Mécs, I. (1998). pH-Dependent activation of the alternative transcriptional factor σ(B) in *Bacillus subtilis*. *FEMS Microbiology Letters*, 165(2), 323–328. [https://doi.org/10.1016/S0378-1097\(98\)00295-X](https://doi.org/10.1016/S0378-1097(98)00295-X)
- Lam, H., Oh, D.-C., Cava, F., Takacs, C. N., Clardy, J., de Pedro, M. A., & Waldor, M. K. (2009). D-Amino Acids Govern Stationary Phase Cell Wall Remodeling in Bacteria. *Science*, 325(5947), 1552–1555. <https://doi.org/10.1126/science.1178123>
- Lazazzera, B. A., Kurtser, I. G., McQuade, R. S., & Grossman, A. D. (1999). An autoregulatory circuit affecting peptide signaling in *Bacillus subtilis*. *Journal of Bacteriology*, 181(17), 5193–5200.
- Liaqat, I., Ahmed, S. I., & Jahan, N. (2013). Biofilm formation and sporulation in *Bacillus subtilis*. *International Journal of Microbiology Research and Reviews*, 1(4), 61–67. Retrieved from <https://pdfs.semanticscholar.org/e6a3/91708da7e86486263a6c25e9f6975b6b84fe.pdf>
- Liu, W.-T., Yang, Y.-L., Xu, Y., Lamsa, A., Haste, N. M., Yang, J. Y., ... Performed, K. P. (2010). Imaging mass spectrometry of intraspecies metabolic exchange revealed the cannibalistic factors of *Bacillus subtilis*, 107(37). <https://doi.org/10.1073/pnas.1008368107>
- Lopez, D., Fischbach, M. A., Chu, F., Losick, R., & Kolter, R. (2009). Structurally diverse natural products that cause potassium leakage trigger multicellularity in *Bacillus subtilis*. *Proceedings of the National Academy of Sciences*, 106(1), 280–285. <https://doi.org/10.1073/pnas.0810940106>
- Losick, R., & Stragier, P. (1992). Crisscross regulation of cell-type-specific gene expression during development in *B. subtilis*. *Nature*, 355(6361), 601–604. <https://doi.org/10.1038/355601a0>
- Manuscript, A., Blood, W., & Count, C. (2009). NIH Public Access, 49(18), 1841–1850. <https://doi.org/10.1016/j.jacc.2007.01.076.White>
- Marlow, V. L., Porter, M., Hobley, L., Kiley, T. B., Swedlow, J. R., Davidson, F. A., & Stanley-Wall, N. R. (2014). Phosphorylated DegU manipulates cell fate differentiation in the *Bacillus subtilis* biofilm. *Journal of Bacteriology*, 196(1), 16–27. <https://doi.org/10.1128/JB.00930-13>
- Martinez, K. A., Kitko, R. D., Mershon, J. P., Adcox, H. E., Malek, K. A., Berkmen, M. B., & Slonczewski, J. L. (2012). Cytoplasmic pH response to acid stress in individual cells of *Escherichia coli* and *Bacillus subtilis* observed by fluorescence ratio imaging microscopy. *Applied and Environmental Microbiology*, 78(10), 3706–14. <https://doi.org/10.1128/AEM.00354-12>
- McLoon, A. L., Guttenplan, S. B., Kearns, D. B., Kolter, R., & Losick, R. (2011). Tracing the domestication of a biofilm-forming bacterium. *Journal of Bacteriology*, 193(8), 2027–34. <https://doi.org/10.1128/JB.01542-10>
- Méndez, M. B., Orsaria, L. M., Philippe, V., Pedrido, M. E., & Grau, R. R. (2004). Novel roles of the master transcription factors SpoOA and sigmaB for survival and sporulation of *Bacillus subtilis* at low growth temperature. *Journal of Bacteriology*, 186(4), 989–1000. <https://doi.org/10.1128/JB.186.4.989-1000.2004>
- Mielich-Süss, B., & Lopez, D. (2015). Molecular mechanisms involved in *Bacillus subtilis* biofilm

- formation. *Environmental Microbiology*, 17(3), 555–565. <https://doi.org/10.1111/1462-2920.12527>
- Molle, V., Fujita, M., Jensen, S. T., Eichenberger, P., González-Pastor, J. E., Liu, J. S., & Losick, R. (2003). The SpoOA regulon of *Bacillus subtilis*. *Molecular Microbiology*, 50(5), 1683–1701. <https://doi.org/10.1046/j.1365-2958.2003.03818.x>
- Morikawa, M. (2006). Beneficial biofilm formation by industrial bacteria *Bacillus subtilis* and related species. *Journal of Bioscience and Bioengineering*, 101(1), 1–8. <https://doi.org/10.1263/JBB.101.1>
- Murray, E. J., Kiley, T. B., & Stanley-Wall, N. R. (2009). A pivotal role for the response regulator DegU in controlling multicellular behaviour. *Microbiology*, 155(1), 1–8. <https://doi.org/10.1099/mic.0.023903-0>
- Nakano, M. M., Dailly, Y. P., Zuber, P., & Clark, D. P. (1997). Characterization of anaerobic fermentative growth of *Bacillus subtilis*: identification of fermentation end products and genes required for growth. *Journal of Bacteriology*, 179(21), 6749–55. <https://doi.org/10.1128/JB.179.21.6749-6755.1997>
- Nakano, M. M., & Hulett, F. M. (1997). Adaptation of *Bacillus subtilis* to oxygen limitation. *FEMS Microbiology Letters*, 157(1), 1–7. [https://doi.org/10.1016/S0378-1097\(97\)00436-9](https://doi.org/10.1016/S0378-1097(97)00436-9)
- Nakano, M. M., Marahiel, M. A., & Zuber, P. (1988). Identification of a genetic locus required for biosynthesis of the lipopeptide antibiotic surfactin in *Bacillus subtilis*. *Journal of Bacteriology*, 170(12), 5662–8. Retrieved from <http://www.ncbi.nlm.nih.gov/pubmed/2848009>
- Nakano, M. M., & Zuber, P. (1993). Mutational analysis of the regulatory region of the srfA operon in *Bacillus subtilis*. *Journal of Bacteriology*, 175(10), 3188–91. Retrieved from <http://www.ncbi.nlm.nih.gov/pubmed/8491732>
- Nguyen, H. T., Razafindralambo, H., Blecker, C., Yapo, C. N. ', Thonart, P., & Delvigne, F. (2014). Author's personal copy Stochastic exposure to sub-lethal high temperature enhances exopolysaccharides (EPS) excretion and improves *Bifidobacterium bifidum* cell survival to freeze-drying. *Biochemical Engineering Journal*, 88, 85–94. Retrieved from <http://www.elsevier.com/authorsrights>
- Nitschke, M., & Pastore, G. M. (2005). Production and properties of a surfactant obtained from *Bacillus subtilis* grown on cassava wastewater. <https://doi.org/10.1016/j.biortech.2005.02.044>
- Nye, T. M., Schroeder, J. W., Kearns, D. B., & Simmons, L. A. (2017). Complete Genome Sequence of Undomesticated *Bacillus subtilis* Strain NCIB 3610. *Genome Announcements*, 5(20). <https://doi.org/10.1128/genomeA.00364-17>
- Ogura, M., & Tsukahara, K. (2010). Autoregulation of the *Bacillus subtilis* response regulator gene *degU* is coupled with the proteolysis of DegU-P by ClpCP. *Molecular Microbiology*, 75(5), 1244–1259. <https://doi.org/10.1111/j.1365-2958.2010.07047.x>
- Ohlsen, K. L., Grimsley, J. K., & Hoch, J. A. (1994). Deactivation of the sporulation transcription factor SpoOA by the SpoOE protein phosphatase. *Developmental Biology*, 91(March), 1756–1760. <https://doi.org/10.1073/PNAS.91.5.1756>

- Oise Hullo, M., Moszer, I., Danchin, A., & Martin-verstraete, I. (2001). CotA of *Bacillus subtilis* Is a Copper-Dependent Laccase. *JOURNAL OF BACTERIOLOGY*, 183(18), 5426–5430. <https://doi.org/10.1128/JB.183.18.5426-5430.2001>
- Ondrusch, N., & Rgen Kreft, J. (2011). Blue and Red Light Modulates SigB-Dependent Gene Transcription, Swimming Motility and Invasiveness in *Listeria monocytogenes*. <https://doi.org/10.1371/journal.pone.0016151>
- Ongena, M., & Jacques, P. (2008). *Bacillus* lipopeptides: versatile weapons for plant disease biocontrol. *Trends in Microbiology*, 16(3), 115–125. <https://doi.org/10.1016/J.TIM.2007.12.009>
- Ongena, M., Jourdan, E., Adam, A., Paquot, M., Brans, A., Joris, B., ... Thonart, P. (2007). Surfactin and fengycin lipopeptides of *Bacillus subtilis* as elicitors of induced systemic resistance in plants. *Environmental Microbiology*, 9(4), 1084–1090. <https://doi.org/10.1111/j.1462-2920.2006.01202.x>
- Padan, E., Bibi, E., Ito, M., & Krulwich, T. A. (2005). Alkaline pH homeostasis in bacteria: New insights. *Biochimica et Biophysica Acta (BBA) - Biomembranes*, 1717(2), 67–88. <https://doi.org/10.1016/J.BBAMEM.2005.09.010>
- Perego, M., Spiegelman, G. B., & Hoch, J. A. (1988). Structure of the gene for the transition state regulator, abrB: regulator synthesis is controlled by the spo0A sporulation gene in *Bacillus subtilis*. *Molecular Microbiology*, 2(6), 689–699. <https://doi.org/10.1111/j.1365-2958.1988.tb00079.x>
- Piggot, P. J., & Hilbert, D. W. (2004). Sporulation of *Bacillus subtilis*. *Current Opinion in Microbiology*, 7, 579–586. <https://doi.org/10.1016/j.mib.2004.10.001>
- Piggot, P. J., & Losick, R. (2002). Sporulation Genes and Intercompartmental Regulation. In *Bacillus subtilis and Its Closest Relatives* (pp. 483–517). American Society of Microbiology. <https://doi.org/10.1128/9781555817992.ch34>
- Propst-Ricciui, C., & Lubin, A. L. B. (1976). Light-Induced Inhibition of Sporulation in *Bacillus licheniformis*. *JOURNAL OF BACTERIOLOGY*, 128(1), 506–609. Retrieved from <https://www.ncbi.nlm.nih.gov/pmc/articles/PMC232885/pdf/jbacter00311-0516.pdf>
- Quisel, J. D., Burkholder, W. F., & Grossman, A. D. (2001). In vivo effects of sporulation kinases on mutant Spo0A proteins in *Bacillus subtilis*. *Journal of Bacteriology*, 183(22), 6573–8. <https://doi.org/10.1128/JB.183.22.6573-6578.2001>
- Quisel, J. D., Burkholder, W. F., & Grossman, A. D. (2001). In Vivo Effects of Sporulation Kinases on Mutant Spo0A Proteins in *Bacillus subtilis*. *JOURNAL OF BACTERIOLOGY*, 183(22), 6573–6578. <https://doi.org/10.1128/JB.183.22.6573-6578.2001>
- Reder, A., Albrecht, D., Gerth, U., & Hecker, M. (2012). Cross-talk between the general stress response and sporulation initiation in *Bacillus subtilis* - the ??B promoter of spo0E represents an AND-gate. *Environmental Microbiology*, 14(10), 2741–2756. <https://doi.org/10.1111/j.1462-2920.2012.02755.x>
- Reder, A., Gerth, U., & Hecker, M. (2012). Integration of oB activity into the decision-making process of sporulation initiation in *Bacillus subtilis*. *Journal of Bacteriology*, 194(5), 1065–1074.

<https://doi.org/10.1128/JB.06490-11>

- Renna, M. C., Najimudin, N., Winik, L. R., & Zahler, S. A. (1993). Regulation of the *Bacillus subtilis* alsS, alsD, and alsR genes involved in post-exponential-phase production of acetoin. *Journal of Bacteriology*, 175(12), 3863–75. <https://doi.org/10.1128/JB.175.12.3863-3875.1993>
- Riesenman, P. J., & Nicholson, W. L. (2000). Role of the spore coat layers in *Bacillus subtilis* spore resistance to hydrogen peroxide, artificial UV-C, UV-B, and solar UV radiation. *Applied and Environmental Microbiology*, 66(2), 620–6. Retrieved from <http://www.ncbi.nlm.nih.gov/pubmed/10653726>
- Roilides, E., Simitsopoulou, M., Katragkou, A., & Walsh, T. J. (2015). How Biofilms Evade Host Defenses. <https://doi.org/10.1128/microbiolspec.MB-0012-2014>
- Romero, D., Aguilar, C., Losick, R., & Kolter, R. (2010). Amyloid fibers provide structural integrity to *Bacillus subtilis* biofilms. *Proceedings of the National Academy of Sciences of the United States of America*, 107(5), 2230–4. <https://doi.org/10.1073/pnas.0910560107>
- Romero, D., Vlamakis, H., Losick, R., & Kolter, R. (2014). Functional analysis of the accessory protein TapA in *Bacillus subtilis* amyloid fiber assembly. *Journal of Bacteriology*, 196(8), 1505–1513. <https://doi.org/10.1128/JB.01363-13>
- Rothstein, D. M., Lazinski, D., Osburne, M. S., & Sonenshein, A. L. (2017). A Mutation in the *Bacillus subtilis* rsbU Gene That Limits RNA Synthesis during Sporulation. *Journal of Bacteriology*, 199(14), JB.00212-17. <https://doi.org/10.1128/JB.00212-17>
- Rudner, D. Z., LeDeaux, J. R., Ireton, K., & Grossman, A. D. (1991). The spoOK locus of *Bacillus subtilis* is homologous to the oligopeptide permease locus and is required for sporulation and competence. *Journal of Bacteriology*, 173(4), 1388–98. Retrieved from <http://www.ncbi.nlm.nih.gov/pubmed/1899858>
- Sharma, P., & Noronha, S. (2014). Comparative Assessment of Factors Involved in Acetoin Synthesis by *Bacillus subtilis* 168. *ISRN Microbiology*, 2014, 578682. <https://doi.org/10.1155/2014/578682>
- Shemesh, M., & Chai, Y. (2013). A combination of glycerol and manganese promotes biofilm formation in *Bacillus subtilis* via the histidine kinase KinD signaling 2 3 Email addresses: Running title: KinD signaling governs biofilm formation. *J. Bacteriol.* <https://doi.org/10.1128/JB.00028-13>
- Silbersack, J., Jürgen, B., Hecker, M., Schneidinger, B., Schmuck, R., & Schweder, T. (2006). An acetoin-regulated expression system of *Bacillus subtilis*. *Applied Microbiology and Biotechnology*, 73(4), 895–903. <https://doi.org/10.1007/s00253-006-0549-5>
- Solomon, J. M., Lazazzera, B. A., & Grossman, A. D. (1996). Purification and characterization of an extracellular peptide factor that affects two different developmental pathways in *Bacillus subtilis*. *Genes & Development*, 10(16), 2014–2024. <https://doi.org/10.1101/gad.10.16.2014>
- Speck* A N, E. L. (1973). Control of Metabolite Secretion in *Bacillus subtilis*. *Journal of General Microbiology*, 78, 261–275. Retrieved from www.microbiologyresearch.org
- Spring, C., York, N., York, N., York, N., & York, N. (1993). Sinl modulates the activity of SinR , a developmental sw tch protein of *Bacillus subtilis* , by protein-protein interaction, 139–148.

- Stanley, N. R., Britton, R. A., Grossman, A. D., & Lazazzera, B. A. (2003). Identification of Catabolite Repression as a Physiological Regulator of Biofilm Formation by *Bacillus subtilis* by Use of DNA Microarrays. *JOURNAL OF BACTERIOLOGY*, 185(6), 1951–1957. <https://doi.org/10.1128/JB.185.6.1951-1957.2003>
- Stanley, N. R., & Lazazzera, B. A. (2004). Environmental signals and regulatory pathways that influence biofilm formation. *Molecular Microbiology*, 52(4), 917–924. <https://doi.org/10.1111/j.1365-2958.2004.04036.x>
- Strauch, M. a, Spiegelman, G. B., Perego, M., Johnson, W. C., Burbulys, D., & Hoch, J. a. (1989). The transition state transcription regulator *abrB* of *Bacillus subtilis* is a DNA binding protein. *The EMBO Journal*, 8(5), 1615–1621.
- Sun, G., Sharkova, E., Chesnut, R., Birkey, † Stephanie, Duggan, M. F., Sorokin, A., ... Marion Hulett, F. (1996). *Regulators of Aerobic and Anaerobic Respiration in Bacillus subtilis*. *JOURNAL OF BACTERIOLOGY* (Vol. 178). Retrieved from <https://www.ncbi.nlm.nih.gov/pmc/articles/PMC177812/pdf/1781374.pdf>
- Taylor, B. L., & Zhulin, I. B. (1999). PAS domains: internal sensors of oxygen, redox potential, and light. *Microbiology and Molecular Biology Reviews : MMBR*, 63(2), 479–506. Retrieved from <http://www.ncbi.nlm.nih.gov/pubmed/10357859>
- Tian, Y., Fan, Y., Liu, J., Zhao, X., & Chen, W. (2016). Effect of nitrogen, carbon sources and agitation speed on acetoin production of *Bacillus subtilis* SF4-3. *Electronic Journal of Biotechnology*, 19, 41–49. <https://doi.org/10.1016/J.EJBT.2015.11.005>
- Tian, Y., Xu, H., Liu, J., Chen, W., Sun, W., & Chen, Y. (2016). Biotechnology & Biotechnological Equipment Construction of acetoin high-producing *Bacillus subtilis* strain Construction of acetoin high-producing *Bacillus subtilis* strain. <https://doi.org/10.1080/13102818.2016.1179592>
- Touré, Y., Ongena, M., Jacques, P., Guiro, A., & Thonart, P. (2004). Role of lipopeptides produced by *Bacillus subtilis* GA1 in the reduction of grey mould disease caused by *Botrytis cinerea* on apple. *Journal of Applied Microbiology*, 96(5), 1151–1160. <https://doi.org/10.1111/j.1365-2672.2004.02252.x>
- Van Der Steen, J. B. ;, Nakasone, Y. ;, Hendriks, J. C. ;, Hellingwerf, K. J., & Biosystems, M. (n.d.). UvA-DARE (Digital Academic Repository) Modeling the functioning of YtvA in the general stress response in *Bacillus subtilis*. <https://doi.org/10.1039/c3mb70124g>
- Van Der Steen, J. B., & Hellingwerf, K. J. (2015). Activation of the General Stress Response of *Bacillus subtilis* by Visible Light. *Photochemistry and Photobiology*, 91(5), 1032–1045. <https://doi.org/10.1111/php.12499>
- Van Loosdrecht, M. C. M., Lyklema, J., Norde, W., & Zehnder, A. J. B. (1989). Bacterial Adhesion: A Physicochemical Approach. *Microb Er*, 17, 1–15. Retrieved from <https://link.springer.com/content/pdf/10.1007%2FBF02025589.pdf>
- Veening, J.-W., Igoshin, O. A., Eijlander, R. T., Nijland, R., Hamoen, L. W., & Kuipers, O. P. (2008). Transient heterogeneity in extracellular protease production by *Bacillus subtilis*. *Molecular Systems Biology*, 4, 184. <https://doi.org/10.1038/msb.2008.18>

- Veening, J. W., Hamoen, L. W., & Kuipers, O. P. (2005). Phosphatases modulate the bistable sporulation gene expression pattern in *Bacillus subtilis*. *Molecular Microbiology*, 56(6), 1481–1494. <https://doi.org/10.1111/j.1365-2958.2005.04659.x>
- Vijay, K., Brody, M. S., Fredlund, E., & Price, C. W. (2000). A PP2C phosphatase containing a PAS domain is required to convey signals of energy stress to the ??(B) transcription factor of *Bacillus subtilis*. *Molecular Microbiology*, 35(1), 180–188. <https://doi.org/10.1046/j.1365-2958.2000.01697.x>
- Vlamakis, H., Chai, Y., Beauregard, P., Losick, R., & Kolter, R. (2013). Sticking together: building a biofilm the *Bacillus subtilis* way. *Nature Reviews Microbiology*, 11. <https://doi.org/10.1038/nrmicro2960>
- Voelker, U., Dufour, A., & Haldenwang, W. G. (1995). The *Bacillus subtilis* rsbU gene product is necessary for RsbX-dependent regulation of σB. *J. Bacteriol.*, 177(1), 114–122. Retrieved from <http://jb.asm.org/cgi/content/abstract/177/1/114>
- Voelker, U., Voelker, A., & Haldenwang, W. G. (1996). Reactivation of the *Bacillus subtilis* anti-sigma B antagonist, RsbV, by stress- or starvation-induced phosphatase activities. *Journal of Bacteriology*, 178(18), 5456–63. <https://doi.org/10.1128/JB.178.18.5456-5463.1996>
- Voelker, U., Voelker, A., Maul, B., Hecker, M., Dufour, A., & Haldenwang, W. G. (1995). Separate mechanisms activate sigma B of *Bacillus subtilis* in response to environmental and metabolic stresses. *Journal of Bacteriology*, 177(13), 3771–80. <https://doi.org/10.1128/JB.177.13.3771-3780.1995>
- Wang, S. T., Setlow, B., Conlon, E. M., Lyon, J. L., Imamura, D., Sato, T., ... Eichenberger, P. (n.d.). The Forespore Line of Gene Expression in *Bacillus subtilis*. <https://doi.org/10.1016/j.jmb.2006.01.059>
- Weber, M. H. W., & Marahiel, M. A. (2002). Coping with the cold: the cold shock response in the Gram-positive soil bacterium *Bacillus subtilis*. <https://doi.org/10.1098/rstb.2002.1078>
- Wilks, J. C., Kitko, R. D., Cleeton, S. H., Lee, G. E., Ugwu, C. S., Jones, B. D., ... Slonczewski, J. L. (2009). Acid and base stress and transcriptomic responses in *Bacillus subtilis*. *Applied and Environmental Microbiology*, 75(4), 981–90. <https://doi.org/10.1128/AEM.01652-08>
- Xenopoulos, P., & Piggot, P. J. (2011). Regulation of growth of the mother cell and chromosome replication during sporulation of *Bacillus subtilis*. *Journal of Bacteriology*, 193(12), 3117–26. <https://doi.org/10.1128/JB.00204-11>
- Ye, R. W., Tao, W., Bedzyk, L., Young, T., Chen, M., & Li, L. (2000). *Grown under Anaerobic Conditions. JOURNAL OF BACTERIOLOGY* (Vol. 182). Retrieved from <https://www.ncbi.nlm.nih.gov/pmc/articles/PMC94617/pdf/jb004458.pdf>
- Yeh, M.-S., Wei, Y.-H., & Chang, J.-S. (2006). Bioreactor design for enhanced carrier-assisted surfactin production with *Bacillus subtilis*. *Process Biochemistry*, 41(8), 1799–1805. <https://doi.org/10.1016/J.PROCBIO.2006.03.027>
- Zhang, S., & Haldenwang, W. G. (2005). Contributions of ATP, GTP, and redox state to nutritional stress activation of the *Bacillus subtilis* sigmaB transcription factor. *Journal of Bacteriology*,

Annexes

187(22), 7554–60. <https://doi.org/10.1128/JB.187.22.7554-7560.2005>

Zhang, W., Seminara, A., Suaris, M., Brenner, M. P., Weitz, D. A., & Angelini, T. E. (2014). Nutrient depletion in *Bacillus subtilis* biofilms triggers matrix production. *New Journal of Physics*, 16(1), 015028. <https://doi.org/10.1088/1367-2630/16/1/015028>

Zhang, Y., Li, S., Liu, L., & Wu, J. (2013). Acetoin production enhanced by manipulating carbon flux in a newly isolated *Bacillus amyloliquefaciens*. <https://doi.org/10.1016/j.biortech.2012.10.036>

Zune, Q., Soyeurt, D., Toye, D., Ongena, M., Thonart, P., & Delvigne, F. (2014). High-energy X-ray tomography analysis of a metal packing biofilm reactor for the production of lipopeptides by *Bacillus subtilis*. *Journal of Chemical Technology & Biotechnology*, 89(3), 382–390. <https://doi.org/10.1002/jctb.4128>

Zune, Q., Telek, S., Calvo, S., Salmon, T., Alchihab, M., Toye, D., & Delvigne, F. (2017). Influence of liquid phase hydrodynamics on biofilm formation on structured packing: Optimization of surfactin production from *Bacillus amyloliquefaciens*. <https://doi.org/10.1016/j.ces.2016.08.023>

Annexes

Annex 1 : Assembly and disassembly of the reactor and the column

4.5. Montage de la colonne

3 parties : le bas, la colonne et le haut.

Le bas est constitué de la base de la colonne, d'un joint, d'une attache tri-clover et d'un raccord. Les 3 s'associent ensemble tel que sur la Figure 30.



Figure 30: Matériel du bas de la colonne (gauche) et assemblage du bas de la colonne (droite) (Illustration du travail de Bachelor de Clément Furrer)

Ensuite, un tuyau PharMed 4.8*8.0mm est placé à l'entrée d'air afin que l'injection se fasse toujours au-dessus du niveau du liquide afin d'éviter la formation de mousse (Figure 31). Le support intérieur de la zone d'aération est ensuite placé par-dessus.

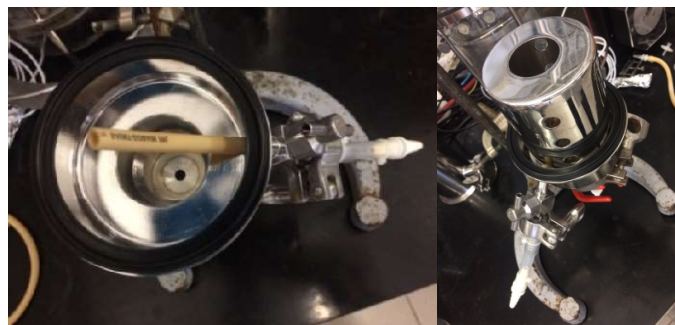


Figure 31: bas de la colonne avec support intérieur et avec le tuyau d'aération Illustration du travail de Bachelor de Clément Furrer)

L'ouverture latérale de la colonne doit être fermée à l'aide d'un joint, d'un bouchon et d'une attache tri-clover (Figure 32).



Figure 32: ouverture latérale de la colonne (Illustration du travail de Bachelor de Clément Furrer)

Rien de particulier ne doit être fait pour la partie du haut. Toutes les pièces sont déjà assemblées. Cependant, des précautions doivent être prises lors de sa manipulation afin d'éviter de briser l'entonnoir et l'état des tuyauteries souples doit être vérifié.

Le bas est attaché à la colonne à l'aide d'un joint et d'une attache tri-clover. Il faut faire attention à placer l'ouverture latérale de la colonne à 90° ou à 180° de l'ouverture pour l'entrée d'air de la partie du bas (Figure 33). Vérifier que le joint est bien positionné.



Figure 33: bas attaché à la colonne

La colonne est attachée à son support à l'aide de 3 pinces à 3 doigts (Figure 33). La pince orange est fixée sur le support dans le bas. La colonne est simplement déposée sur cette pince. Les 2 autres sont fixées au milieu et en haut de la tige. Elles vont maintenir la colonne bien droite et empêcher qu'elle ne bouge autour de son axe. Les 2 pinces sont d'abord ouvertes quasiment complètement. Puis, une fois que la colonne est placée, on utilise un niveau pour s'assurer que la colonne soit bien droite. Les 2 pinces noires sont ensuite refermées.

Une fois cela effectué, on peut placer les 6 packings Sulzer 83/53 dans la colonne (Figure 34). Le premier packing doit être placé perpendiculairement à l'entrée d'air et doit toucher le support intérieur de la zone d'aération. Les suivants sont ensuite placés de manière à avoir un angle de 90°C entre eux afin d'augmenter le cisaillement du liquide. Les garnissages sont numérotés et doivent être placés suivant cet ordre. Des ailettes sont présentes sur les packings. Elles doivent toujours être orientées vers le haut.



Si les packings ne sont pas bien enfoncés, l'entonnoir risque de les toucher et d'être endommagé.



Figure 34: Packing

Ensuite, le haut de la colonne peut être placé et attaché à l'aide d'un joint noir et d'une attache triclover. Le condenseur doit être placé de manière à être sur la droite pour faciliter les rattachements ultérieurs (Figure 35). Lors de la stérilisation, les prises du condenseur doivent être emballées dans de l'aluminium.

La colonne est ensuite placée sur la table entre le box de contrôle et le réacteur.



Figure 35: Colonne sur son support

Des tuyaux en silicone ID5-ED9mm équipés de connecteurs sont installés à 4 endroits sur la colonne. Le premier tuyau d'une longueur de 180cm est placé entre la colonne et le haut du capteur infrarouge (Figure 36). Le 2^{ème} est accroché au condenseur. Il est équipé d'un Y qui permet d'avoir,

d'une part, un tuyau en silicone ID5-ED9mm vers un berlin contenant de l'eau de javel (400ml d'eau pour 50ml d'eau de javel) ainsi qu'un autre équipé d'un filtre 0.2µm PTFE Sartorius Midistar 2000 qui permet de maintenir la colonne à pression atmosphérique en laissant l'air entrer ou sortir dans la colonne de manière stérile (Figure 36). Le 3^{ème}tuyau d'une longueur totale de 174cm divisé en deux partie à l'aide d'un tuyau PharMed 3.20*6.40mm dont les dimensions sont 20cm, relie le bas de la colonne à la prise d'ajout du bio-réacteur. Ce tuyau permet le retour du liquide au sein du fermenteur à l'aide d'une pompe 323 watsonmarlow. Le 4^{ème} tuyau permet l'injection de l'oxygène. Ce tuyau est équipé d'un filtre 0.2µm PTFE Sartorius Midistar 2000 qui est entouré de 2 pinces de Mohr.



Figure 36: Tuyau en silicone de la colonne

4.6. Calibrage de la sonde PH

Le calibrage de la sonde pH PHI K8 200 doit être effectué avant de monter le réacteur. Le capuchon contenant du KCl 3mol/L est dévissé puis enlevé et la sonde est rincée puis épongée avec du papier sans être frottée pour éviter de la griffer. Le contenu du capuchon est jeté et celui-ci est rincé. La sonde pH est branchée au moniteur en veillant à ce que la sonde de la température PT100 le soit également (la sonde de température est dans le réacteur).

La sonde est placée dans la solution à pH 7. Sur l'écran du moniteur, choisir l'unité de travail (ici UNIT 1) aller dans « mode » puis « calibration » puis « 7pH» puis « ok ». Attendre ensuite plus au moins 5 minutes le temps que la sonde se stabilise. Puis « calibration 7 » puis « ok », rincer avec l'eau distillée du kit pH. Placer ensuite la sonde dans la solution à pH 4. Appuyer sur « OK » sur le moniteur puis attendre que ça se stabilise avant de nouveau pousser sur « ok ». Ensuite, enlever le câble qui relie la sonde au moniteur et remettre le capuchon de protection noir sur la sonde. Vérifier la présence du joint blanc transparent au niveau du connecteur de la sonde.

La sonde est placée dans un berlin rempli d'eau en attendant d'être autoclavée avec le réacteur.



Le couvercle du réacteur ne s'enlève jamais avec la sonde encore attachée sur celui-ci.

4.7. Montage du réacteur

Composition du couvercle du bio-réacteurB plus Sartorius 2 Litres : Voir figure 37.

Le couvercle du réacteur est composé notamment d'un bouchon d'ajout à 4 entrées pour l'injection de l'acide, la base et le saccharose pour notre cas de figure (Figure 37). Le couvercle du réacteur est déposé de manière à placer les 4 embouts pour l'acide, la base et le saccharose à l'avant (Figure 37). Il faut veiller à ce que le joint entre le couvercle et le réacteur soit bien présent et humidifié lors du montage pour augmenter l'adhésion. Le couvercle est ensuite vissé en quinconce par 3 vis dont une possède une tubulure. Elle est disposée côté entrer et sortie double enveloppe de la cuve en verre.



Figure 37: Couvercle du réacteur annoté

Les extrémités de la double enveloppe sont protégées par un tuyau en silicium (Figure 38).



Figure 38: Double enveloppe

Le câble de la sonde de température est enroulé et attaché à la poignée à l'aide d'un collier colson et la prise de connexion est entourée d'aluminium.

L'arrivée d'air est située entre la sonde pH et le condenseur sur l'entrée du Sparger (Figure 37). Il faut lui adjoindre un tuyau en silicone ID5-ED9mm relié à un filtre Sartorius (attention au sens du gaz sur le filtre) fermé de part et d'autre par des pinces de Mohr. Ce câble est ensuite enroulé à la poigné du réacteur (Figure 39).

La sonde pO₂ (Hamilton Visiferm DO) est placée à gauche de la sonde de température (Figure 37). S'assurer de la présence des 2 joints, le noir sur la sonde et le blanc sur le couvercle du fermenteur et puis visser la sonde avec une clé de 199mm. L'extrémité de la sonde est recouverte d'un morceau de tuyau en silicone (Figure 39).



Figure 39: Couvercle du réacteur avec sonde pO₂ et tuyau d'aération

Le condenseur est vissé au couvercle (Figure 40). La barre en fer soutenant le condenseur n'est fixée qu'après la stérilisation mais est placée puis retirée lors de la mise en place de celui-ci afin de valider la position correcte sur le fermenteur. Les 2 connecteurs rapides du condenseur sont emballés dans de l'aluminium pour les protéger lors de la stérilisation. Au dessus du condenseur est fixé un tuyau en silicone ID5-ED9mm auquel est accroché un raccord en Y. Ce dernier permet de relier 2 tuyaux en silicone ID5-ED9mm, l'un est équipé d'un filtre 0.2µm PTFE Sartorius qui est entouré de pince de Mohr et l'extrémité de l'autre est emballé d'un morceau de papier à autoclave et équipé d'une pince Mohr non fermée. Elle sera fermée lors de la sortie de l'autoclave. Cette sortie permet l'équilibre des pressions lors de l'autoclavage du bio-réacteur.



Figure 40: Condenseur du réacteur

Les 4 entrées d'ajouts rassemblés ensemble sont les prises pour le saccharose, l'acide et la base. La 4^{ème} prise n'est pas utilisée et doit être fermée à l'aide d'un tuyau en silicium ID5-ED9mm de 5cm accompagné d'un connecteur et d'une pince à Mohr pour fermer le tout.

Les 3 tuyaux en silicium ID5-ED9mm reliant le réacteur aux bouteilles d'acide, de saccharose et de base sont d'une longueur suffisante pour passer par le moniteur (+-1m). Les bouteilles ont un couvercle présentant 2 entrées. L'une est connectée à un tuyau en silicium ID5-ED9mm fixé sur le dessus du capuchon de la bouteille de Schott et présente un filtre Sartorius 0.2µm PTFE (Minisart SRP) fermé à l'aide d'un bouchon et à l'autre est accroché à un tuyau en silicium de 5cm qui rentre à l'intérieur de la bouteille (Figure 41). Les 2 tuyaux sont ensuite fermés à l'aide de pinces de Mohr (Figure 41). Les solutions de saccharose et d'acide (H3PO4 40%) sont ajoutées dans les bouteilles avant la stérilisation. La bouteille de base (NH3 17%) est remplie seulement après le passage dans l'autoclave. Les étiquettes de la bouteille d'acide et de la base sont annotées en rouge de leur nom et de leur concentration. Les informations pour le saccharose sont inscrites en noir.



Figure 41: bouteille d'acide à gauche et montage à l'intérieur à droite

La sortie du réacteur est située à droite des 4 entrées d'ajouts pour le saccharose, la base et l'acide (Figure 37). A cette prise est accroché un tuyau en silicium ID5-ED9mm de 5cm fermé par une pince

de Mohr et équipé à son extrémité d'un raccord en Y (POLYPROPYL Y CONN 8MM) (Figure 42). Cet Y va servir à la prise d'échantillons et à la recirculation entre la sortie du bio-réacteur et l'entrée bas de la chambre d'analyse de l'infrarouge. L'Y est relié par une de ses extrémités à un petit tuyau en silicone ID3-ED6 mm de 5 cm fermé à son extrémité par un bouchon luer lock. Sur l'autre extrémité du Y est installé un tuyau en silicone ID5-ED9mm de 102cm relié à un tuyau PharMed 3.2*6.4mm de 33cm qui sera placé dans la pompe MCP-Process. Un tuyau en silicone ID5-ED9mm de 190.5cm est ensuite placé à son extrémité pour être relié au système infrarouge. Une pince de Mohr est placé à l'entrée du tuyau afin que le milieu ne remonte pas dedans pendant l'autoclavage.



Figure 42: Sortie du réacteur

Le tuyau pour l'entrée du réacteur se fait via une prise située à gauche des 4 entrées d'ajouts pour le saccharose, la base et l'acide (Figure 37). Avant la stérilisation, un tuyau en silicone ID5-ED9mm de 4cm relié à un connecteur est placé sur l'embout et fermé ensuite par une pince Mohr tel qu'indiqué sur la Figure 43. Ce tuyau sera relié au montage déjà effectué sur la colonne après la stérilisation.



Figure 43: Entrée dans le réacteur

Lorsque tout est placé, les 1,3L du milieu optimized sans le glucose sont versés dans le réacteur à l'aide d'un entonnoir par l'entrée de la sonde pH. Puis, la sonde pH est installée après avoir été calibrée. Pour la placer sur le couvercle, il faut veiller à ce que le joint blanc entre le couvercle et la sonde soit bien présent. La sonde est ensuite essuyée puis vissée à la main au couvercle.

Les tuyaux encore libre sont attachés au réacteur (Figure 44). Le tout peut maintenant être autoclavé à 121°C pendant 20 minutes.



Figure 44: réacteur prêt avant l'autoclave

4.8. Jour précédent le lancement du réacteur (après l'autoclavage)

Libérer les différents tuyaux de la colonne en enlevant les colsons et faire de même pour les tuyaux sur la poignée de droite du réacteur. Fixer le condenseur au réacteur à l'aide de la tige en fer (Figure 45).



Figure 45: tige du condenseur

Ensuite, il faut brancher les câbles du condenseur au réacteur.



Brancher la prise mâle du condenseur sur la prise femelle du box de contrôle en premier et seulement après la prise femelle du condenseur.

Le long tuyau en silicone du condenseur de la colonne est baigné dans un berlin contenant un mélange d'eau de javel et d'eau (400ml d'eau pour 50ml d'eau de javel). Une boucle est formée avec le tuyau et il est attaché à l'aide d'un collier colson au fermenteur afin d'éviter qu'il ne se croque (voir Figure 46). Le tuyau en silicone relié à l'entrée de la colonne est attaché à la structure de l'infrarouge afin de le stabiliser.

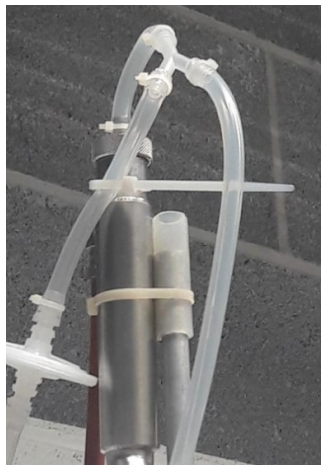


Figure 46: Condenseur de la colonne

Les sondes pH et pO₂ sont ensuite branchées au moniteur en faisant attention de ne pas les confondre. Puis les tuyaux de la poignée de gauche du réacteur sont relâchés.

La bouteille de saccharose est placée à coté du moniteur afin de pouvoir passer son tuyau dans la pompe de celui-ci. Le tuyau doit être placé dans le bon sens dans la pompe afin que le saccharose s'écoule dans le réacteur et pas l'inverse. Le saccharose est branché à la pompe AFOAM1. Ensuite, faire de même avec les 2 autres bouteilles en vérifiant les correspondances des produits avec les pompes.



Les lunettes de sécurité sont obligatoires pour cette manipulation.

Les câbles de la double enveloppe (Figure 47) sont ensuite fixés. La prise mâle est branchée en haut et la prise femelle en bas. Ils sont ensuite reliés au moniteur.



Figure 47: câble de la double enveloppe

Le moteur peut maintenant être fixé. Il est placé de manière légèrement décalé au condenseur pour éviter qu'ils ne se gênent. D'une main, tenir le moteur bien droit et de l'autre visser la vis de manière forte à l'aide d'un tournevis en croix (Figure 48).



Figure 48: Moteur du rotor

Les tuyaux qui doivent être liés à la capsule infrarouge sont placés sur les grilles pour éviter qu'ils ne se croquent.

Les pompes MCP-Process ISMATEC et 323 Watson Marlow sont installées l'une à côté de l'autre (Figure 20). Les tuyaux PharMed 4.8*8.0mm y sont placés en faisant attention au sens de pompage. La pompe verte (MCP-Process ISMATEC) pompe dans le sens des aiguilles d'une montre. La sortie de la colonne est située à droite dans la pompe (Figure 49).



Figure 49: Pompe

La capsule à infrarouge doit être lavée avec du Bacillol (effectue un CIP). La taille de l'espace choisi est de 1mm. 2 tuyaux en silicone ID5-ED9mm sont installés de part et d'autre de la capsule suivi d'un connecteur et d'un autre tuyau en silicone fermé par des pinces. 25ml de Bacillol est introduit dans ce montage pendant 24h. Une fois désinfectée, la capsule est vidée et rincée à l'aide d'eau distillée stérile. Si la capsule n'est pas branchée immédiatement au système, un tuyau en silicone fermé par une pince de Mohr est attaché au connecteur et le tout est soutenu par un colson (Figure 50). Les 2

câbles renfermant les fibres sont branché dans le bas de la capsule (le sens n'a pas d'importance). La capsule est ensuite fixée à la grille en fer à l'aide de 2 colliers colsons tel que sur la Figure 50.



Figure 50: Installation capsule infrarouge

5. Lancement du réacteur le jour-J

Tout d'abord, en condition non aérée et non agitée, il faut vérifier à l'aide d'une lampe l'opacité du milieu.

L'agitation et la température sont réglées respectivement sur 400rpm et 30°C ou 37°C.

Ensuite, on injecte le glucose en allumant la pompe d'AFOM1. Le mode manuel est enclenché sur le moniteur : dans « main » (Figure 51), aller sur pompe et pousser sur « on » puis « ok ». Attendre que la bouteille de Schott se vide complètement puis pousser sur le sigle de la pompe et appuyer sur « off » puis sur « ok ».



Figure 51: écran moniteur

Ensuite, l'alimentation en oxygène et le pH doivent être réglés. L'oxygène est calibré sur 0,1l/min et le pH sur 6,95.

Pour l'oxygène : aller sur « controller » puis « GAZF1 » (tout en bas sur l'écran) puis appuyer sur « set point » et encoder 0,1l/min. Puis, mettre le mode automatique et enlever les 2 pinces autour du filtre de l'alimentation en oxygène. Enlever les pinces en suivant le sens du flux d'oxygène. Quand cela est fait, la pince de Mohr du tuyau baignant dans l'eau de javel est enlevée.

Les pinces de l'acide et de la base sont enlevées puis les pompes d'acide et de bases sont mises en marche sur le mode automatique grâce à la même démarche que pour le glucose.



Les pinces de l'acide et de la base sont enlevées avant l'actionnement des pompes.

Pour calibrer l'oxygène, aller dans «calibration » puis dans « sensor » puis « pO21 » puis « mode » puis « calibration air » puis « 100% ». Il faut ensuite attendre que ça se stabilise.

Le chauffage de la colonne est assuré par un bain-marie figure (Julabo 12) (Figure 52) et un tuyau en silicone ID8-ED12mm accroché au bain par l'arrière de l'appareil et fermement fixé à l'aide de colson. Le tuyau de chauffage est collé au tuyau en silicone reliant la capsule infrarouge et la colonne à l'aide d'isolant pour tuyauterie (Climasap). La colonne est quant à elle isolée thermiquement grâce à de l'isolant pour tuyauterie en laine de verre fermé par des bandes adhésives.

Le bain marie peut ensuite être allumé à la température désirée (Figure 52). Celle-ci est ajustée afin de se rapprocher de la température optimale. La température de l'arrivée de la culture à l'entrée de la colonne est mesurée à l'aide d'un thermomètre infrarouge (Fluke IR thermometer). En fonction de la valeur de cette dernière, la température du bain est ajustée.



Figure 52 : bain marie (Julabo 12)

La préculture peut maintenant être ajoutée. Sous la flamme, la préculture du Schott de 250ml peut être versée dans le Schott qui contenait le glucose. La pompe peut être enclenchée en cliquant sur la pompe puis sur « AFOM1 » puis « on » puis « OK ». Lorsque la bouteille Schott est vide, la pompe est arrêtée via la même démarche en encodant « off ».

Des informations sur le réacteur sont encodées sur l'ordinateur près des réacteurs (Figure 53). Dans biostat, cliquer sur le 1^{er} (dans ce cas-ci), aller dans « start batch » puis de nouveau « start batch ». Dans description, toujours encoder la date au format américain avec le prénom et la première lettre du nom de l'utilisateur suivi du nom de la souche, exemple : 2018_03_07 justine K GA1. On peut ensuite y ajouter ce que l'on veut.

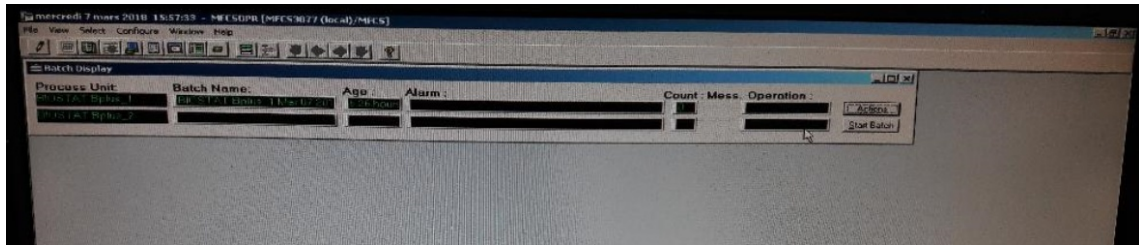


Figure 53: écran ordinateur

Un chronomètre donnant l'âge de la culture est visible dans « Trend ».

La capsule d'infrarouge (MINIPLANT Transmission cell IN243 de Bruker) est branchée au circuit (Figure 54) sous flamme.

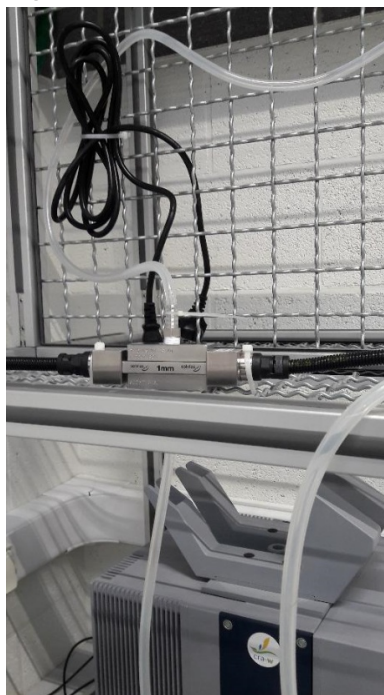


Figure 54: Capsule infrarouge branchée au système

Le montage complet est illustré par la Figure 55.

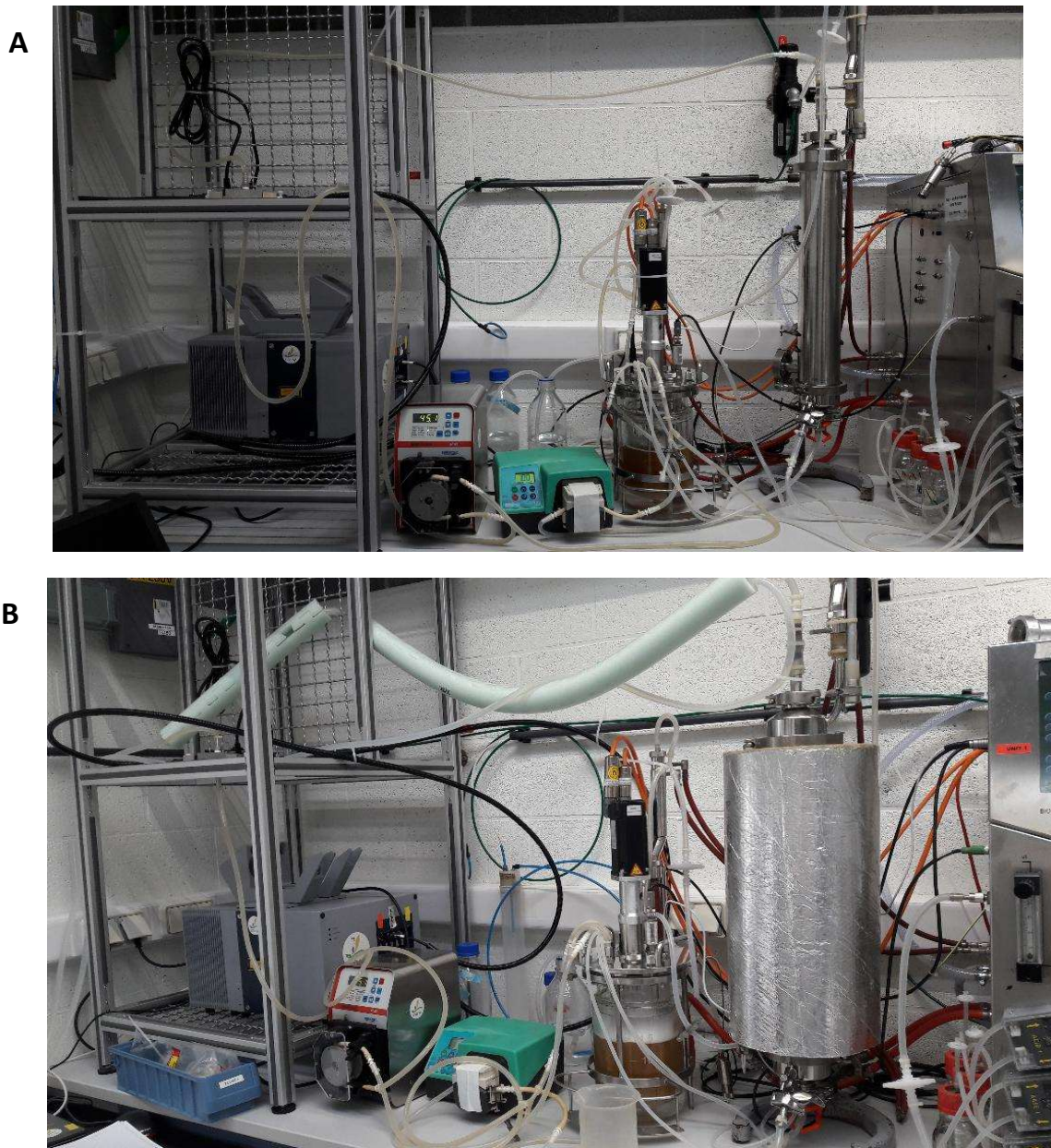


Figure 55: Montage complet sans chauffage de la colonne (A) avec (B)

5.1. Lancement de la recirculation

2 heures après que le réacteur ait été lancé, la recirculation est enclenchée. La pompe MCP-process est allumée et réglée sur 45,1rpm (44,7ml/min).

Le système infrarouge est allumé via l'ordinateur (Matrix-F FT-NIR spectrometer Bucker).

Le tuyau d'entrée du réacteur est branché au réacteur sous flamme puis il est attaché au moteur avec un colson. Ensuite, la pompe 323 Watson Marlow est allumée et réglée sur 100rpm.

Les aérations peuvent maintenant être interverties. Une pince de Mohr est placée sur le tuyau d'aération du réacteur après le filtre et le tuyau est accroché au moteur afin que le filtre soit placé en hauteur. La vanne d'aération dans le bas de la colonne est ouverte (Figure 56). La pince de Mohr du tuyau relié au condenseur qui baigne dans l'eau de javel est ensuite ouverte afin de permettre l'évacuation de l'air.



Figure 56: Vanne d'aération de la colonne

Les condenseurs sont interchangés entre le fermenteur et la colonne. La prise femelle est retirée en premier puis la mâle. Pour rebrancher le condenseur, c'est l'inverse, la prise mâle est branchée avant la femelle.

6. Démontage et nettoyage



Ce protocole n'est valable que pour des micro-organismes de type sauvage de classe 1 et non OGM.

L'infrarouge est d'abord arrêté.

Le sens de la pompe MCP-process est inversé afin de vidanger les tuyaux. Quand le tuyau est vide, la pompe MCP-process est arrêtée.

Le tuyau d'entrée de la colonne (tuyau du dessus de la colonne) est débranché et reconnecté au tuyau de la sortie du réacteur. Le tuyau est lavé avec de l'eau contenant du Bacillol (-+ 500ml d'eau). L'eau est introduite via le tuyau en silicone utilisé pour la prise d'échantillon. L'eau de lavage est récupérée dans une bouteille Schott et est ensuite jetée. Un deuxième lavage est ensuite effectué avec 100ml de bacillol dans de l'eau. Cette eau est conservée dans les tuyaux pour le moment.

Quand la colonne est complètement vidée, la pompe 323 Watson Marlow est arrêtée et le tuyau PharMed 4.8*8.0mm en est ôté.

Sur le moniteur, arrêter l'agitation et la mesure du pH, de l'oxygène et de la température.

6.1. Démontage de la colonne

L'isolant de tuyauterie est ôté des tuyaux après leurs vidanges dans le bain marie. Le tuyau de chauffage est ensuite enlevé ainsi que la laine de roche recouvrant la colonne.

La colonne est ensuite déconnectée du réacteur. Le tuyau de l'entrée du réacteur est débranché puis relié au haut de la colonne (le connecteur est laissé sur le réacteur).

Le tuyau d'entrée d'air de la colonne est retiré du moniteur et le tuyau baignant dans l'eau de javel est retiré de son bain. Le condenseur est ensuite enlevé (prise femelle avant mâle). Les tuyaux encore libre de la colonne y sont accrochés à l'aide de colliers colsons.

On peut maintenant dévisser les 2 pinces noires et prendre la colonne. Cette dernière est amenée dans la zone de nettoyage. Elle est couchée entre les 2 éviers et les colliers colsons en sont ôtés.

Pour le nettoyage, il y a 2 cas de figure en fonction de l'étude ou non du biofilm dans la colonne.

- Si on n'a pas besoin de le conserver, il suffit de brancher la colonne par un tuyau en silicone à l'évier pour la nettoyer puis de l'ouvrir.
- Dans l'autre cas, le tuyau du haut de la colonne est débranché de celui du bas. La colonne est ensuite ouverte par le haut. Un marteau avec embouts en plastique peut être utilisé pour faciliter l'ouverture. Le bas de la colonne est enlevé après. Maintenant, les packings peuvent être récoltés.

Toute les pièces sont lavées avec du savon Dreft puis rincées à l'eau efa (eau froide adoucie). Les packings sont juste rincés et immersés dans un récipient pour être autoclavés. Si des biofilms sont encore accrochés aux packings, les garnissages sont préalablement trempés dans un berlin contenant 10% de soude. Les lunettes de sécurité sont nécessaires pour cette étape. Les tuyaux en silicone sont rincés à l'extérieur et à l'intérieur à l'eau. Si des filtres sont encore présent sur les tuyaux, les ôter avant le lavage. Les pièces sont ensuite placées sur la table.



L'entonnoir du haut de la colonne doit être manipulé avec précaution et les pièces du haut de la colonne ne doivent jamais être séparées.

6.2. Démontage du réacteur

Enlever les tuyaux de l'acide et de la base de la pompe et mettre les bouteilles au sol afin que les tuyaux se vident complètement. Cela fait, une pince de Mohr peut être placée sur les fils de l'acide et de la base. Les 4 tuyaux peuvent maintenant être ôtés.



Aucune goutte d'acide et de base ne doit rester dans les tuyaux entre la pince et le réacteur.

Les sondes pO₂, pH et température sont déconnectées (les sondes pH et pO₂ du réacteur et la sonde de température du moniteur). Le fil de la sonde de température est enroulé à la poignée du réacteur.

D'une main le moteur du réacteur est dévissé et tenu de l'autre. Il est ensuite déposé sur le moniteur.

Les tuyaux encore libres sont attachés au réacteur. Les 2 tuyaux de la double enveloppe sont débranchés du moniteur et connectés ensemble. Le réacteur est ensuite amené dans la zone de nettoyage une fois qu'il est configuré comme sur la Figure 57.



Figure 57: réacteur prêt au lavage

Une fois dans l'évier, les colsons sont ôtés. La sonde de température est sortie de l'évier pour éviter de la mouiller. La sonde pO₂ (Hamilton Visiferm DO) est dévissée avec une clé 17 mm et la sonde pH avec les mains.

Remettre le capuchon de la prise de la sonde pH sur la sonde puis, la rincer à l'eau chaude et remplir le capuchon transparent de KCl 3M (au-dessus de l'évier) à ras-bord. La sonde est ensuite remise dans son capuchon. Le tout est ensuite rincé à l'eau. La sonde est placée dans une bouteille et remise près de la machine infrarouge. La sonde pO₂ est rincée et le capuchon jaune y est remis.

Les tuyaux d'entrée et de sortie d'air sont déconnectés et mis sur le côté ainsi que les filtres. Le condenseur est enlevé. Le tuyau de sortie du condenseur est branché à l'eau de ville et ainsi rincé. Les câbles de la double enveloppe sont enlevés de celle-ci et la double enveloppe est vidée. Des morceaux de tuyaux en silicone sont placés afin de protéger les sorties (Figure 58).



Figure 58: réacteur pendant le lavage

Puis, les derniers tuyaux encore sur le réacteur sont enlevés. Les 3 vis du réacteur sont dévissées en quinconce et le couvercle est enlevé. 20ml d'eau de javel sont versés dans le réacteur. Le couvercle est lavé au savon Dreft et puis de l'eau est aspergée dans les spargers du couvercle.

Le contenu du réacteur est vidé dans un berlin puis vider directement dans la buse de l'évier. Puis, la cuve est lavée au savon Dreft et rincée. Le couvercle peut maintenant être replacé et revisser en quinconce. La sonde de température est remise sur le couvercle.

La bouteille de saccharose est lavée à l'eau de ville. La bouteille de base est vidée dans la bouteille de NH₃ Waste (au-dessus de l'évier) dans la hotte à solvant. Le tuyau en silicone de la bouteille de NH₃ est jeté après chaque utilisation. La bouteille et le couvercle sont ensuite rincés à l'eau froide. Le tuyau de chaque bouteille d'acide est enroulé autour de celle-ci (Figure 59). Puis les bouteilles sont replacées sur le réacteur (Figure 29).



Figure 59: bouteille de base (gauche) et bouteille sur réacteur (droite)

Le tuyau toujours rempli de Bacillol au niveau de l'infrarouge est vidé. La pompe est rallumée pour la vidange. Les tuyaux sont retirés des pompes et les tuyaux en silicone de part et d'autre de l'infrarouge sont coupés. Les tuyaux et les bouteilles sont rincés.

Annex 2: Code on Matlab for compartments model (part determinist)

```

function dCdt = modelcolonneqdifer(t,C)

%% Parameters
n=250 %number of compartments in the column
%global n part of the model allowing the study of the impact of value variations of one parameter
v = 0.082/n; %liquid volume in the column. 110 seconds are required for the beginning of the liquid release. Then, in 110 sec with a recirculation flow of 0.000745L/s (44.7ml/min), volume in column equals 0,082
q1 = 0.000745*0.010; %flow q1 in lateral compartments
q2 = 0.000745*0.01; %flow q2 in lateral compartments
q = 0; %flow between lateral compartments; its valued was studied before but then, was fixed to 0.
Q = 0.0007450-q1% recirculation flow minus flow entering in lateral compartments
k = 0*Q; %adsorption rate in the biofilm column in s^-1 (considered as a fraction of the main flow rate Q) equals 0 here

%% Flow matrix
% Vectors for diagonal matrix
x=[Q/V q/V];
y=repmat (x,1, n);
o=[q2/V q1/V];
p=repmat (o,1, n);
z=[1 0];
w=repmat (z,1, n);
V6=y(1:n+1);
V0=p(1:n+1);
V1=-V6-V0;
V2=w(1:n)*(q1/V);
V3 = y(1:n-1);
V4 = w(1:n)*(q2/V);

% Diagonal matrix from vectors V1, V2, V3 and V4
M1 = diag(V1);
M2 = diag(V2,-1);
M3 = diag (V3,-2);
M4 = diag (V4,1);

% Flow matrix assembly
M = M1+M2+M4+M3;

%% Adding chemical reaction
K = ones(1,n+1).*k;
%K(1) = 0;
Mat_trans= M;
save Mat_trans Mat_trans;
%part non used here

%% ODEs
dCdt = (M*C)-k*C;

```

On another page:

```

%global n
%n_array=1:1:100;
%for i=1:numel(n_array)
%n =n_array(i);
% part of the model allowing the study of the impact of value variations of one parameter

```

```

n=250;%number of compartments
init = zeros(1,n+1); %terms to initiate concentration in all compartments equals to 0
init(1)=1; %terms to initiate concentration of the first compartment equals to 1
[t C] = ode15S('modelcolonnedififer',0:300,init);

x=max(C(:,n));
C(:,n)=C(:,n)/x;
%terms to make values of the model proportional to 1

A= xlsread('donneetraceurair2.xlsx');
%lecture of experimental data (traceur)

figure(1),plot(A(:,1),A(:,2),'o', t, C(:,n))
xlabel('Time (sec)')
ylabel('Relative cells concentration')
%Terms to create figure with experimental data and model curve

%hold on
%end
% part of the model allowing the study of the impact of value variations of one parameter

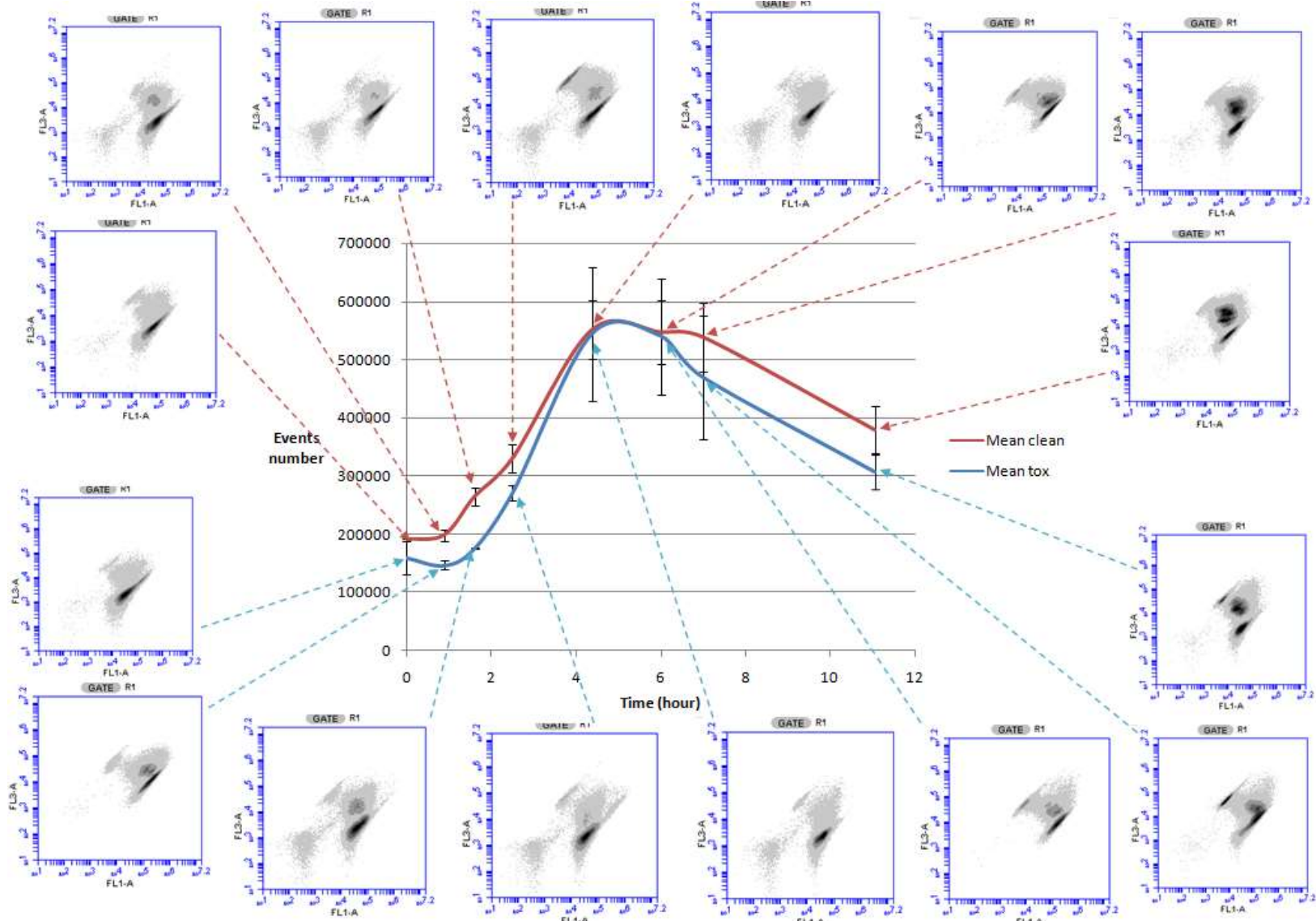
```

Annex 3: Comparison test between fresh culture growing in fresh Optimized medium and in medium take out of the reactor

For this test, fresh culture was putted in 5ml of fresh Optimized medium added to 5ml of sterile distilled water (for clean samples) or to 5ml of the medium sampled in the reactor after 28h of cell culture (for tox samples). Thereby, nutrients concentration is quite higher in samples with medium from reactor (0.52g/L more sucrose). This test was done with an initial OD600 of 1,5 (A) and 0,1 (B).

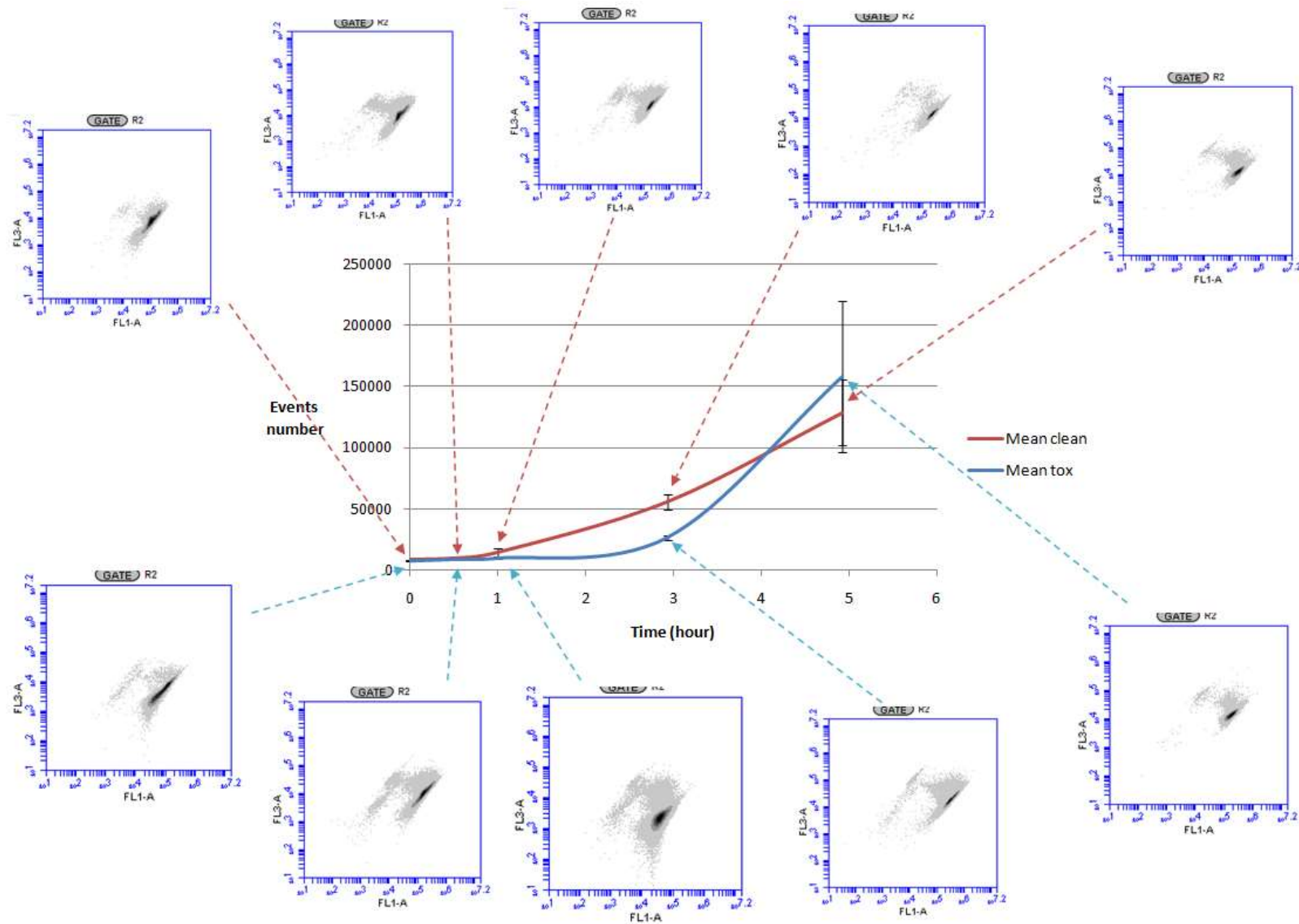
Annexes

A



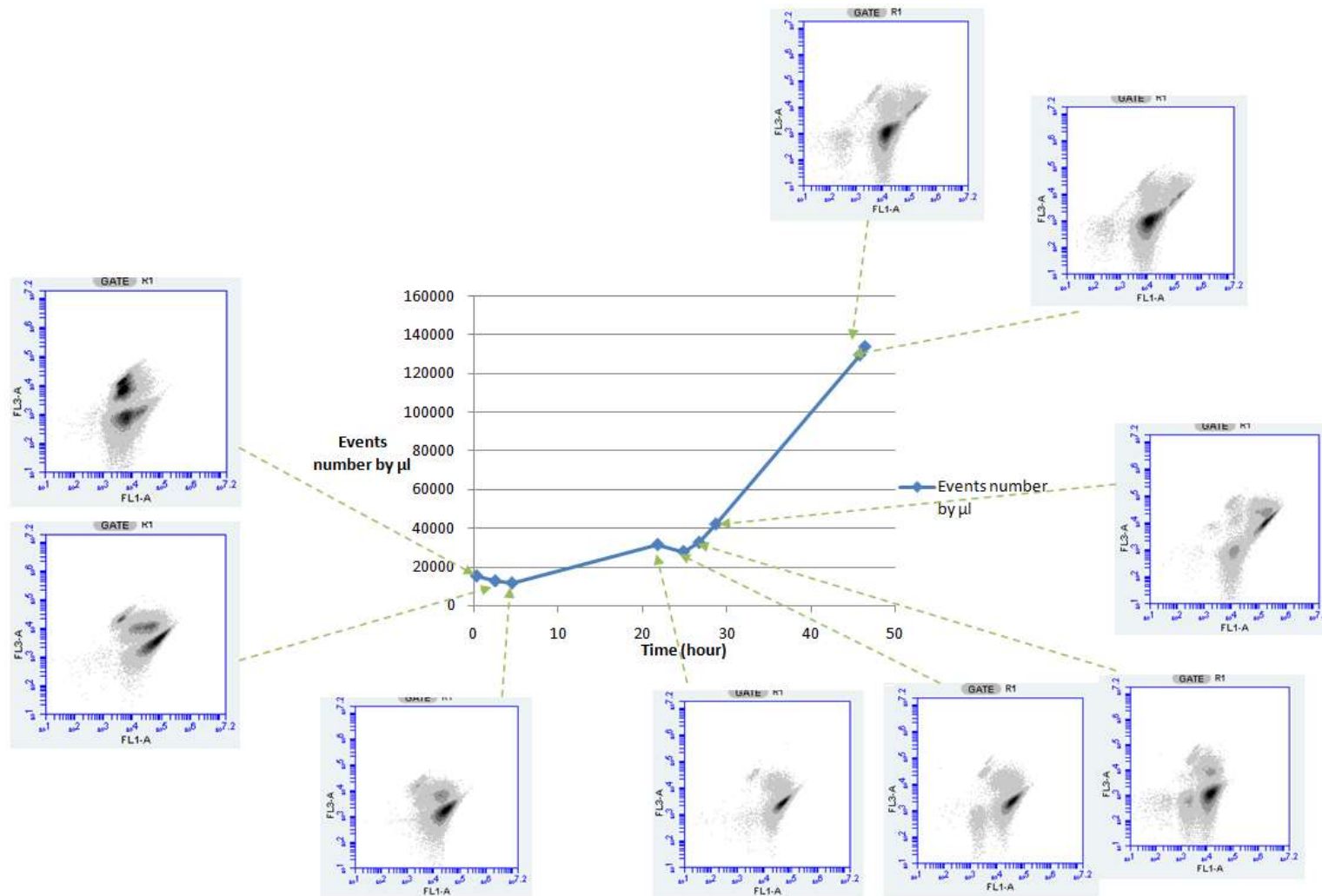
Annexes

B



Annexes

Annex 4: Evolution of events number of *B. amyloliquefaciens* by μl and cells activity measured with a cytometer in FL1 and FL3 i biofilm reactor with MSgg



Annex 5: Evolution of the numbers of events by μl of *B. amyloliquefaciens* growing in microplates in MSgg (red) and in Optimized medium (blue)

